 CMES, vol.65, no.3, pp.259-341, 2010

Variable Kinematics and Advanced Variational Statements for Free Vibrations Analysis of Piezoelectric Plates and Shells

E. Carrera, S. Brischetto[1] and M. Cinefra[2]

Abstract: This paper investigates the problem of free vibrations of multilayered plates and shells embedding anisotropic and thickness polarized piezoelectric layers. Carrera's Unified Formulation (CUF) has been employed to implement a large variety of electro-mechanical plate/shell theories. So-called Equivalent Single Layer and Layer Wise variable descriptions are employed for mechanical and electrical variables; linear to fourth order expansions are used in the thickness direction z in terms of power of z or Legendre polynomials. Various forms are considered for the Principle of Virtual Displacements (PVD) and Reissner's Mixed Variational Theorem (RMVT) to derive consistent differential electro-mechanical governing equations. The effect of electro-mechanical stiffness has been evaluated in both PVD and RMVT frameworks, while the effect of continuity of transverse variables (transverse shear and normal stresses and transverse normal electric displacement) has been addressed by comparing various forms of RMVT. According to CUF, governing equations related to a given variational statement have been written in terms of fundamental nuclei whose form is independent of the order of expansion and of the adopted variable description. The numerical results have been restricted to simply supported orthotropic plates and shells, for which exact three-dimensional solutions are available. A large numerical investigation has been conducted to compute fundamental and higher vibrations modes. An exhaustive numerical evaluation of assumptions, related to the various PVD and RMVT forms, is given. Classical, higher-order, layer-wise and mixed assumptions have been compared to available three-dimensional solutions. The convenience of hierarchical approaches based on CUF is shown, along with the suitability of the implemented RMVT forms to accurately trace the free vibration response of piezoelectric plates and shells. RMVT applications permit the vibration modes of transverse electro-mechanical variables

[1] Corresponding author: Salvatore Brischetto, Department of Aeronautics and Space Engineering, Politecnico di Torino, Corso Duca degli Abruzzi, 24, 10129 Torino, Italy. Tel: +39.011.564.6869, Fax: +39.011.564.6899, Email: salvatore.brischetto@polito.it.

[2] Department of Aeronautics and Space Engineering, Politecnico di Torino, Italy

to be accurately evaluated in the thickness plate/shell direction

.

Keywords: multilayered plates; multilayered shells; thickness polarized piezoelectric layers; electro-mechanical coupling; Principle of Virtual Displacements; Reissner's Mixed Variational Theorem; layer wise; equivalent single layer; vibrations modes.

1 Introduction

Piezoelectric materials are one of the most suitable solutions for the design of smart structures [Im and Atluri (1989)]. These materials use the so-called piezoelectric effect, which consists of a linear energy conversion between the mechanical and electric field and viceversa, and this conversion leads to a direct or converse piezoelectric effect, respectively [Ikeda (1990)]. The main applications of smart structures are: vibration and noise damping, shape adaptation of aerodynamic surfaces, active aeroelastic control, shape control of optical and electro-magnetic devices and health monitoring. Exhaustive overviews on possible applications of smart structures have been given by Rao and Sunar (1994), Crawley (1994), Chopra (1996), Tani et al. (1998), Sunar and Rao (1999), and more recently by Chopra (2002) and Yang (2006). In most applications, smart structures are multilayered anisotropic plates and shells with strong electro-mechanical coupling. The layers can be made of traditional metallic or advanced composite materials, as well as sandwich structures. Piezoelectric layers are embedded in the structures in various forms: one or more sensor layers (or patches); one or more actuator layers (or patches); a combination of one or more sensor/actuator layers. Several topics are of interest in the application of smart structures as well as in their computational simulation: material modelings, structural modelings and control algorithms. The attention of this work is restricted to advanced structural modelings for multilayered thickness polarized piezoelectric plates and shells with emphasis on the vibration response. In addition to the afore mentioned review papers, further overviews on modelling are those in Benjeddou (2000), Robbins and Chopra (2006) and Carrera and Boscolo (2007). As in any other multilayered structure, improved refined models for multilayered plates should account for:

- an accurate description of the interlaminar conditions, such as the Zig-Zag (ZZ) form of displacement in the thickness direction z (rapid change in slope in correspondence to each layer interface) and the Interlaminar Continuity (IC) of transverse stresses at each layer interface.

In Carrera (1995) and Carrera (1997b), ZZ and IC conditions are referred to as C_z^0-requirements. ZZ and IC can be introduced into Equivalent Single Layer ESL theories by implementing various techniques; according to Reddy (2004), the number of displacement variables should be kept independent of the number of constitutive layers in the ESL models, while the same variables depend on each layer in Layer Wise LW cases. A discussion on a historical review of so-called zig-zag theories has been given in Carrera (2003). Recent works about zigzag models for the analysis of multilayered piezoelectric structures have been proposed by Kapuria (2004a), Kapuria (2004b), Kapuria and Achary (2005a) and Kapuria and Kulkarni (2008). In Carrera (2001) it was established that the Reissner's Mixed Variational Theorem (RMVT) [Reissner (1984)] should be considered as the natural extension of the Principle of Virtual Displacements (PVD) to multilayered structures in view of the fullfillment of C_z^0-requirements. RMVT in fact, permits the compatibility conditions of transverse shear and normal stress components to be enforced.

The fulfillment of C_z^0-requirements remains a crucial point in the development of appropriate two-dimensional models for multilayered plates and shells embedding piezolectric layers. Figure 1 shows the distribution of mechanical and electrical variables in layered plates made of piezoelectric layers. Displacement, in-plane stress components, electrical potential, transverse stress components and transverse normal electrical displacement are shown. An extended 'electrical' form of RMVT permits the continuity of transverse normal electrical displacement to be fulfilled at each layer interface as well as the direct evaluation of the electrical charge [Carrera et al. (2008); Carrera and Nali (2009)]. An alternative method has been proposed in Chen and Hwu (2010), where the use of Green's function permits to exactly satisfy the interface continuity conditions and no meshes are needed along the interface, in this approach the materials can be any kinds of piezoelectric or anisotropic elastic materials. The Green's function is also employed by Wu and Chen (2007) to investigate the dynamic responses of several piezoelectric materials in order to yield the displacement or stress fields in the time domain directly.

The attention of the present paper is restricted to a free vibration analysis of multilayered plates and shells embedding thickness polarized piezoelectric layers. The afore mentioned review papers discuss most of the available works on this topic. However, a short review of works which are relevant for this paper is given in the following. Three-dimensional exact solutions for the free vibration problem have been provided by Heyliger and Saravanos (1995), where frequencies for the first three modes are given for both thick and thin multilayered piezoelectric plates. Kapuria and Achary (2005b) proposed a three-dimensional piezoelasticity solution for hybrid cross-ply plates where a real mass density, different from the unit value suggested in Heyliger and Saravanos (1995), was considered. Kapuria and Achary

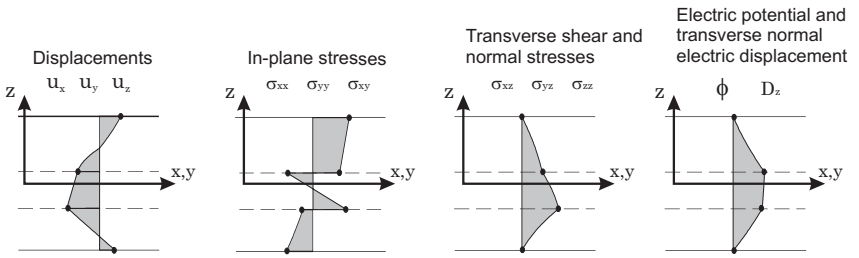

Figure 1: C_z^0-requirements for multilayered piezoelectric plates. Zig-Zag form and Interlaminar Continuity for some mechanical and electrical variables. For shell geometry the reference system (x,y,z) is replaced by (α,β,z).

(2005b) investigated also hybrid sandwich configurations where the different values of the mass density for the embedded layers were more relevant. Du et al. (2006) investigated the thickness vibrations of a piezoelectric plate using an exact solution obtained for materials with general anisotropy; the effects of a uniform biasing acceleration were also considered. A three dimensional theory is presented in Zhu et al. (2003) for the dynamic stability analysis of piezoelectric circular cylindrical shells. In this case, results indicate that piezoelectric effects and electric field have a minor effect on the unstable region with respect to the geometric parameters and the rigidity of constituent materials. A three dimensional solution for dynamic analysis of thick laminated shell panels is illustrated in Shakeri et al. (2006), direct and inverse effects of piezoelectric materials are considered. Applications of CLT and FSDT to piezoelectric plates have been given by Tiersten (1969) and Mindlin (1972). In He et al. (1998), numerical and experimental results have been compared for free vibration analysis of thin plates embedding metallic and piezoceramic layers, but the transverse normal strain/stress effects were not taken into account. An annular plate has been considered in Duan et al (2005), where the free vibration analysis has been conducted using very simple models such as the Kirchhoff and Reissner-Mindlin plate models; different boundary conditions have been investigated and FEM solutions have been considered. In Heidary and Eslami (2006), the linear response of thermopiezoelectric plates is given using the Hamilton principle and the finite element method. Linear shape functions are used and the First order Shear deformation Theory (FSDT) of laminated plates is considered. Thermally induced vibration amplitudes are suppressed through application of electric potential differences across the piezoelectric layers attached to the surfaces of the composite plate. The numerical studies demonstrate the effectiveness of thermal environment, as well as the piezo-control of these thermal deformations

using piezoelectric structures. As example of a refined theory, the work by Yang and Yu (1993), is mentioned. The electric field generated by stresses (electrical stiffness) was not considered in this work. Refined ESL models have been discussed by Benjeddou and Deü (2001). ESL formulation, taking into account ZZ and IC, has been discussed by Ossadzow-David and Touratier (2004). Pan and Heyliger (2002) have shown natural frequencies and shape modes for sandwich piezoelectric/piezocomposite plates using analytical solutions. Mitchell and Reddy (1995) introduced a Layer-Wise (LW) description of the electric potential, while an Equivalent Single Layer (ESL) description was retained for displacements. Han et al. (2005) have considered the coupling between the elastic and electric field in each element when characteristics surface waves in hybrid multilayered piezoelectric plates have been investigated. Cupial (2005) has remarked that the capability of a two-dimensional model to predict vibration modes plays a fundamental role in both noise damping and health monitoring problems. Ramirez et al. (2006) calculated the natural frequencies and through-thickness mode behavior of simply supported and cantilever laminates. An approximated solution for free vibration problems of two-dimensional magneto-electro-elastic laminates has been presented to determine their fundamental behavior. The solution for the elastic displacements, electric potential and magnetic potential is obtained by combining a discrete layer approach with the Ritz method. Free vibrations of multilayered piezoelectric composite plates can be also found in Zhang et al. (2006), where an analysis was performed using the differential quadratic (DQ) technique to solve three-dimensional piezoelasticity equations. Solutions for piezoelectric laminates are possible if the DQ layer-wise modelling technique is implemented. Becker et al. (2006) have proposed a finite element modelling methodology which incorporates both piezoelectric coupling effects and the electrical dynamics of the employed passive electrical circuits. The effects of the electric boundary conditions and the influence of the direction of polarization are investigated in Dziatkiewicz and Fedelinski (2007) for the free vibrations of two-dimensional piezoelectric structures using the dual reciprocity boundary element method. Further works about shell geometries are listed in the following. In Wang et al. (2005) the dynamic solution for a multilayered orthotropic piezoelectric hollow cylinder is obtained by means of a solution split in two parts: a quasi-static solution in addition to a dynamic one; displacements, stresses and electric potential are finally obtained. Numerical results for layered piezoelectric spherical caps and indication of their behavior are given in Wu and Heyliger (2001). First, only elastic shells are examined to test the accuracy of the formulation, then solutions for piezoelectric shells are given, they could be a means of comparison for other techniques and methods. In Zheng et al. (2004) a refined hybrid piezoelectric shell element formulation is developed for mechanical analysis and active vibration control of laminated structures bonded to piezoelectric sensors

and actuators. Benjeddou et al. (2001a) and Benjeddou et al. (2001b) consider shells of revolution, a finite element implementation is presented. Open circuit and closed circuit configurations are investigated and different types of modes are considered, such as bending, radial and torsion ones.

Applications of CUF to piezolectric plates were first given in Carrera (1997a), ZZ and IC were introduced in the First order Shear Deformation Theory (FSDT). Ballhause et al. (2005) gave closed-form solutions for the free vibration problem of multilayered piezoelectric plates; a quasi-3D formulation was obtained by employing Carrera's Unified Formulation (CUF) [Carrera (1995)] and the Principle of Virtual Displacements (PVD) was extended to the electro-mechanical case. The closed form solution proposed by Ballhause et al. (2005) for plates was extended to shell geometry by D'Ottavio et al. (2006). CUF is a variable kinematic framework which permits a large variety of electro-mechanical plate/shell theories to be implemented: Equivalent Single Layer (ESL) and Layer Wise (LW) variable descriptions are employed for mechanical and electrical variables; linear to fourth-order expansions are used in the thickness direction z, in terms of power of z and/or Legendre polynomials. According to CUF, all the governing equations related to a given variational statement have been written in terms of fundamental nuclei, and their form is independent of the order of expansion as well as of the adopted variable description.

It can be concluded that CUF variable kinematic modelings as well as the use of mixed variational statements could be used to construct appropriate theories for the analysis of piezoelectric plates and shells in view of the fulfillment of the C_z^0-requirements. The present paper gives a complete discussion of available CUF modelings, and applications of various classical (PVD) and advanced (RMVT) statements for the free vibration problems of piezoelectric plates and shells. In particular, the CUF variable kinematics models are implemented according to the following variational statements:

- $PVD(\boldsymbol{u})$, the electrical stiffness is neglected ($\boldsymbol{u}$ indicates displacement variables).
- $RMVT(\boldsymbol{u},\boldsymbol{\sigma}_n)$, the electrical stiffness is neglected and transverse shear/normal stresses IC are a priori fulfilled ($\boldsymbol{\sigma}_n$ denotes transverse shear/normal stresses).
- $PVD(\boldsymbol{u},\Phi)$, the electrical stiffness is included (Φ is the electric potential).
- $RMVT(\boldsymbol{u},\Phi,\boldsymbol{\sigma}_n)$, transverse shear/normal stresses IC are a priori fulfilled.
- $RMVT(\boldsymbol{u},\Phi,\mathscr{D}_n)$, transverse normal electric displacement IC is a priori fulfilled ($\mathscr{D}_n$ is the transverse normal electric displacement).

- $RMVT(\boldsymbol{u}, \Phi, \boldsymbol{\sigma}_n, \mathscr{D}_n)$, transverse shear/normal stresses and transverse normal electric displacement IC are a priori fulfilled.

Other applications of RMVT and CUF to piezoelectric plates and shells have been given in Carrera and Boscolo (2007), Carrera et al. (2008), Carrera and Nali (2009), Carrera and Brischetto (2007a), Carrera and Brischetto (2007b) and D'Ottavio and Kröplin (2006). In Carrera and Boscolo (2007) the FEM static analysis of multilayered piezoelectric plates was given, in the proposed variational statements the case $RMVT(\boldsymbol{u}, \Phi, \mathscr{D}_n)$ was not considered. Carrera et al. (2008) was an extension of Carrera and Boscolo (2007), where the magnetic field is also considered. In Carrera and Nali (2009) the $RMVT(\boldsymbol{u}, \Phi, \mathscr{D}_n)$ case was introduced but only static FEM analysis of multilayered piezoelectric plates was considered. In Carrera and Brischetto (2007a) and Carrera and Brischetto (2007b) $RMVT(\boldsymbol{u}, \Phi, \boldsymbol{\sigma}_n)$ and $RMVT(\boldsymbol{u}, \Phi, \boldsymbol{\sigma}_n, \mathscr{D}_n)$ were extended to the static and dynamic analysis of multilayered piezoelectric shells, respectively. D'Ottavio and Kröplin (2006) extended the $RMVT(\boldsymbol{u}, \Phi, \boldsymbol{\sigma}_n)$ to piezoelectric laminates, this variational statement was employed for the free-vibration problem of multilayered piezoelectric shells. The present paper gives an exhaustive discussion about each possible extension of PVD and RMVT variational statement to electro-mechanical analysis of plates and shells, with emphasis to those variational statements not included in the above cited works. The governing differential equations related to the various formulations are given and their closed-form solutions are discussed. A numerical investigation is made to evaluate fundamental and higher-order modes. The in-house academic MUL2 code [MUL2 (2009)] has been used. Comparisons of classical, higher-order, layer-wise and mixed assumptions are made. Evaluations of the effect of interlaminar continuity is given.

The paper has been organized as follows. The various extensions of PVD and RMVT to electro-mechanical analysis are discussed in Section 2; the related consistent constitutive equations are derived in the same section. Geometrical relations for plates and shells are described in Section 3, while CUF is dealt with in detail in Section 4. The governing equations for the dynamic analysis of piezoelectric plates and shells are derived in Section 5. Closed-form solutions are given in Section 6. Governing eigenvalues problem can be found in Section 7. The results are discussed in Section 8 and the main conclusions are drawn in Section 9. Some appendices quote a few details of the considered formulations in order to see the main differences for fundamental nuclei in the case of plate geometry and those in the case of shell geometry (both open spherical and cylindrical cases).

2 The considered variational statements

The Principle of Virtual Displacements (PVD) is extended to the electro-mechanical case by simply adding the virtual internal electric work to the mechanical one. Constitutive equations are obtained from the quadratic form of the Gibbs free-energy function, written in the case of linear interaction between the mechanical and electrical field [Ikeda (1990); Rogacheva (1994)]. Hooke's well-known law for the pure mechanical problem can be considered as a particular case of the more general constitutive equations written for the electro-mechanical case [Carrera et al. (2008)].

Three different extensions of Reissner's Mixed Variational Theorem (RMVT) to an electro-mechanical case are here discussed; for each proposed extension, the constitutive equations must be rearranged and written coherently with the employed variational statement [Carrera et al. (2008)].

2.1 Extended PVD cases

The PVD($\boldsymbol{u}$) case

For a multilayered plate or shell, including orthotropic layers, in the case of pure mechanical problem, the PVD states:

$$\mathrm{PVD}(\boldsymbol{u}) : \int_V (\delta\boldsymbol{\varepsilon}_{pG}^T \boldsymbol{\sigma}_{pC} + \delta\boldsymbol{\varepsilon}_{nG}^T \boldsymbol{\sigma}_{nC}) dV = \delta L^e + \delta L^{in}, \tag{1}$$

subscripts C and G indicate the substitution of constitutive and geometrical relations, respectively. For plate geometry $\boldsymbol{u} = (u_x, u_y, u_z)$ is the displacement vector; $\boldsymbol{\sigma}_p = (\sigma_{xx}, \sigma_{yy}, \sigma_{xy})$ and $\boldsymbol{\sigma}_n = (\sigma_{xz}, \sigma_{yz}, \sigma_{zz})$ are the in-plane and out-plane stress components, respectively. $\boldsymbol{\varepsilon}_p = (\varepsilon_{xx}, \varepsilon_{yy}, \gamma_{xy})$ and $\boldsymbol{\varepsilon}_n = (\gamma_{xz}, \gamma_{yz}, \varepsilon_{zz})$ are the in-plane and out-plane strain components, respectively. δL^e is the virtual external work and δL^{in} is the virtual inertial work.

This form of PVD does not include electrical stiffness, so it is denoted as PVD($\boldsymbol{u}$) due to the fact that the displacements are the only primary variables. For shell geometry a curvilinear reference system (α,β,z) is employed in place of the rectilinear one (x,y,z) for the plate (see also Figure 2).

The PVD($\boldsymbol{u}$,Φ) case

PVD is extended to the electro-mechanical case by simply adding the internal electric work:

$$\mathrm{PVD}(\boldsymbol{u}, \Phi) : \int_V (\delta\boldsymbol{\varepsilon}_{pG}^T \boldsymbol{\sigma}_{pC} + \delta\boldsymbol{\varepsilon}_{nG}^T \boldsymbol{\sigma}_{nC} - \delta\boldsymbol{\mathscr{E}}_{pG}^T \boldsymbol{\mathscr{D}}_{pC} - \delta\boldsymbol{\mathscr{E}}_{nG}^T \boldsymbol{\mathscr{D}}_{nC}) dV = \delta L^e + \delta L^{in}, \tag{2}$$

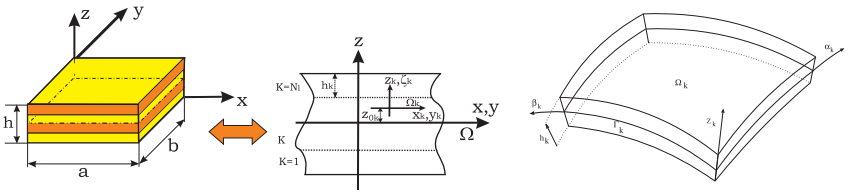

a) *b)*

Figure 2: Geometry and notation for a multilayered plate (a) and a multilayered shell (b).

where $\boldsymbol{\mathscr{E}}_p = (\mathscr{E}_x, \mathscr{E}_y)$, $\boldsymbol{\mathscr{E}}_n = (\mathscr{E}_z)$ and $\boldsymbol{\mathscr{D}}_p = (\mathscr{D}_x, \mathscr{D}_y)$, $\boldsymbol{\mathscr{D}}_n = (\mathscr{D}_z)$ are the in-plane and out-plane electric field and electric displacement components, respectively. Both displacement and electric potential are primary variables in PVD($\boldsymbol{u}$,Φ).

In case of electro-mechanical problem the constitutive equations are obtained from the Gibbs free-energy function G [Ikeda (1990); Rogacheva (1994)]:

$$G(\varepsilon\ ,\mathscr{E}\ ) = \frac{1}{2}\boldsymbol{\varepsilon}^T \boldsymbol{C}\boldsymbol{\varepsilon} - \frac{1}{2}\boldsymbol{\mathscr{E}}^T \boldsymbol{\varepsilon}\boldsymbol{\mathscr{E}} - \boldsymbol{\mathscr{E}}^T \boldsymbol{e}\boldsymbol{\varepsilon}\ . \tag{3}$$

$\boldsymbol{C}$ is the matrix of elastic coefficients, $\boldsymbol{e}$ is the matrix of piezoelectric coefficients, $\boldsymbol{\varepsilon}$ is the matrix of dielectric coefficients. The [6×6] matrix $\boldsymbol{C}$ for an orthotropic material in the structural reference system assumes the following form [Reddy (2004)]:

$$\boldsymbol{C} = \begin{bmatrix} C_{11} & C_{12} & C_{16} & 0 & 0 & C_{13} \\ C_{12} & C_{22} & C_{26} & 0 & 0 & C_{23} \\ C_{16} & C_{26} & C_{66} & 0 & 0 & C_{36} \\ 0 & 0 & 0 & C_{55} & C_{45} & 0 \\ 0 & 0 & 0 & C_{45} & C_{44} & 0 \\ C_{13} & C_{23} & C_{36} & 0 & 0 & C_{33} \end{bmatrix} = \begin{bmatrix} \mathbf{C}_{pp} & \mathbf{C}_{pn} \\ \mathbf{C}_{np} & \mathbf{C}_{nn} \end{bmatrix}, \tag{4}$$

where $\mathbf{C}_{pp}$, $\mathbf{C}_{pn}$, $\mathbf{C}_{np}$ and $\mathbf{C}_{nn}$ are the [3×3] sub-matrices related to in-plane p and out-plane n strain/stress components.

The matrices for the piezoelectric coupling and for the dielectric coefficients, when

the poling direction 3 coincides with the layer z direction, are:

$$\boldsymbol{e} = \begin{bmatrix} 0 & 0 & 0 & e_{15} & e_{14} & 0 \\ 0 & 0 & 0 & e_{25} & e_{24} & 0 \\ e_{31} & e_{32} & e_{36} & 0 & 0 & e_{33} \end{bmatrix}, \quad \boldsymbol{\varepsilon} = \begin{bmatrix} \varepsilon_{11} & \varepsilon_{12} & 0 \\ \varepsilon_{21} & \varepsilon_{22} & 0 \\ 0 & 0 & \varepsilon_{33} \end{bmatrix}. \tag{5}$$

Stresses and electric displacement are obtained upon direct differentiation of G as it follows:

$$\boldsymbol{\sigma} = \frac{\partial G}{\partial \boldsymbol{\varepsilon}} = \frac{\partial}{\partial \boldsymbol{\varepsilon}}\left(\frac{1}{2}\boldsymbol{\varepsilon}^T \boldsymbol{C}\boldsymbol{\varepsilon} - \frac{1}{2}\boldsymbol{\mathscr{E}}^T \boldsymbol{\varepsilon}\boldsymbol{\mathscr{E}} - \boldsymbol{\mathscr{E}}^T \boldsymbol{e}\boldsymbol{\varepsilon}\right) = \boldsymbol{C}\boldsymbol{\varepsilon} - \boldsymbol{e}^T \boldsymbol{\mathscr{E}}, \tag{6}$$

$$\boldsymbol{\mathscr{D}} = -\frac{\partial G}{\partial \boldsymbol{\mathscr{E}}} = -\frac{\partial}{\partial \boldsymbol{\mathscr{E}}}\left(\frac{1}{2}\boldsymbol{\varepsilon}^T \boldsymbol{C}\boldsymbol{\varepsilon} - \frac{1}{2}\boldsymbol{\mathscr{E}}^T \boldsymbol{\varepsilon}\boldsymbol{\mathscr{E}} - \boldsymbol{\mathscr{E}}^T \boldsymbol{e}\boldsymbol{\varepsilon}\right) = \boldsymbol{e}\boldsymbol{\varepsilon} + \boldsymbol{\varepsilon}\boldsymbol{\mathscr{E}}. \tag{7}$$

$\boldsymbol{\mathscr{E}} = (\mathscr{E}_x, \mathscr{E}_y, \mathscr{E}_z)$ is the [3×1] electric field vector, $\boldsymbol{\varepsilon} = (\varepsilon_{xx}, \varepsilon_{yy}, \gamma_{xy}, \gamma_{xz}, \gamma_{yz}, \varepsilon_{zz})$ is the [6×1] strain vector, $\boldsymbol{\sigma} = (\sigma_{xx}, \sigma_{yy}, \sigma_{xy}, \sigma_{xz}, \sigma_{yz}, \sigma_{zz})$ is the [6×1] stress vector, $\boldsymbol{\mathscr{D}} = (\mathscr{D}_x, \mathscr{D}_y, \mathscr{D}_z)$ is the [3×1] electric displacement vector.

The correspondent constitutive equations are herein split in in-plane and out-plane components:

$$\boldsymbol{\sigma}_{pC} = \frac{\partial G}{\partial \boldsymbol{\varepsilon}_p} = \boldsymbol{C}_{pp}\boldsymbol{\varepsilon}_{pG} + \boldsymbol{C}_{pn}\boldsymbol{\varepsilon}_{nG} - \boldsymbol{e}_{pp}^T \boldsymbol{\mathscr{E}}_{pG} - \boldsymbol{e}_{np}^T \boldsymbol{\mathscr{E}}_{nG}, \tag{8}$$

$$\boldsymbol{\sigma}_{nC} = \frac{\partial G}{\partial \boldsymbol{\varepsilon}_n} = \boldsymbol{C}_{np}\boldsymbol{\varepsilon}_{pG} + \boldsymbol{C}_{nn}\boldsymbol{\varepsilon}_{nG} - \boldsymbol{e}_{pn}^T \boldsymbol{\mathscr{E}}_{pG} - \boldsymbol{e}_{nn}^T \boldsymbol{\mathscr{E}}_{nG}, \tag{9}$$

$$\boldsymbol{\mathscr{D}}_{pC} = -\frac{\partial G}{\partial \boldsymbol{\mathscr{E}}_p} = \boldsymbol{e}_{pp}\boldsymbol{\varepsilon}_{pG} + \boldsymbol{e}_{pn}\boldsymbol{\varepsilon}_{nG} + \boldsymbol{\varepsilon}_{pp}\boldsymbol{\mathscr{E}}_{pG} + \boldsymbol{\varepsilon}_{pn}\boldsymbol{\mathscr{E}}_{nG}, \tag{10}$$

$$\boldsymbol{\mathscr{D}}_{nC} = -\frac{\partial G}{\partial \boldsymbol{\mathscr{E}}_n} = \boldsymbol{e}_{np}\boldsymbol{\varepsilon}_{pG} + \boldsymbol{e}_{nn}\boldsymbol{\varepsilon}_{nG} + \boldsymbol{\varepsilon}_{np}\boldsymbol{\mathscr{E}}_{pG} + \boldsymbol{\varepsilon}_{nn}\boldsymbol{\mathscr{E}}_{nG}, \tag{11}$$

where

$$\mathbf{e}_{pp} = \begin{bmatrix} 0 & 0 & 0 \\ 0 & 0 & 0 \end{bmatrix}, \ \mathbf{e}_{pn} = \begin{bmatrix} e_{15} & e_{14} & 0 \\ e_{25} & e_{24} & 0 \end{bmatrix}, \tag{12}$$

$$\mathbf{e}_{np} = \begin{bmatrix} e_{31} & e_{32} & e_{36} \end{bmatrix}, \ \mathbf{e}_{nn} = \begin{bmatrix} 0 & 0 & e_{33} \end{bmatrix},$$

$$\boldsymbol{\varepsilon}_{pp} = \begin{bmatrix} \varepsilon_{11} & \varepsilon_{12} \\ \varepsilon_{12} & \varepsilon_{22} \end{bmatrix}, \ \boldsymbol{\varepsilon}_{pn} = \begin{bmatrix} 0 \\ 0 \end{bmatrix}, \ \boldsymbol{\varepsilon}_{np} = \begin{bmatrix} 0 & 0 \end{bmatrix}, \ \boldsymbol{\varepsilon}_{nn} = \begin{bmatrix} \varepsilon_{33} \end{bmatrix}.$$

From Eqs.(8)-(11), in case of pure mechanical problem, the classical Hooke law is obtained:

$$\boldsymbol{\sigma}_p = \boldsymbol{C}_{pp}\boldsymbol{\varepsilon}_p + \boldsymbol{C}_{pn}\boldsymbol{\varepsilon}_n \ , \tag{13}$$

$$\boldsymbol{\sigma}_n = \boldsymbol{C}_{np}\boldsymbol{\varepsilon}_p + \boldsymbol{C}_{nn}\boldsymbol{\varepsilon}_n \ . \tag{14}$$

Eqs.(8)-(11) are the consistent constitutive equations for the variational statement PVD($\boldsymbol{u}$,Φ) at Eq.(2), while Eqs.(13) and (14) are the constitutive equations consistent to the PVD($\boldsymbol{u}$) in Eq.(1).

For shell geometry a curvilinear reference system (α,β,z) is employed in place of the rectilinear one (x,y,z) for the plate (see also Figure 2).

2.2 Extended RMVT cases

The RMVT($\boldsymbol{u}$,Φ,$\boldsymbol{\sigma}_n$) case

Reissner's Mixed Variational Theorem (RMVT) for the pure mechanical case assumes transverse shear/normal stresses and displacement as independent variables [Reissner (1984)]:

$$\mathrm{R}MVT(\boldsymbol{u},\boldsymbol{\sigma}_n) : \int_V (\delta\boldsymbol{\varepsilon}_{pG}^T\boldsymbol{\sigma}_{pC} + \delta\boldsymbol{\varepsilon}_{nG}^T\boldsymbol{\sigma}_{nM} + \delta\boldsymbol{\sigma}_{nM}^T(\boldsymbol{\varepsilon}_{nG} - \boldsymbol{\varepsilon}_{nC}))dV = \delta L^e + \delta L^{in} \ , \tag{15}$$

a Lagrange multiplier $\delta\boldsymbol{\sigma}_{nM}$ is added to permit to assume a priori interlaminar continuous transverse stresses $\boldsymbol{\sigma}_{nM}$ (subscript M means modelled variables). RMVT permits therefore the fulfillment a priori of C_z^0-requirements for transverse shear/normal stresses.

A partial extension of RMVT to electro-mechanical problems is obtained simply adding the virtual internal electric work [Carrera and Brischetto (2007a)]:

$$\begin{aligned}\mathrm{R}MVT(\boldsymbol{u},\Phi,\boldsymbol{\sigma}_n) : \int_V (&\delta\boldsymbol{\varepsilon}_{pG}^T\boldsymbol{\sigma}_{pC} + \delta\boldsymbol{\varepsilon}_{nG}^T\boldsymbol{\sigma}_{nM} + \delta\boldsymbol{\sigma}_{nM}^T(\boldsymbol{\varepsilon}_{nG} - \boldsymbol{\varepsilon}_{nC}) - \\ &\delta\boldsymbol{\mathscr{E}}_{pG}^T\boldsymbol{\mathscr{D}}_{pC} - \delta\boldsymbol{\mathscr{E}}_{nG}^T\boldsymbol{\mathscr{D}}_{nC})dV = \delta L^e + \delta L^{in} \ ,\end{aligned} \tag{16}$$

displacement $\boldsymbol{u}$, electric potential Φ and transverse shear/normal stresses $\boldsymbol{\sigma}_n$ are primary variables. The related constitutive equations are obtained from Eqs.(8)-(11) by considering $\boldsymbol{\sigma}_p$, $\boldsymbol{\varepsilon}_n$, $\boldsymbol{\mathscr{D}}_p$ and $\boldsymbol{\mathscr{D}}_n$:

$$\boldsymbol{\sigma}_{pC} = \hat{\boldsymbol{C}}_{\sigma_p\varepsilon_p}\boldsymbol{\varepsilon}_{pG} + \hat{\boldsymbol{C}}_{\sigma_p\sigma_n}\boldsymbol{\sigma}_{nM} + \hat{\boldsymbol{C}}_{\sigma_p\mathscr{E}_p}\boldsymbol{\mathscr{E}}_{pG} + \hat{\boldsymbol{C}}_{\sigma_p\mathscr{E}_n}\boldsymbol{\mathscr{E}}_{nG} \ , \tag{17}$$

$$\boldsymbol{\varepsilon}_{nC} = \hat{\boldsymbol{C}}_{\varepsilon_n\varepsilon_p}\boldsymbol{\varepsilon}_{pG} + \hat{\boldsymbol{C}}_{\varepsilon_n\sigma_n}\boldsymbol{\sigma}_{nM} + \hat{\boldsymbol{C}}_{\varepsilon_n\mathscr{E}_p}\boldsymbol{\mathscr{E}}_{pG} + \hat{\boldsymbol{C}}_{\varepsilon_n\mathscr{E}_n}\boldsymbol{\mathscr{E}}_{nG} \ , \tag{18}$$

$$\boldsymbol{\mathscr{D}}_{pC} = \hat{\boldsymbol{C}}_{\mathscr{D}_p\varepsilon_p}\boldsymbol{\varepsilon}_{pG} + \hat{\boldsymbol{C}}_{\mathscr{D}_p\sigma_n}\boldsymbol{\sigma}_{nM} + \hat{\boldsymbol{C}}_{\mathscr{D}_p\mathscr{E}_p}\boldsymbol{\mathscr{E}}_{pG} + \hat{\boldsymbol{C}}_{\mathscr{D}_p\mathscr{E}_n}\boldsymbol{\mathscr{E}}_{nG} \ , \tag{19}$$

$$\mathscr{D}_{nC} = \hat{\boldsymbol{C}}_{\mathscr{D}_n\varepsilon_p}\boldsymbol{\varepsilon}_{pG} + \hat{\boldsymbol{C}}_{\mathscr{D}_n\sigma_n}\boldsymbol{\sigma}_{nM} + \hat{\boldsymbol{C}}_{\mathscr{D}_n\mathscr{E}_p}\mathscr{E}_{pG} + \hat{\boldsymbol{C}}_{\mathscr{D}_n\mathscr{E}_n}\mathscr{E}_{nG} \,, \tag{20}$$

where:

$$\begin{aligned}
&\hat{\boldsymbol{C}}_{\sigma_p\varepsilon_p} = \boldsymbol{C}_{pp} - \boldsymbol{C}_{pn}\boldsymbol{C}_{nn}^{-1}\boldsymbol{C}_{np} \,, \quad \hat{\boldsymbol{C}}_{\sigma_p\sigma_n} = \boldsymbol{C}_{pn}\boldsymbol{C}_{nn}^{-1} \,, \quad \hat{\boldsymbol{C}}_{\sigma_p\mathscr{E}_p} = \boldsymbol{C}_{pn}\boldsymbol{C}_{nn}^{-1}\boldsymbol{e}_{pn}^T - \boldsymbol{e}_{pp}^T \,, \\
&\hat{\boldsymbol{C}}_{\sigma_p\mathscr{E}_n} = \boldsymbol{C}_{pn}\boldsymbol{C}_{nn}^{-1}\boldsymbol{e}_{nn}^T - \boldsymbol{e}_{np}^T \,, \quad \hat{\boldsymbol{C}}_{\varepsilon_n\varepsilon_p} = -\boldsymbol{C}_{nn}^{-1}\boldsymbol{C}_{np} \,, \quad \hat{\boldsymbol{C}}_{\varepsilon_n\sigma_n} = \boldsymbol{C}_{nn}^{-1} \,, \\
&\hat{\boldsymbol{C}}_{\varepsilon_n\mathscr{E}_p} = \boldsymbol{C}_{nn}^{-1}\boldsymbol{e}_{np} \,, \quad \hat{\boldsymbol{C}}_{\varepsilon_n\mathscr{E}_n} = \boldsymbol{C}_{nn}^{-1}\boldsymbol{e}_{nn} \,, \quad \hat{\boldsymbol{C}}_{\mathscr{D}_p\varepsilon_p} = \boldsymbol{e}_{pp} - \boldsymbol{e}_{pn}\boldsymbol{C}_{nn}^{-1}\boldsymbol{C}_{np} \,, \\
&\hat{\boldsymbol{C}}_{\mathscr{D}_p\sigma_n} = \boldsymbol{e}_{pn}\boldsymbol{C}_{nn}^{-1} \,, \quad \hat{\boldsymbol{C}}_{\mathscr{D}_p\mathscr{E}_p} = \boldsymbol{e}_{pn}\boldsymbol{C}_{nn}^{-1}\boldsymbol{e}_{pn}^T + \boldsymbol{\varepsilon}_{pp} \,, \\
&\hat{\boldsymbol{C}}_{\mathscr{D}_p\mathscr{E}_n} = \boldsymbol{e}_{pn}\boldsymbol{C}_{nn}^{-1}\boldsymbol{e}_{nn}^T + \boldsymbol{\varepsilon}_{pn} \,, \quad \hat{\boldsymbol{C}}_{\mathscr{D}_n\varepsilon_p} = \boldsymbol{e}_{np} - \boldsymbol{e}_{nn}\boldsymbol{C}_{nn}^{-1}\boldsymbol{C}_{np} \,, \quad \hat{\boldsymbol{C}}_{\mathscr{D}_n\sigma_n} = \boldsymbol{e}_{nn}\boldsymbol{C}_{nn}^{-1} \,, \\
&\hat{\boldsymbol{C}}_{\mathscr{D}_n\mathscr{E}_p} = \boldsymbol{e}_{nn}\boldsymbol{C}_{nn}^{-1}\boldsymbol{e}_{pn}^T + \boldsymbol{\varepsilon}_{np} \,, \quad \hat{\boldsymbol{C}}_{\mathscr{D}_n\mathscr{E}_n} = \boldsymbol{e}_{nn}\boldsymbol{C}_{nn}^{-1}\boldsymbol{e}_{nn}^T + \boldsymbol{\varepsilon}_{nn} \,.
\end{aligned} \tag{21}$$

RMVT($\boldsymbol{u}$,$\boldsymbol{\sigma}_n$) for the pure mechanical case can be considered as a particular case of the RMVT($\boldsymbol{u}$,Φ,$\boldsymbol{\sigma}_n$). That is Eqs.(17)-(20) degenerate for the pure mechanical case as:

$$\boldsymbol{\sigma}_{pC} = \hat{\boldsymbol{C}}_{\sigma_p\varepsilon_p}\boldsymbol{\varepsilon}_{pG} + \hat{\boldsymbol{C}}_{\sigma_p\sigma_n}\boldsymbol{\sigma}_{nM} \,, \tag{22}$$

$$\boldsymbol{\varepsilon}_{nC} = \hat{\boldsymbol{C}}_{\varepsilon_n\varepsilon_p}\boldsymbol{\varepsilon}_{pG} + \hat{\boldsymbol{C}}_{\varepsilon_n\sigma_n}\boldsymbol{\sigma}_{nM} \,. \tag{23}$$

The RMVT($\boldsymbol{u}$,Φ,$\mathscr{D}_n$) case

The second extension of RMVT to electro-mechanical case, implemented in this work, considers the transverse normal electric displacement $\mathscr{D}_n$ as primary variable, for details readers can refer to Carrera and Nali (2009):

$$\begin{aligned}
\mathrm{R}MVT(\boldsymbol{u},\Phi,\mathscr{D}_n) : \int_V (&\delta\boldsymbol{\varepsilon}_{pG}^T\boldsymbol{\sigma}_{pC} + \delta\boldsymbol{\varepsilon}_{nG}^T\boldsymbol{\sigma}_{nC} - \delta\mathscr{E}_{pG}^T\mathscr{D}_{pC} - \delta\mathscr{E}_{nG}^T\mathscr{D}_{nM} - \\
&\delta\mathscr{D}_{nM}^T(\mathscr{E}_{nG} - \mathscr{E}_{nC}))dV = \delta L^e + \delta L^{in} \,,
\end{aligned} \tag{24}$$

the added Lagrange multiplier $\delta\mathscr{D}_{nM}$ permits to assume an independent interlaminar continuous transverse normal electric displacement $\mathscr{D}_n$.

The constitutive equations are obtained from Eqs.(8)-(11) by expressing $\boldsymbol{\sigma}_p$, $\boldsymbol{\sigma}_n$, $\mathscr{D}_p$ and $\mathscr{E}_n$:

$$\boldsymbol{\sigma}_{pC} = \bar{\boldsymbol{C}}_{\sigma_p\varepsilon_p}\boldsymbol{\varepsilon}_{pG} + \bar{\boldsymbol{C}}_{\sigma_p\varepsilon_n}\boldsymbol{\varepsilon}_{nG} + \bar{\boldsymbol{C}}_{\sigma_p\mathscr{E}_p}\mathscr{E}_{pG} + \bar{\boldsymbol{C}}_{\sigma_p\mathscr{D}_n}\mathscr{D}_{nM} \,, \tag{25}$$

$$\boldsymbol{\sigma}_{nC} = \bar{\boldsymbol{C}}_{\sigma_n\varepsilon_p}\boldsymbol{\varepsilon}_{pG} + \bar{\boldsymbol{C}}_{\sigma_n\varepsilon_n}\boldsymbol{\varepsilon}_{nG} + \bar{\boldsymbol{C}}_{\sigma_n\mathscr{E}_p}\mathscr{E}_{pG} + \bar{\boldsymbol{C}}_{\sigma_n\mathscr{D}_n}\mathscr{D}_{nM} \,, \tag{26}$$

$$\mathscr{D}_{pC} = \bar{\boldsymbol{C}}_{\mathscr{D}_p\varepsilon_p}\boldsymbol{\varepsilon}_{pG} + \bar{\boldsymbol{C}}_{\mathscr{D}_p\varepsilon_n}\boldsymbol{\varepsilon}_{nG} + \bar{\boldsymbol{C}}_{\mathscr{D}_p\mathscr{E}_p}\mathscr{E}_{pG} + \bar{\boldsymbol{C}}_{\mathscr{D}_p\mathscr{D}_n}\mathscr{D}_{nM} \,, \tag{27}$$

$$\mathscr{E}_{nC} = \bar{\boldsymbol{C}}_{\mathscr{E}_n\varepsilon_p}\boldsymbol{\varepsilon}_{pG} + \bar{\boldsymbol{C}}_{\mathscr{E}_n\varepsilon_n}\boldsymbol{\varepsilon}_{nG} + \bar{\boldsymbol{C}}_{\mathscr{E}_n\mathscr{E}_p}\mathscr{E}_{pG} + \bar{\boldsymbol{C}}_{\mathscr{E}_n\mathscr{D}_n}\mathscr{D}_{nM} \,, \tag{28}$$

where:

$$\bar{\boldsymbol{C}}_{\sigma_p\varepsilon_p} = \boldsymbol{C}_{pp} + \boldsymbol{e}_{np}^T\boldsymbol{\varepsilon}_{nn}^{-1}\boldsymbol{e}_{np} \,, \quad \bar{\boldsymbol{C}}_{\sigma_p\varepsilon_n} = \boldsymbol{C}_{pn} + \boldsymbol{e}_{np}^T\boldsymbol{\varepsilon}_{nn}^{-1}\boldsymbol{e}_{nn} \,, \quad \bar{\boldsymbol{C}}_{\sigma_p\mathscr{E}_p} = \boldsymbol{e}_{np}^T\boldsymbol{\varepsilon}_{nn}^{-1}\boldsymbol{\varepsilon}_{np} - \boldsymbol{e}_{pp}^T \,,$$

$$\begin{aligned}
&\bar{\boldsymbol{C}}_{\sigma_p\mathscr{D}_n} = -\boldsymbol{e}_{np}^T\boldsymbol{\varepsilon}_{nn}^{-1}\ , \quad \bar{\boldsymbol{C}}_{\sigma_n\varepsilon_p} = \boldsymbol{C}_{np} + \boldsymbol{e}_{nn}^T\boldsymbol{\varepsilon}_{nn}^{-1}\boldsymbol{e}_{np}\ , \quad \bar{\boldsymbol{C}}_{\sigma_n\varepsilon_n} = \boldsymbol{C}_{nn} + \boldsymbol{e}_{nn}^T\boldsymbol{\varepsilon}_{nn}^{-1}\boldsymbol{e}_{nn}\ ,\\
&\bar{\boldsymbol{C}}_{\sigma_n\mathscr{E}_p} = \boldsymbol{e}_{nn}^T\boldsymbol{\varepsilon}_{nn}^{-1}\boldsymbol{\varepsilon}_{np} - \boldsymbol{e}_{pn}^T\ , \quad \bar{\boldsymbol{C}}_{\sigma_n\mathscr{D}_n} = -\boldsymbol{e}_{nn}^T\boldsymbol{\varepsilon}_{nn}^{-1}\ , \quad \bar{\boldsymbol{C}}_{\mathscr{D}_p\varepsilon_p} = \boldsymbol{e}_{pp} - \boldsymbol{\varepsilon}_{pn}\boldsymbol{\varepsilon}_{nn}^{-1}\boldsymbol{e}_{np}\ ,\\
&\bar{\boldsymbol{C}}_{\mathscr{D}_p\varepsilon_n} = \boldsymbol{e}_{pn} - \boldsymbol{\varepsilon}_{pn}\boldsymbol{\varepsilon}_{nn}^{-1}\boldsymbol{e}_{nn}\ , \quad \bar{\boldsymbol{C}}_{\mathscr{D}_p\mathscr{E}_p} = \boldsymbol{\varepsilon}_{pp} - \boldsymbol{\varepsilon}_{pn}\boldsymbol{\varepsilon}_{nn}^{-1}\boldsymbol{\varepsilon}_{np}\ , \quad \bar{\boldsymbol{C}}_{\mathscr{D}_p\mathscr{D}_n} = \boldsymbol{\varepsilon}_{pn}\boldsymbol{\varepsilon}_{nn}^{-1}\ ,\\
&\bar{\boldsymbol{C}}_{\mathscr{E}_n\varepsilon_p} = -\boldsymbol{\varepsilon}_{nn}^{-1}\boldsymbol{e}_{np}\ , \quad \bar{\boldsymbol{C}}_{\mathscr{E}_n\varepsilon_n} = -\boldsymbol{\varepsilon}_{nn}^{-1}\boldsymbol{e}_{nn}\ , \quad \bar{\boldsymbol{C}}_{\mathscr{E}_n\mathscr{E}_p} = -\boldsymbol{\varepsilon}_{nn}^{-1}\boldsymbol{\varepsilon}_{np} \quad \bar{\boldsymbol{C}}_{\mathscr{E}_n\mathscr{D}_n} = \boldsymbol{\varepsilon}_{nn}^{-1}\ .
\end{aligned} \tag{29}$$

To be noticed that in this RMVT case, the constitutive equations for pure mechanical case cannot be derived as a particular case of Eqs.(25)-(28) because the modelled variables are different: transverse stresses in Eq.(16) and transverse normal electric displacement in Eq.(24), in fact, two different Lagrange multipliers are considered.

The RMVT($\boldsymbol{u},\Phi,\boldsymbol{\sigma}_n,\mathscr{D}_n$) case

The third, full extension case of RMVT to electro-mechanical problems considers both transverse shear/normal stresses $\boldsymbol{\sigma}_n$ and transverse normal electrical displacement $\mathscr{D}_n$ as primary variables:

$$\begin{aligned}
RMVT(\boldsymbol{u},\Phi,\boldsymbol{\sigma}_n,\mathscr{D}_n) : \int_V (&\delta\boldsymbol{\varepsilon}_{pG}^T\boldsymbol{\sigma}_{pC} + \delta\boldsymbol{\varepsilon}_{nG}^T\boldsymbol{\sigma}_{nM} - \delta\boldsymbol{\mathscr{E}}_{pG}^T\mathscr{D}_{pC} - \delta\boldsymbol{\mathscr{E}}_{nG}^T\mathscr{D}_{nM} +\\
&\delta\boldsymbol{\sigma}_{nM}^T(\boldsymbol{\varepsilon}_{nG} - \boldsymbol{\varepsilon}_{nC}) - \delta\mathscr{D}_{nM}^T(\boldsymbol{\mathscr{E}}_{nG} - \boldsymbol{\mathscr{E}}_{nC}))dV = \delta L^e + \delta L^{in}\ .
\end{aligned} \tag{30}$$

The full extension of RMVT permits the complete fulfillment of C_z^0-requirements for both transverse shear/normal stresses and transverse normal electric displacement.

The constitutive equations are obtained from Eqs.(8)-(11) by expressing $\boldsymbol{\sigma}_p$, $\boldsymbol{\varepsilon}_n$, $\mathscr{D}_p$ and $\boldsymbol{\mathscr{E}}_n$:

$$\boldsymbol{\sigma}_{pC} = \tilde{\boldsymbol{C}}_{\sigma_p\varepsilon_p}\boldsymbol{\varepsilon}_{pG} + \tilde{\boldsymbol{C}}_{\sigma_p\sigma_n}\boldsymbol{\sigma}_{nM} + \tilde{\boldsymbol{C}}_{\sigma_p\mathscr{E}_p}\boldsymbol{\mathscr{E}}_{pG} + \tilde{\boldsymbol{C}}_{\sigma_p\mathscr{D}_n}\mathscr{D}_{nM}\ , \tag{31}$$

$$\boldsymbol{\varepsilon}_{nC} = \tilde{\boldsymbol{C}}_{\varepsilon_n\varepsilon_p}\boldsymbol{\varepsilon}_{pG} + \tilde{\boldsymbol{C}}_{\varepsilon_n\sigma_n}\boldsymbol{\sigma}_{nM} + \tilde{\boldsymbol{C}}_{\varepsilon_n\mathscr{E}_p}\boldsymbol{\mathscr{E}}_{pG} + \tilde{\boldsymbol{C}}_{\varepsilon_n\mathscr{D}_n}\mathscr{D}_{nM}\ , \tag{32}$$

$$\mathscr{D}_{pC} = \tilde{\boldsymbol{C}}_{\mathscr{D}_p\varepsilon_p}\boldsymbol{\varepsilon}_{pG} + \tilde{\boldsymbol{C}}_{\mathscr{D}_p\sigma_n}\boldsymbol{\sigma}_{nM} + \tilde{\boldsymbol{C}}_{\mathscr{D}_p\mathscr{E}_p}\boldsymbol{\mathscr{E}}_{pG} + \tilde{\boldsymbol{C}}_{\mathscr{D}_p\mathscr{D}_n}\mathscr{D}_{nM}\ , \tag{33}$$

$$\boldsymbol{\mathscr{E}}_{nC} = \tilde{\boldsymbol{C}}_{\mathscr{E}_n\varepsilon_p}\boldsymbol{\varepsilon}_{pG} + \tilde{\boldsymbol{C}}_{\mathscr{E}_n\sigma_n}\boldsymbol{\sigma}_{nM} + \tilde{\boldsymbol{C}}_{\mathscr{E}_n\mathscr{E}_p}\boldsymbol{\mathscr{E}}_{pG} + \tilde{\boldsymbol{C}}_{\mathscr{E}_n\mathscr{D}_n}\mathscr{D}_{nM}\ . \tag{34}$$

The explicit form of the matrices in Eqs.(31)-(34) is:

$$\begin{aligned}
\tilde{\boldsymbol{C}}_{\sigma_p\varepsilon_p} &= \boldsymbol{C}_{pp} - \boldsymbol{C}_{pn}\boldsymbol{C}_{nn}^{-1}\boldsymbol{C}_{np} - (\boldsymbol{C}_{pn}\boldsymbol{C}_{nn}^{-1}\boldsymbol{e}_{nn}^T - \boldsymbol{e}_{np}^T)(\boldsymbol{e}_{nn}\boldsymbol{C}_{nn}^{-1}\boldsymbol{e}_{nn}^T + \boldsymbol{\varepsilon}_{nn})^{-1}\\
&\quad (\boldsymbol{e}_{np} - \boldsymbol{e}_{nn}\boldsymbol{C}_{nn}^{-1}\boldsymbol{C}_{np})\ ,\\
\tilde{\boldsymbol{C}}_{\sigma_p\sigma_n} &= \boldsymbol{C}_{pn}\boldsymbol{C}_{nn}^{-1} - (\boldsymbol{C}_{pn}\boldsymbol{C}_{nn}^{-1}\boldsymbol{e}_{nn}^T - \boldsymbol{e}_{np}^T)(\boldsymbol{e}_{nn}\boldsymbol{C}_{nn}^{-1}\boldsymbol{e}_{nn}^T + \boldsymbol{\varepsilon}_{nn})^{-1}(\boldsymbol{e}_{nn}\boldsymbol{C}_{nn}^{-1})\ ,\\
\tilde{\boldsymbol{C}}_{\sigma_p\mathscr{E}_p} &= \boldsymbol{C}_{pn}\boldsymbol{C}_{nn}^{-1}\boldsymbol{e}_{pn}^T - \boldsymbol{e}_{pp}^T - (\boldsymbol{C}_{pn}\boldsymbol{C}_{nn}^{-1}\boldsymbol{e}_{nn}^T - \boldsymbol{e}_{np}^T)(\boldsymbol{e}_{nn}\boldsymbol{C}_{nn}^{-1}\boldsymbol{e}_{nn}^T + \boldsymbol{\varepsilon}_{nn})^{-1}
\end{aligned}$$

$$
\begin{aligned}
&(\boldsymbol{e}_{nn}\boldsymbol{C}_{nn}^{-1}\boldsymbol{e}_{pn}^{T}+\boldsymbol{\varepsilon}_{np})\ ,\\
\tilde{\boldsymbol{C}}_{\sigma_p\mathscr{D}_n} &= (\boldsymbol{C}_{pn}\boldsymbol{C}_{nn}^{-1}\boldsymbol{e}_{nn}^{T}-\boldsymbol{e}_{pn}^{T})(\boldsymbol{e}_{nn}\boldsymbol{C}_{nn}^{-1}\boldsymbol{e}_{nn}^{T}+\boldsymbol{\varepsilon}_{nn})^{-1}\ ,\\
\tilde{\boldsymbol{C}}_{\varepsilon_n\varepsilon_p} &= -\boldsymbol{C}_{nn}^{-1}\boldsymbol{C}_{np}-\boldsymbol{C}_{nn}^{-1}\boldsymbol{e}_{nn}^{T}(\boldsymbol{e}_{nn}\boldsymbol{C}_{nn}^{-1}\boldsymbol{e}_{nn}^{T}+\boldsymbol{\varepsilon}_{nn})^{-1}(\boldsymbol{e}_{nn}\boldsymbol{C}_{nn}^{-1}\boldsymbol{C}_{np}-\boldsymbol{e}_{np})\ ,\\
\tilde{\boldsymbol{C}}_{\varepsilon_n\sigma_n} &= \boldsymbol{C}_{nn}^{-1}-\boldsymbol{C}_{nn}^{-1}\boldsymbol{e}_{nn}^{T}(\boldsymbol{e}_{nn}\boldsymbol{C}_{nn}^{-1}\boldsymbol{e}_{nn}^{T}+\boldsymbol{\varepsilon}_{nn})^{-1}\boldsymbol{e}_{nn}\boldsymbol{C}_{nn}^{-1}\ ,\\
\tilde{\boldsymbol{C}}_{\varepsilon_n\mathscr{E}_p} &= \boldsymbol{C}_{nn}^{-1}\boldsymbol{e}_{pn}^{T}-\boldsymbol{C}_{nn}^{-1}\boldsymbol{e}_{nn}^{T}(\boldsymbol{e}_{nn}\boldsymbol{C}_{nn}^{-1}\boldsymbol{e}_{nn}^{T}+\boldsymbol{\varepsilon}_{nn})^{-1}(\boldsymbol{e}_{nn}\boldsymbol{C}_{nn}^{-1}\boldsymbol{e}_{np}+\boldsymbol{\varepsilon}_{np})\ ,\\
\tilde{\boldsymbol{C}}_{\varepsilon_n\mathscr{D}_n} &= \boldsymbol{C}_{nn}^{-1}\boldsymbol{e}_{nn}^{T}(\boldsymbol{e}_{nn}\boldsymbol{C}_{nn}^{-1}\boldsymbol{e}_{nn}^{T}+\boldsymbol{\varepsilon}_{nn})^{-1}\ ,\\
\tilde{\boldsymbol{C}}_{\mathscr{D}_p\varepsilon_p} &= \boldsymbol{e}_{pp}-\boldsymbol{e}_{pn}\boldsymbol{C}_{nn}^{-1}\boldsymbol{C}_{np}-\boldsymbol{e}_{pn}\boldsymbol{C}_{nn}^{-1}\boldsymbol{e}_{nn}^{T}(\boldsymbol{e}_{nn}\boldsymbol{C}_{nn}^{-1}\boldsymbol{e}_{nn}^{T}+\boldsymbol{\varepsilon}_{nn})^{-1}(\boldsymbol{e}_{np}-\boldsymbol{e}_{nn}\boldsymbol{C}_{nn}^{-1}\boldsymbol{C}_{np})\\
&\quad -\boldsymbol{\varepsilon}_{pn}(\boldsymbol{e}_{nn}\boldsymbol{C}_{nn}^{-1}\boldsymbol{e}_{nn}^{T}+\boldsymbol{\varepsilon}_{nn})^{-1}(\boldsymbol{e}_{np}-\boldsymbol{e}_{nn}\boldsymbol{C}_{nn}^{-1}\boldsymbol{C}_{np})\ , \qquad (35)\\
\tilde{\boldsymbol{C}}_{\mathscr{D}_p\sigma_n} &= \boldsymbol{e}_{pn}\boldsymbol{C}_{nn}^{-1}-\boldsymbol{e}_{pn}\boldsymbol{C}_{nn}^{-1}\boldsymbol{e}_{nn}^{T}(\boldsymbol{e}_{nn}\boldsymbol{C}_{nn}^{-1}\boldsymbol{e}_{nn}^{T}+\boldsymbol{\varepsilon}_{nn})^{-1}\boldsymbol{e}_{nn}\boldsymbol{C}_{nn}^{-1}\\
&\quad -\boldsymbol{\varepsilon}_{pn}(\boldsymbol{e}_{nn}\boldsymbol{C}_{nn}^{-1}\boldsymbol{e}_{nn}^{T}+\boldsymbol{\varepsilon}_{nn})^{-1}\boldsymbol{e}_{nn}\boldsymbol{C}_{nn}^{-1}\ ,\\
\tilde{\boldsymbol{C}}_{\mathscr{D}_p\mathscr{E}_p} &= \boldsymbol{\varepsilon}_{pp}+\boldsymbol{e}_{pn}\boldsymbol{C}_{nn}^{-1}\boldsymbol{e}_{pn}^{T}-\boldsymbol{e}_{pn}\boldsymbol{C}_{nn}^{-1}\boldsymbol{e}_{nn}^{T}(\boldsymbol{e}_{nn}\boldsymbol{C}_{nn}^{-1}\boldsymbol{e}_{nn}^{T}+\boldsymbol{\varepsilon}_{nn})^{-1}(\boldsymbol{e}_{nn}\boldsymbol{C}_{nn}^{-1}\boldsymbol{e}_{np}+\boldsymbol{\varepsilon}_{np})\\
&\quad -\boldsymbol{\varepsilon}_{np}(\boldsymbol{e}_{nn}\boldsymbol{C}_{nn}^{-1}\boldsymbol{e}_{nn}^{T}+\boldsymbol{\varepsilon}_{nn})^{-1}(\boldsymbol{e}_{nn}\boldsymbol{C}_{nn}^{-1}\boldsymbol{e}_{pn}^{T}+\boldsymbol{\varepsilon}_{np})\ ,\\
\tilde{\boldsymbol{C}}_{\mathscr{D}_p\mathscr{D}_n} &= \boldsymbol{e}_{pn}\boldsymbol{C}_{nn}^{-1}\boldsymbol{e}_{nn}^{T}(\boldsymbol{e}_{nn}\boldsymbol{C}_{nn}^{-1}\boldsymbol{e}_{nn}^{T}+\boldsymbol{\varepsilon}_{nn})^{-1}+\boldsymbol{\varepsilon}_{pn}(\boldsymbol{e}_{nn}\boldsymbol{C}_{nn}^{-1}\boldsymbol{e}_{nn}^{T}+\boldsymbol{\varepsilon}_{nn})\ ,\\
\tilde{\boldsymbol{C}}_{\mathscr{E}_n\varepsilon_p} &= -(\boldsymbol{e}_{nn}\boldsymbol{C}_{nn}^{-1}\boldsymbol{e}_{nn}^{T}+\boldsymbol{\varepsilon}_{nn})^{-1}(\boldsymbol{e}_{pn}^{T}-\boldsymbol{e}_{nn}\boldsymbol{C}_{nn}^{-1}\boldsymbol{C}_{np})\ ,\\
\tilde{\boldsymbol{C}}_{\mathscr{E}_n\sigma_n} &= -(\boldsymbol{e}_{nn}\boldsymbol{C}_{nn}^{-1}\boldsymbol{e}_{nn}^{T}+\boldsymbol{\varepsilon}_{nn})^{-1}\boldsymbol{e}_{nn}\boldsymbol{C}_{nn}^{-1}\ ,\\
\tilde{\boldsymbol{C}}_{\mathscr{E}_n\mathscr{E}_p} &= -(\boldsymbol{e}_{nn}\boldsymbol{C}_{nn}^{-1}\boldsymbol{e}_{nn}^{T}+\boldsymbol{\varepsilon}_{nn})^{-1}(\boldsymbol{e}_{nn}\boldsymbol{C}_{nn}^{-1}\boldsymbol{e}_{pn}^{T}+\boldsymbol{\varepsilon}_{np})\ ,\\
\tilde{\boldsymbol{C}}_{\mathscr{E}_n\mathscr{D}_n} &= (\boldsymbol{e}_{nn}\boldsymbol{C}_{nn}^{-1}\boldsymbol{e}_{nn}^{T}+\boldsymbol{\varepsilon}_{nn})^{-1}\ .
\end{aligned}
$$

3 Geometrical relations

Shells are bi-dimensional structures in which one dimension (in general the thickness in z direction) is negligible with respect to the other two in-plane dimensions. Geometry and the reference system are indicated in Figure 2. The square of an infinitesimal linear segment in the layer, the associated infinitesimal area and volume are given by:

$$ds_k^2 = {H_\alpha^k}^2\, d\alpha_k^2 \ + \ {H_\beta^k}^2\, d\beta_k^2 + {H_z^k}^2\, dz_k^2\ , \qquad (36)$$

$$d\Omega_k = H_\alpha^k H_\beta^k\, d\alpha_k\, d\beta_k\ , \qquad (37)$$

$$dV_k = H_\alpha^k\, H_\beta^k\, H_z^k\, d\alpha_k\, d\beta_k\, dz_k\ , \qquad (38)$$

where the metric coefficients are:

$$H_\alpha^k = A^k(1+z_k/R_\alpha^k),\quad H_\beta^k = B^k(1+z_k/R_\beta^k),\quad H_z^k = 1\ . \qquad (39)$$

k denotes the k-layer of the multilayered shell; R_α^k and R_β^k are the principal radii of curvature along the coordinates α_k and β_k, respectively. A^k and B^k are the coeffi-

cients of the first fundamental form of Ω_k (Γ_k is the Ω_k boundary). In this paper, the attention has been restricted to shells with constant radii of curvature (cylindrical, open spherical panels, toroidal geometries) for which $A^k = B^k = 1$. Details for shells are reported in Leissa (1973). Eqs.(36)-(38) demonstrate as a LW representation of the curvature terms is employed for both ESL and LW kinematics models.

Geometrical relations permit to express the in-plane $\boldsymbol{\varepsilon}_p$ and out-plane $\boldsymbol{\varepsilon}_n$ strains in terms of displacement $\boldsymbol{u}$, and the in-plane components $\boldsymbol{\mathscr{E}}_p$ and out-plane components $\boldsymbol{\mathscr{E}}_n$ of electric field in terms of the electric potential Φ. The following relations hold:

$$\begin{aligned}
&\boldsymbol{\varepsilon}^k_{pG} = [\varepsilon^k_{\alpha\alpha}, \varepsilon^k_{\beta\beta}, \gamma^k_{\alpha\beta}]^T = (\boldsymbol{D}^k_p + \boldsymbol{A}^k_p)\, \boldsymbol{u}^k, \\
&\boldsymbol{\varepsilon}^k_{nG} = [\gamma^k_{\alpha z}, \gamma^k_{\beta z}, \varepsilon^k_{zz}]^T = (\boldsymbol{D}^k_{n\Omega} + \boldsymbol{D}^k_{nz} - \boldsymbol{A}^k_n)\, \boldsymbol{u}^k\,, \\
&\boldsymbol{\mathscr{E}}^k_{pG} = [\mathscr{E}^k_\alpha, \mathscr{E}^k_\beta]^T = -\boldsymbol{D}^k_{e\Omega}\, \Phi^k\,,\ \boldsymbol{\mathscr{E}}^k_{nG} = [\mathscr{E}^k_z]^T = -\boldsymbol{D}^k_{en}\, \Phi^k\,.
\end{aligned} \tag{40}$$

The explicit form of the introduced arrays follows:

$$\boldsymbol{D}^k_p = \begin{bmatrix} \frac{\partial_\alpha}{H^k_\alpha} & 0 & 0 \\ 0 & \frac{\partial_\beta}{H^k_\beta} & 0 \\ \frac{\partial_\beta}{H^k_\beta} & \frac{\partial_\alpha}{H^k_\alpha} & 0 \end{bmatrix}, \quad \boldsymbol{D}^k_{n\Omega} = \begin{bmatrix} 0 & 0 & \frac{\partial_\alpha}{H^k_\alpha} \\ 0 & 0 & \frac{\partial_\beta}{H^k_\beta} \\ 0 & 0 & 0 \end{bmatrix}, \quad \boldsymbol{D}^k_{nz} = \begin{bmatrix} \partial_z & 0 & 0 \\ 0 & \partial_z & 0 \\ 0 & 0 & \partial_z \end{bmatrix}, \tag{41}$$

$$\boldsymbol{D}^k_{e\Omega} = \begin{bmatrix} \frac{\partial_\alpha}{H^k_\alpha} \\ \frac{\partial_\beta}{H^k_\beta} \end{bmatrix}, \quad \boldsymbol{D}^k_{en} = \begin{bmatrix} \partial_z \end{bmatrix}, \quad \boldsymbol{A}^k_p = \begin{bmatrix} 0 & 0 & \frac{1}{H^k_\alpha R^k_\alpha} \\ 0 & 0 & \frac{1}{H^k_\beta R^k_\beta} \\ 0 & 0 & 0 \end{bmatrix}, \quad \boldsymbol{A}^k_n = \begin{bmatrix} \frac{1}{H^k_\alpha R^k_\alpha} & 0 & 0 \\ 0 & \frac{1}{H^k_\beta R^k_\beta} & 0 \\ 0 & 0 & 0 \end{bmatrix}.$$

Geometrical relations for shells degenerate in those for plates when the radii of curvature R^k_α and R^k_β are infinite, and metric coefficients H^k_α and H^k_β are equal to one (see Eq.(44)).

In the case of plate geometry the square of an infinitesimal linear segment, the associated infinitesimal area and volume of the generic k-layer are given by:

$$ds^2_k = dx^2_k + dy^2_k + dz^2_k\,, \quad d\Omega_k = dx_k\, dy_k\,, \quad dV_k = dx_k\, dy_k\, dz_k\,, \tag{42}$$

(x,y,z) is the orthogonal cartesian reference system and k is the indicative of the layer, the following relations hold:

$$\begin{aligned}
&\boldsymbol{\varepsilon}^k_{pG} = [\varepsilon^k_{xx}, \varepsilon^k_{yy}, \gamma^k_{xy}]^T = \boldsymbol{D}_p\, \boldsymbol{u}^k\,,\ \boldsymbol{\varepsilon}^k_{nG} = [\gamma^k_{xz}, \gamma^k_{yz}, \varepsilon^k_{zz}]^T = (\boldsymbol{D}_{n\Omega} + \boldsymbol{D}_{nz})\, \boldsymbol{u}^k \\
&\boldsymbol{\mathscr{E}}^k_{pG} = [\mathscr{E}^k_x, \mathscr{E}^k_y]^T = -\boldsymbol{D}_{e\Omega}\, \Phi^k\,,\ \boldsymbol{\mathscr{E}}^k_{nG} = [\mathscr{E}^k_z]^T = -\boldsymbol{D}_{en}\, \Phi^k\,.
\end{aligned} \tag{43}$$

The explicit form of the introduced arrays follows:

$$\boldsymbol{D}_p = \begin{bmatrix} \partial_x & 0 & 0 \\ 0 & \partial_y & 0 \\ \partial_y & \partial_x & 0 \end{bmatrix} , \quad \boldsymbol{D}_{n\Omega} = \begin{bmatrix} 0 & 0 & \partial_x \\ 0 & 0 & \partial_y \\ 0 & 0 & 0 \end{bmatrix} , \quad \boldsymbol{D}_{nz} = \begin{bmatrix} \partial_z & 0 & 0 \\ 0 & \partial_z & 0 \\ 0 & 0 & \partial_z \end{bmatrix} , \tag{44}$$

$$\boldsymbol{D}_{e\Omega} = \begin{bmatrix} \partial_x \\ \partial_y \end{bmatrix} , \quad \boldsymbol{D}_{en} = \begin{bmatrix} \partial_z \end{bmatrix} .$$

4 Variable kinematics plate/shell modelings via Carrera's Unified Formulation

Carrera's Unified Formulation (CUF) is a technique that permits to handle in a unified manner a large variety of bi-dimensional plate/shell models. CUF [Carrera (1995); Carrera (2002)] permits to express the considered three-dimensional 3D variables in terms of a set of thickness functions depending only on the thickness coordinate z and two-dimensional variables depending on the in-plane coordinates (x,y). According to CUF, the governing equations are written in terms of a few fundamental nuclei which do not formally depend on: - the order of expansion N used in the z-direction; - variables description (Layer Wise (LW) or Equivalent Single Layer (ESL)). By expanding these fundamental nuclei in according to opportune indexes, the governing equations of the structure can be obtained. For a generic 3D variable $\boldsymbol{a}$, the following expression is written:

$$\boldsymbol{a}(x,y,z) = F_\tau(z)\boldsymbol{a}_\tau(x,y) , \tag{45}$$

the same is done for its variation:

$$\delta\boldsymbol{a}(x,y,z) = F_s(z)\delta\boldsymbol{a}_s(x,y) . \tag{46}$$

The order of expansion ranges from first to fourth order, and depending on the used thickness functions, a model can be: ESL when the variable is assumed for the whole multilayer (see Figure 3) and LW when the variable is considered for each layer (see Figure 4). In case of an ESL theory, zig-zag forms of displacement variables can be accounted (see Figure 5) by means of Murakami function [Murakami (1986); Carrera (2004)]. The expansion used in Eqs.(45) and (46) are also employed for shell geometry when a curvilinear reference system (α,β,z) is assumed.

4.1 Equivalent Single Layer theories

In case of electro-mechanical problem the assumed variables are the displacements $\boldsymbol{u}$ and the electric potential Φ. If Reissner's Mixed Variational Theorem (RMVT) is

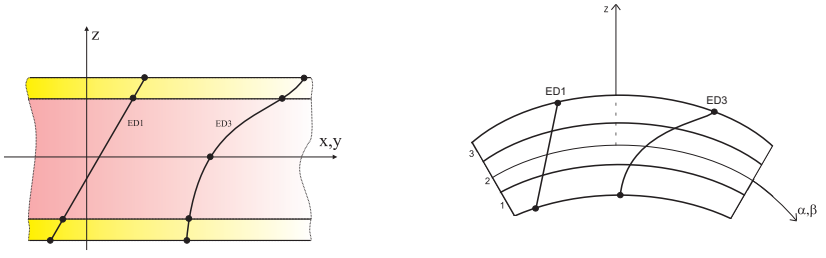

a) *b)*

Figure 3: Generic variable through the thickness direction z in Equivalent Single Layer form for plate (a) and shell (b) geometries.

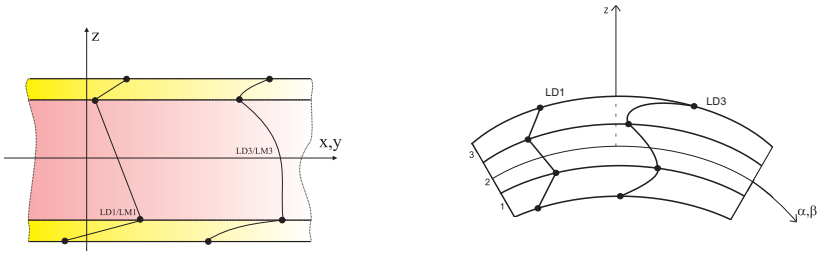

a) *b)*

Figure 4: Generic variable through the thickness direction z in Layer Wise form for plate (a) and shell (b) geometries.

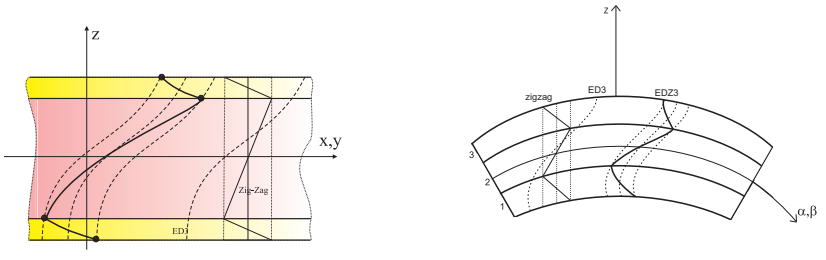

a) *b)*

Figure 5: Addition of Murakami zig-zag function to ESL models for plate (a) and shell (b) geometries.

used, other variables such as transverse shear/normal stresses $\boldsymbol{\sigma}_n$ and/or transverse normal electric displacement $\mathscr{D}_n$ can be also assumed. In this work only the displacement $\boldsymbol{u}$ can be modelled as ESL or LW, the other variables are always assumed in LW form. So a model is said ESL or LW depending on the choice made for the displacement variables.

The expansion in the thickness direction z for ESL theories coincides to Taylor expansion:

$$\boldsymbol{u} = F_0\,\boldsymbol{u}_0 + F_1\,\boldsymbol{u}_1 + \ldots + F_N\,\boldsymbol{u}_N = F_\tau\,\boldsymbol{u}_\tau \;\; with \;\; \tau = 0,1,\ldots,N\,, \tag{47}$$

N is the order of expansion and the thickness functions are:

$$F_0 = z^0 = 1,\;\; F_1 = z^1 = z,\;\; \ldots,\;\; F_N = z^N, \tag{48}$$

the order of expansion N ranges from 1 to 4, that is from linear to fourth order.

Typical zig-zag form of displacements can be recovered by means of Murakami zigzag function (MZZF) [Murakami (1986)] as described in Figure 5. This function is $M(z) = (-1)^k \zeta^k$ where $\zeta_k = 2z_k/h_k$ is a non-dimensional layer coordinate (z_k is the physical coordinate of the k-layer whose thickness is h_k) which goes from -1 to $+1$:

$$\boldsymbol{u} = F_0\,\boldsymbol{u}_0 + F_1\,\boldsymbol{u}_1 + \ldots + F_N\,\boldsymbol{u}_N + (-1)^k\zeta_k\boldsymbol{u}_Z = F_\tau\,\boldsymbol{u}_\tau + (-1)^k\zeta_k\boldsymbol{u}_Z \tag{49}$$

with $\tau = 0,1,\ldots,N$.

The exponent k changes the sign of the zig-zag term in each layer. Such an artifice permits one to reproduce the discontinuity of the first derivative of the displacement variables in the z-direction, see Figure 5.

4.2 Layer Wise theories

In the case of Layer Wise (LW) models, the considered variables are modelled in each layer k. For electro-mechanical problems the expansions in z direction are:

$$\begin{aligned}(\boldsymbol{u}^k, \boldsymbol{\sigma}^k_{nM}, \Phi^k, \mathscr{D}^k_{nM}) &= F_t\;(\boldsymbol{u}^{\boldsymbol{k}}, \boldsymbol{\sigma}^k_{nM}, \Phi^k, \mathscr{D}^k_{nM})_t \;+\; F_b\;(\boldsymbol{u}^{\boldsymbol{k}}, \boldsymbol{\sigma}^k_{nM}, \Phi^k, \mathscr{D}^k_{nM})_b \\ &\quad + F_r(\boldsymbol{u}^{\boldsymbol{k}}, \boldsymbol{\sigma}^k_{nM}, \Phi^k, \mathscr{D}^k_{nM})_r \\ &= F_\tau\;(\boldsymbol{u}^{\boldsymbol{k}}, \boldsymbol{\sigma}^k_{nM}, \Phi^k, \mathscr{D}^k_{nM})_\tau\end{aligned} \tag{50}$$

where

$$\tau = t,b,r \;\; with \;\; r = 2,\ldots,N\,, \tag{51}$$

t and b are the top and bottom values, and r the higher order terms of expansion. The thickness functions $F_\tau(\zeta_k)$ have been defined at the k-layer level, they are a

linear combination of Legendre polynomials $P_j = P_j(\zeta_k)$ of the jth-order defined in ζ_k-domain ($-1 \leq \zeta_k \leq 1$). The first five Legendre polynomials are:

$$P_0 = 1,\ P_1 = \zeta_k,\ P_2 = \frac{(3{\zeta_k}^2 - 1)}{2},\ P_3 = \frac{5{\zeta_k}^3}{2} - \frac{3\zeta_k}{2},\ P_4 = \frac{35{\zeta_k}^4}{8} - \frac{15{\zeta_k}^2}{4} + \frac{3}{8}\,, \tag{52}$$

and:

$$F_t = \frac{P_0 + P_1}{2},\ F_b = \frac{P_0 - P_1}{2},\ F_r = P_r - P_{r-2} \quad with \quad r = 2, \ldots, N\,. \tag{53}$$

The chosen functions have the following interesting properties:

$$\zeta_k = 1 \quad : F_t = 1;\ F_b = 0;\ F_r = 0\ , \tag{54}$$

$$\zeta_k = -1 \ : F_t = 0;\ F_b = 1;\ F_r = 0\ . \tag{55}$$

Eqs.(54) and (55) permit to consider interface values of the variables as unknown variables, this fact permits to impose the compatibility and/or equilibrium conditions at each layer interface.

4.3 Acronyms system

Several refined and advanced two-dimensional models can be obtained according to what in Sections 4.1 and 4.2. Depending on the used variational statement (PVD or RMVT), variables description (LW, ESL or ESL with MZZF), order of expansion N in z, a large variety of kinematics plate/shell theories is obtained. A system of acronyms is given in order to denote these models. The first letter indicates the multilayer approach which can be Equivalent Single Layer (E) or Layer Wise (L). The second letter refers to the employed variational statement: D for Principle of Virtual Displacements and M for Reissner's Mixed Variational Theorem. The number N indicates the order of expansion used in the z-direction (from 1 to 4). In the case of ESL approach, a letter Z can be added if the zigzag effect of displacements is considered by means of MZZF. Summarizing, $ED1 - ED4$ are ESL models based on PVD and $EM1 - EM4$ are ESL models based on RMVT. If Murakami zigzag function is used, these equivalent single layer models are indicated as $EDZ1 - EDZ3$ and $EMZ1 - EMZ3$, respectively. In the case of layer wise approaches, the letter L is considered in place of E, so the acronyms are $LD1 - LD4$ and $LM1 - LM4$. Classical theories such as Classical Lamination Theory (CLT) and First order Shear Deformation Theory (FSDT) can be obtained as particular cases of $ED1$ theory simply imposing a constant value of u_z through the thickness direction. An appropriate application of penalty technique to shear correction factor leads to CLT.

5 Governing equations

The steps to obtain the consistent governing equations are: - choice of the opportune variational statement (PVD or RMVT); - substitutions of consistent constitutive equations; - use of geometrical relations for plates and shells; - introduction of CUF for the two-dimensional approximation.

5.1 The classical PVD electro-mechanical case

The complete procedure to obtain governing equations, boundary conditions and fundamental nuclei for PVD case extended to electro-mechanical problem is here discussed (see Ballhause et al. (2005)). The variational statement, as obtained in Eq.(2), and written for a multilayered structure is:

$$\begin{aligned} \mathrm{PVD}(\boldsymbol{u},\Phi) : \sum_{k=1}^{N_l} \{ \int_{\Omega_k} \int_{A_k} \{ \delta\boldsymbol{\varepsilon}^{kT}_{pG} \boldsymbol{\sigma}^{k}_{pC} + \delta\boldsymbol{\varepsilon}^{kT}_{nG} \boldsymbol{\sigma}^{k}_{nC} - \delta\boldsymbol{\mathscr{E}}^{kT}_{pG} \boldsymbol{\mathscr{D}}^{k}_{pC} - \delta\boldsymbol{\mathscr{E}}^{kT}_{nG} \boldsymbol{\mathscr{D}}^{k}_{nC} \} d\Omega_k dz_k \} \\ = \sum_{k=1}^{N_l} (\delta L^{k}_{in} + \delta L^{k}_{e}) \, , \end{aligned} \tag{56}$$

where k denotes the layer and N_l is the number of layers embedded in the multilayered structure. Ω_k is the in-plane integration domain, A_k denotes domain in the z direction. Upon substitution of the correspondent constitutive equations (Eqs.(8)-(11)) in Eq.(56) one has:

$$\begin{aligned} &\sum_{k=1}^{N_l} \{ \int_{\Omega_k} \int_{A_k} \{ \delta\boldsymbol{\varepsilon}^{kT}_{pG} (\boldsymbol{C}^{k}_{pp} \boldsymbol{\varepsilon}^{k}_{pG} + \boldsymbol{C}^{k}_{pn} \boldsymbol{\varepsilon}^{k}_{nG} - \boldsymbol{e}^{kT}_{pp} \boldsymbol{\mathscr{E}}^{k}_{pG} - \boldsymbol{e}^{kT}_{np} \boldsymbol{\mathscr{E}}^{k}_{nG}) + \\ &\delta\boldsymbol{\varepsilon}^{kT}_{nG} (\boldsymbol{C}^{k}_{np} \boldsymbol{\varepsilon}^{k}_{pG} + \boldsymbol{C}^{k}_{nn} \boldsymbol{\varepsilon}^{k}_{nG} - \boldsymbol{e}^{kT}_{pn} \boldsymbol{\mathscr{E}}^{k}_{pG} - \boldsymbol{e}^{kT}_{nn} \boldsymbol{\mathscr{E}}^{k}_{nG}) - \\ &\delta\boldsymbol{\mathscr{E}}^{kT}_{pG} (\boldsymbol{e}^{k}_{pp} \boldsymbol{\varepsilon}^{k}_{pG} + \boldsymbol{e}^{k}_{pn} \boldsymbol{\varepsilon}^{k}_{nG} + \boldsymbol{\varepsilon}^{k}_{pp} \boldsymbol{\mathscr{E}}^{k}_{pG} + \boldsymbol{\varepsilon}^{k}_{pn} \boldsymbol{\mathscr{E}}^{k}_{nG}) - \\ &\delta\boldsymbol{\mathscr{E}}^{kT}_{nG} (\boldsymbol{e}^{k}_{np} \boldsymbol{\varepsilon}^{k}_{pG} + \boldsymbol{e}^{k}_{nn} \boldsymbol{\varepsilon}^{k}_{nG} + \boldsymbol{\varepsilon}^{k}_{np} \boldsymbol{\mathscr{E}}^{k}_{pG} + \boldsymbol{\varepsilon}^{k}_{nn} \boldsymbol{\mathscr{E}}^{k}_{nG}) \} d\Omega_k dz_k \} = \sum_{k=1}^{N_l} (\delta L^{k}_{in} + \delta L^{k}_{e}) \, . \end{aligned} \tag{57}$$

5.1.1 Plate geometry

If the geometrical relations for plate geometry (Eqs.(43)) are substituted where the subscript G appears in Eq.(57), the PVD becomes:

$$\begin{aligned}
&\sum_{k=1}^{N_l}\{\int_{\Omega_k}\int_{A_k}\{(\boldsymbol{D}_p\delta\boldsymbol{u}^k)^T(\boldsymbol{C}^k_{pp}\boldsymbol{D}_p\boldsymbol{u}^k+\boldsymbol{C}^k_{pn}(\boldsymbol{D}_{n\Omega}+\boldsymbol{D}_{nz})\boldsymbol{u}^k+\boldsymbol{e}^{kT}_{pp}\boldsymbol{D}_{e\Omega}\Phi^k+\boldsymbol{e}^{kT}_{np}\boldsymbol{D}_{en}\Phi^k)+\\
&((\boldsymbol{D}_{n\Omega}+\boldsymbol{D}_{nz})\delta\boldsymbol{u}^k)^T(\boldsymbol{C}^k_{np}\boldsymbol{D}_p\boldsymbol{u}^k+\boldsymbol{C}^k_{nn}(\boldsymbol{D}_{n\Omega}+\boldsymbol{D}_{nz})\boldsymbol{u}^k+\boldsymbol{e}^{kT}_{pn}\boldsymbol{D}_{e\Omega}\Phi^k+\boldsymbol{e}^{kT}_{nn}\boldsymbol{D}_{en}\Phi^k)-\\
&(-\boldsymbol{D}_{e\Omega}\delta\Phi^k)^T(\boldsymbol{e}^k_{pp}\boldsymbol{D}_p\boldsymbol{u}^k+\boldsymbol{e}^k_{pn}(\boldsymbol{D}_{n\Omega}+\boldsymbol{D}_{nz})\boldsymbol{u}^k-\boldsymbol{\varepsilon}^k_{pp}\boldsymbol{D}_{e\Omega}\Phi^k-\boldsymbol{\varepsilon}^k_{pn}\boldsymbol{D}_{en}\Phi^k)-\\
&(-\boldsymbol{D}_{en}\delta\Phi^k)^T(\boldsymbol{e}^k_{np}\boldsymbol{D}_p\boldsymbol{u}^k+\boldsymbol{e}^k_{nn}(\boldsymbol{D}_{n\Omega}+\boldsymbol{D}_{nz})\boldsymbol{u}^k-\boldsymbol{\varepsilon}^k_{np}\boldsymbol{D}_{e\Omega}\Phi^k-\boldsymbol{\varepsilon}^k_{nn}\boldsymbol{D}_{en}\Phi^k)\}d\Omega_k dz_k\}\\
&=\sum_{k=1}^{N_l}(\delta L^k_{in}+\delta L^k_e)\ .
\end{aligned} \tag{58}$$

Upon substitution of two-dimensional approximation by means of CUF, the following form is obtained:

$$\begin{aligned}
&\sum_{k=1}^{N_l}\{\int_{\Omega_k}\int_{A_k}\{\left(\boldsymbol{D}_p\delta\boldsymbol{u}^k_s\right)^T F_s\left(\boldsymbol{C}^k_{pp}\boldsymbol{D}_p F_\tau\boldsymbol{u}^k_\tau+\right.\\
&\left.\boldsymbol{C}^k_{pn}(\boldsymbol{D}_{n\Omega}+\boldsymbol{D}_{nz})F_\tau\boldsymbol{u}^k_\tau+\boldsymbol{e}^{kT}_{pp}\boldsymbol{D}_{e\Omega}F_\tau\Phi^k_\tau+\boldsymbol{e}^{kT}_{np}\boldsymbol{D}_{en}F_\tau\Phi^k_\tau\right)+\\
&\left((\boldsymbol{D}_{n\Omega}+\boldsymbol{D}_{nz})\delta\boldsymbol{u}^k_s\right)^T F_s\left(\boldsymbol{C}^k_{np}\boldsymbol{D}_p F_\tau\boldsymbol{u}^k_\tau+\right.\\
&\left.\boldsymbol{C}^k_{nn}(\boldsymbol{D}_{n\Omega}+\boldsymbol{D}_{nz})F_\tau\boldsymbol{u}^k_\tau+\boldsymbol{e}^{kT}_{pn}\boldsymbol{D}_{e\Omega}F_\tau\Phi^k_\tau+\boldsymbol{e}^{kT}_{nn}\boldsymbol{D}_{en}F_\tau\Phi^k_\tau\right)-\\
&\left(-\boldsymbol{D}_{e\Omega}\delta\Phi^k_s\right)^T F_s\left(\boldsymbol{e}^k_{pp}\boldsymbol{D}_p F_\tau\boldsymbol{u}^k_\tau+\boldsymbol{e}^k_{pn}(\boldsymbol{D}_{n\Omega}+\boldsymbol{D}_{nz})F_\tau\boldsymbol{u}^k_\tau-\right.\\
&\left.\boldsymbol{\varepsilon}^k_{pp}\boldsymbol{D}_{e\Omega}F_\tau\Phi^k_\tau-\boldsymbol{\varepsilon}^k_{pn}\boldsymbol{D}_{en}F_\tau\Phi^k_\tau\right)-\left(-\boldsymbol{D}_{en}\delta\Phi^k_s\right)^T F_s\left(\boldsymbol{e}^k_{np}\boldsymbol{D}_p F_\tau\boldsymbol{u}^k_\tau+\right.\\
&\left.\boldsymbol{e}^k_{nn}(\boldsymbol{D}_{n\Omega}+\boldsymbol{D}_{nz})F_\tau\boldsymbol{u}^k_\tau-\boldsymbol{\varepsilon}^k_{np}\boldsymbol{D}_{e\Omega}F_\tau\Phi^k_\tau-\boldsymbol{\varepsilon}^k_{nn}\boldsymbol{D}_{en}F_\tau\Phi^k_\tau\right)\}d\Omega_k dz_k\}=\sum_{k=1}^{N_l}(\delta L^k_{in}+\delta L^k_e)\ .
\end{aligned} \tag{59}$$

In order to obtain a strong form of differential equations on the domain Ω_k, as well as the correspondence boundary conditions on edge Γ_k, the integration by parts must be employed. This latter permits to move the differential operator from the infinitesimal variation of the generic variable $\delta\boldsymbol{a}^k$ to the finite quantity $\boldsymbol{a}^k$ [Carrera (2002)]. For a generic variable $\boldsymbol{a}^k$, the integration by parts states:

$$\int_{\Omega_k}\left((\boldsymbol{D}_\Omega)\delta\boldsymbol{a}^k\right)^T\boldsymbol{a}^k d\Omega_k=$$

$$-\int_{\Omega_k}\delta\boldsymbol{a}^{kT}\left((\boldsymbol{D}_\Omega)^T\boldsymbol{a}^k\right)d\Omega_k+\int_{\Gamma_k}\delta\boldsymbol{a}^{kT}\left((\boldsymbol{I}_\Omega)^T\boldsymbol{a}^k\right)d\Gamma_k\,, \quad (60)$$

where $\Omega = p, n\Omega, e\Omega$. The following additional arrays have been introduced to perform integration by parts:

$$\mathbf{I}_p=\begin{bmatrix}1&0&0\\0&1&0\\1&1&0\end{bmatrix};\mathbf{I}_{n\Omega}=\begin{bmatrix}0&0&1\\0&0&1\\0&0&0\end{bmatrix};\mathbf{I}_{e\Omega}=\begin{bmatrix}1\\1\end{bmatrix}. \quad (61)$$

After the integration by parts, the PVD assumes the following form:

$$\begin{aligned}
&\sum_{k=1}^{N_l}\{\int_{\Omega_k}\int_{A_k}\{\delta\boldsymbol{u}_s^{kT}[(-\boldsymbol{D}_p)^TF_s(\boldsymbol{C}_{pp}^k\boldsymbol{D}_pF_\tau\boldsymbol{u}_\tau^k+\\
&\boldsymbol{C}_{pn}^k(\boldsymbol{D}_{n\Omega}+\boldsymbol{D}_{nz})F_\tau\boldsymbol{u}_\tau^k+\boldsymbol{e}_{pp}^{kT}\boldsymbol{D}_{e\Omega}F_\tau\Phi_\tau^k+\boldsymbol{e}_{np}^{kT}\boldsymbol{D}_{en}F_\tau\Phi_\tau^k)]+\\
&\delta\boldsymbol{u}_s^{kT}[(-\boldsymbol{D}_{n\Omega}+\boldsymbol{D}_{nz})^TF_s(\boldsymbol{C}_{np}^k\boldsymbol{D}_pF_\tau\boldsymbol{u}_\tau^k+\\
&\boldsymbol{C}_{nn}^k(\boldsymbol{D}_{n\Omega}+\boldsymbol{D}_{nz})F_\tau\boldsymbol{u}_\tau^k+\boldsymbol{e}_{pn}^{kT}\boldsymbol{D}_{e\Omega}F_\tau\Phi_\tau^k+\boldsymbol{e}_{nn}^{kT}\boldsymbol{D}_{en}F_\tau\Phi_\tau^k)]+\\
&\delta\Phi_s^{kT}[(-\boldsymbol{D}_{e\Omega})^TF_s(\boldsymbol{e}_{pp}^k\boldsymbol{D}_pF_\tau\boldsymbol{u}_\tau^k+\boldsymbol{e}_{pn}^k(\boldsymbol{D}_{n\Omega}+\boldsymbol{D}_{nz})F_\tau\boldsymbol{u}_\tau^k-\\
&\boldsymbol{\varepsilon}_{pp}^k\boldsymbol{D}_{e\Omega}F_\tau\Phi_\tau^k-\boldsymbol{\varepsilon}_{pn}^k\boldsymbol{D}_{en}F_\tau\Phi_\tau^k)]+\delta\Phi_s^{kT}[(\boldsymbol{D}_{en})^TF_s(\boldsymbol{e}_{np}^k\boldsymbol{D}_pF_\tau\boldsymbol{u}_\tau^k+\\
&\boldsymbol{e}_{nn}^k(\boldsymbol{D}_{n\Omega}+\boldsymbol{D}_{nz})F_\tau\boldsymbol{u}_\tau^k-\boldsymbol{\varepsilon}_{np}^k\boldsymbol{D}_{e\Omega}F_\tau\Phi_\tau^k-\boldsymbol{\varepsilon}_{nn}^k\boldsymbol{D}_{en}F_\tau\Phi_\tau^k)]\}d\Omega_kdz_k\}\\
&+\sum_{k=1}^{N_l}\{\int_{\Gamma_k}\int_{A_k}\{\delta\boldsymbol{u}_s^{kT}[\boldsymbol{I}_p^TF_s(\boldsymbol{C}_{pp}^k\boldsymbol{D}_pF_\tau\boldsymbol{u}_\tau^k+\\
&\boldsymbol{C}_{pn}^k(\boldsymbol{D}_{n\Omega}+\boldsymbol{D}_{nz})F_\tau\boldsymbol{u}_\tau^k+\boldsymbol{e}_{pp}^{kT}\boldsymbol{D}_{e\Omega}F_\tau\Phi_\tau^k+\boldsymbol{e}_{np}^{kT}\boldsymbol{D}_{en}F_\tau\Phi_\tau^k)]+\\
&\delta\boldsymbol{u}_s^{kT}[\boldsymbol{I}_{n\Omega}^TF_s(\boldsymbol{C}_{np}^k\boldsymbol{D}_pF_\tau\boldsymbol{u}_\tau^k+\\
&\boldsymbol{C}_{nn}^k(\boldsymbol{D}_{n\Omega}+\boldsymbol{D}_{nz})F_\tau\boldsymbol{u}_\tau^k+\boldsymbol{e}_{pn}^{kT}\boldsymbol{D}_{e\Omega}F_\tau\Phi_\tau+\boldsymbol{e}_{nn}^{kT}\boldsymbol{D}_{en}F_\tau\Phi_\tau^k)]+\\
&\delta\Phi_s^{kT}[\boldsymbol{I}_{e\Omega}^TF_s(\boldsymbol{e}_{pp}^k\boldsymbol{D}_pF_\tau\boldsymbol{u}_\tau^k+\boldsymbol{e}_{pn}^k(\boldsymbol{D}_{n\Omega}+\boldsymbol{D}_{nz})F_\tau\boldsymbol{u}_\tau^k-\\
&\boldsymbol{\varepsilon}_{pp}^k\boldsymbol{D}_{e\Omega}F_\tau\Phi_\tau^k-\boldsymbol{\varepsilon}_{pn}^k\boldsymbol{D}_{en}F_\tau\Phi_\tau^k)]\}d\Gamma_kdz_k\}\\
&=-\sum_{k=1}^{N_l}\{\int_{\Omega_k}\int_{A_k}(\delta\boldsymbol{u}_s^{kT}\rho^kF_sF_\tau\ddot{\boldsymbol{u}}_\tau^k)d\Omega_kdz_k\}+\sum_{k=1}^{N_l}\{\int_{\Omega_k}\delta\boldsymbol{u}_s^{kT}F_s\boldsymbol{p}_u^k+\delta\Phi_s^{kT}F_s\boldsymbol{p}_\Phi^k)d\Omega_k\}\,.
\end{aligned} \quad (62)$$

The governing equations on the domain Ω^k are:

$$\begin{aligned}
\delta\boldsymbol{u}_s^k&:\boldsymbol{K}_{uu}^{k\tau s}\boldsymbol{u}_\tau^k+\boldsymbol{K}_{u\Phi}^{k\tau s}\Phi_\tau^k=\boldsymbol{P}_{us}^k-\boldsymbol{M}^{k\tau s}\ddot{\boldsymbol{u}}_\tau^k\,, \quad (63)\\
\delta\Phi_s^k&:\boldsymbol{K}_{\Phi u}^{k\tau s}\boldsymbol{u}_\tau^k+\boldsymbol{K}_{\Phi\Phi}^{k\tau s}\Phi_\tau^k=\boldsymbol{P}_{\Phi s}^k\,,
\end{aligned}$$

where $\ddot{\boldsymbol{u}}^k_\tau$ denotes the second derivative with respect to the time of the displacement components. $\boldsymbol{M}^{k\tau s}$ is the fundamental nucleus for the inertial array. $\boldsymbol{K}^{k\tau s}_{uu}$, $\boldsymbol{K}^{k\tau s}_{u\Phi}$, $\boldsymbol{K}^{k\tau s}_{\Phi u}$ and $\boldsymbol{K}^{k\tau s}_{\Phi\Phi}$ are the so-called fundamental nuclei of electro-mechanical stiffness array. $\boldsymbol{P}^k_{us}$ and $\boldsymbol{P}^k_{\Phi s}$ are the consistent variationally mechanical and electric loads, respectively.
Boundary conditions of Dirichlet type are:

$$\begin{aligned} \boldsymbol{u}^k_\tau &= \bar{\boldsymbol{u}}^k_\tau \,, \\ \Phi^k_\tau &= \bar{\Phi}^k_\tau \,, \end{aligned} \tag{64}$$

Boundary conditions of Neumann type are:

$$\begin{aligned} &\boldsymbol{\Pi}^{k\tau s}_{uu}\boldsymbol{u}^k_\tau + \boldsymbol{\Pi}^{k\tau s}_{u\Phi}\Phi^k_\tau = \boldsymbol{\Pi}^{k\tau s}_{uu}\bar{\boldsymbol{u}}^k_\tau + \boldsymbol{\Pi}^{k\tau s}_{u\Phi}\bar{\Phi}^k_\tau \,, \\ &\boldsymbol{\Pi}^{k\tau s}_{\Phi u}\boldsymbol{u}^k_\tau + \boldsymbol{\Pi}^{k\tau s}_{\Phi\Phi}\Phi^k_\tau = \boldsymbol{\Pi}^{k\tau s}_{\Phi u}\bar{\boldsymbol{u}}^k_\tau + \boldsymbol{\Pi}^{k\tau s}_{\Phi\Phi}\bar{\Phi}^k_\tau \,. \end{aligned} \tag{65}$$

The fundamental nuclei are:

$$\begin{aligned} \boldsymbol{K}^{k\tau s}_{uu} = \int_{A_k} \Big[&[-\boldsymbol{D}_p]^T \boldsymbol{C}^k_{pp}\boldsymbol{D}_p + [-\boldsymbol{D}_p]^T \boldsymbol{C}^k_{pn}[\boldsymbol{D}_{n\Omega} + \boldsymbol{D}_{nz}] + \\ &[-\boldsymbol{D}_{n\Omega} + \boldsymbol{D}_{nz}]^T \boldsymbol{C}^k_{np}\boldsymbol{D}_p + [-\boldsymbol{D}_{n\Omega} + \boldsymbol{D}_{nz}]^T \boldsymbol{C}^k_{nn}[\boldsymbol{D}_{n\Omega} + \boldsymbol{D}_{nz}] \Big] F_\tau F_s \, dz \,, \end{aligned} \tag{66}$$

$$\begin{aligned} \boldsymbol{K}^{k\tau s}_{u\Phi} = -\int_{A_k} \Big[&[-\boldsymbol{D}_p]^T \boldsymbol{e}^{kT}_{pp}\boldsymbol{D}_{e\Omega} + [-\boldsymbol{D}_p]^T \boldsymbol{e}^{kT}_{np}\boldsymbol{D}_{en} + \\ &[-\boldsymbol{D}_{n\Omega} + \boldsymbol{D}_{nz}]^T \boldsymbol{e}^{kT}_{pn}\boldsymbol{D}_{e\Omega} + [-\boldsymbol{D}_{n\Omega} + \boldsymbol{D}_{nz}]^T \boldsymbol{e}^{kT}_{nn}\boldsymbol{D}_{en} \Big] F_\tau F_s \, dz \,, \end{aligned} \tag{67}$$

$$\begin{aligned} \boldsymbol{K}^{k\tau s}_{\Phi u} = -\int_{A_k} \Big[&[-\boldsymbol{D}_{e\Omega}]^T (\boldsymbol{e}^k_{pp}\boldsymbol{D}_p + \boldsymbol{e}^k_{pn}[\boldsymbol{D}_{n\Omega} + \boldsymbol{D}_{nz}] + [\boldsymbol{D}_{en}]^T (\boldsymbol{e}^k_{np}\boldsymbol{D}_p + \\ &\boldsymbol{e}^k_{nn}[\boldsymbol{D}_{n\Omega} + \boldsymbol{D}_{nz}]) \Big] F_\tau F_s \, dz \,, \end{aligned} \tag{68}$$

$$\begin{aligned} \boldsymbol{K}^{k\tau s}_{\Phi\Phi} = -\int_{A_k} \Big[&[-\boldsymbol{D}_{e\Omega}]^T (-\boldsymbol{\varepsilon}^k_{pp}\boldsymbol{D}_{e\Omega}) + [-\boldsymbol{D}_{e\Omega}]^T (-\boldsymbol{\varepsilon}^k_{pn}\boldsymbol{D}_{en}) + \\ &[\boldsymbol{D}_{en}]^T (-\boldsymbol{\varepsilon}^k_{np}\boldsymbol{D}_{e\Omega}) + [\boldsymbol{D}_{en}]^T (-\boldsymbol{\varepsilon}^k_{nn}\boldsymbol{D}_{en}) \Big] F_\tau F_s \, dz \,. \end{aligned} \tag{69}$$

The inertial array is:

$$\boldsymbol{M}^{k\tau s} = \int_{A_k} \boldsymbol{I} \, \rho^k F_\tau F_s \, dz \,, \tag{70}$$

where ρ^k is the mass density for each layer k, and $\boldsymbol{I}$ is the identity matrix of dimension [3×3].

The *nuclei* for the boundary conditions are:

$$\boldsymbol{\Pi}_{uu}^{k\tau s} = \int_{A_k} \Big[\boldsymbol{I}_p^T \boldsymbol{C}_{pp}^k \boldsymbol{D}_p + \boldsymbol{I}_p^T \boldsymbol{C}_{pn}^k [\boldsymbol{D}_{n\Omega} + \boldsymbol{D}_{nz}] + \boldsymbol{I}_{n\Omega}^T \boldsymbol{C}_{np}^k \boldsymbol{D}_p + \boldsymbol{I}_{n\Omega}^T \boldsymbol{C}_{nn}^k [\boldsymbol{D}_{n\Omega} + \boldsymbol{D}_{nz}] \Big] F_\tau F_s \, dz, \quad (71)$$

$$\boldsymbol{\Pi}_{u\Phi}^{k\tau s} = \int_{A_k} \Big[\boldsymbol{I}_p^T \boldsymbol{e}_{pp}^{kT} \boldsymbol{D}_{e\Omega} + \boldsymbol{I}_p^T \boldsymbol{e}_{np}^{kT} \boldsymbol{D}_{en} + \boldsymbol{I}_{n\Omega}^T \boldsymbol{e}_{pn}^{kT} \boldsymbol{D}_{e\Omega} + \boldsymbol{I}_{n\Omega}^T \boldsymbol{e}_{nn}^{kT} \boldsymbol{D}_{en} \Big] F_\tau F_s \, dz \,, \quad (72)$$

$$\boldsymbol{\Pi}_{\Phi u}^{k\tau s} = -\int_{A_k} \Big[\boldsymbol{I}_{e\Omega}^T (\boldsymbol{e}_{pp}^k \boldsymbol{D}_p + \boldsymbol{e}_{pn}^k [\boldsymbol{D}_{n\Omega} + \boldsymbol{D}_{nz}]) \Big] F_\tau F_s \, dz \,, \quad (73)$$

$$\boldsymbol{\Pi}_{\Phi\Phi}^{k\tau s} = -\int_{A_k} \Big[\boldsymbol{I}_{e\Omega}^T (-\boldsymbol{\varepsilon}_{pp}^k \boldsymbol{D}_{e\Omega}) + \boldsymbol{I}_{e\Omega}^T (-\boldsymbol{\varepsilon}_{pn}^k \boldsymbol{D}_{en}) \Big] F_\tau F_s \, dz \,. \quad (74)$$

5.1.2 Shell geometry

If the geometrical relations for shell geometry (Eqs.(40)) are substituted where the subscript G appears in Eq.(57), the PVD becomes:

$$\begin{aligned}
&\sum_{k=1}^{N_l} \{ \int_{\Omega_k} \int_{A_k} \{ ((\boldsymbol{D}_p^k + \boldsymbol{A}_p^k) \delta \boldsymbol{u}^k)^T (\boldsymbol{C}_{pp}^k (\boldsymbol{D}_p^k + \boldsymbol{A}_p^k) \boldsymbol{u}^k + \boldsymbol{C}_{pn}^k (\boldsymbol{D}_{n\Omega}^k + \boldsymbol{D}_{nz}^k - \boldsymbol{A}_n^k) \boldsymbol{u}^k + \\
&\boldsymbol{e}_{pp}^{kT} \boldsymbol{D}_{e\Omega}^k \Phi^k + \boldsymbol{e}_{np}^{kT} \boldsymbol{D}_{en}^k \Phi^k) + \\
&((\boldsymbol{D}_{n\Omega}^k + \boldsymbol{D}_{nz}^k - \boldsymbol{A}_n^k) \delta \boldsymbol{u}^k)^T (\boldsymbol{C}_{np}^k (\boldsymbol{D}_p^k + \boldsymbol{A}_p^k) \boldsymbol{u}^k + \boldsymbol{C}_{nn}^k (\boldsymbol{D}_{n\Omega}^k + \boldsymbol{D}_{nz}^k - \boldsymbol{A}_n^k) \boldsymbol{u}^k + \\
&\boldsymbol{e}_{pn}^{kT} \boldsymbol{D}_{e\Omega}^k \Phi^k + \boldsymbol{e}_{nn}^{kT} \boldsymbol{D}_{en}^k \Phi^k) - \\
&(-\boldsymbol{D}_{e\Omega}^k \delta \Phi^k)^T (\boldsymbol{e}_{pp}^k (\boldsymbol{D}_p^k + \boldsymbol{A}_p^k) \boldsymbol{u}^k + \\
&\boldsymbol{e}_{pn}^k (\boldsymbol{D}_{n\Omega}^k + \boldsymbol{D}_{nz}^k - \boldsymbol{A}_n^k) \boldsymbol{u}^k - \boldsymbol{\varepsilon}_{pp}^k \boldsymbol{D}_{e\Omega}^k \Phi^k - \boldsymbol{\varepsilon}_{pn}^k \boldsymbol{D}_{en}^k \Phi^k) - \\
&(-\boldsymbol{D}_{en}^k \delta \Phi^k)^T (\boldsymbol{e}_{np}^k (\boldsymbol{D}_p^k + \boldsymbol{A}_p^k) \boldsymbol{u}^k + \boldsymbol{e}_{nn}^k (\boldsymbol{D}_{n\Omega}^k + \boldsymbol{D}_{nz}^k - \boldsymbol{A}_n^k) \boldsymbol{u}^k - \\
&\boldsymbol{\varepsilon}_{np}^k \boldsymbol{D}_{e\Omega}^k \Phi^k - \boldsymbol{\varepsilon}_{nn}^k \boldsymbol{D}_{en}^k \Phi^k) \} d\Omega_k dz_k \} = \sum_{k=1}^{N_l} (\delta L_{in}^k + \delta L_e^k) \,. \quad (75)
\end{aligned}$$

Upon substitution of two-dimensional approximation, by means of CUF, the following form is obtained:

$$
\begin{aligned}
&\sum_{k=1}^{N_l}\{\int_{\Omega_k}\int_{A_k}\{\left((\boldsymbol{D}_p^k+\boldsymbol{A}_p^k)\delta\boldsymbol{u}_s^k\right)^T F_s\big(\boldsymbol{C}_{pp}^k(\boldsymbol{D}_p^k+\boldsymbol{A}_p^k)F_\tau\boldsymbol{u}_\tau^k+\\
&\boldsymbol{C}_{pn}^k(\boldsymbol{D}_{n\Omega}^k+\boldsymbol{D}_{nz}^k-\boldsymbol{A}_n^k)F_\tau\boldsymbol{u}_\tau^k+\boldsymbol{e}_{pp}^{kT}\boldsymbol{D}_{e\Omega}^k F_\tau\Phi_\tau^k+\boldsymbol{e}_{np}^{kT}\boldsymbol{D}_{en}^k F_\tau\Phi_\tau^k\big)+\\
&\left((\boldsymbol{D}_{n\Omega}^k+\boldsymbol{D}_{nz}^k-\boldsymbol{A}_n^k)\delta\boldsymbol{u}_s^k\right)^T F_s\big(\boldsymbol{C}_{np}^k(\boldsymbol{D}_p^k+\boldsymbol{A}_p^k)F_\tau\boldsymbol{u}_\tau^k+\\
&\boldsymbol{C}_{nn}^k(\boldsymbol{D}_{n\Omega}^k+\boldsymbol{D}_{nz}^k-\boldsymbol{A}_n^k)F_\tau\boldsymbol{u}_\tau^k+\boldsymbol{e}_{pn}^{kT}\boldsymbol{D}_{e\Omega}^k F_\tau\Phi_\tau^k+\boldsymbol{e}_{nn}^{kT}\boldsymbol{D}_{en}^k F_\tau\Phi_\tau^k\big)-\\
&\left(-\boldsymbol{D}_{e\Omega}^k\delta\Phi_s^k\right)^T F_s\big(\boldsymbol{e}_{pp}^k(\boldsymbol{D}_p^k+\boldsymbol{A}_p^k)F_\tau\boldsymbol{u}_\tau^k+\boldsymbol{e}_{pn}^k(\boldsymbol{D}_{n\Omega}^k+\boldsymbol{D}_{nz}^k-\boldsymbol{A}_n^k)F_\tau\boldsymbol{u}_\tau^k-\\
&\boldsymbol{\varepsilon}_{pp}^k\boldsymbol{D}_{e\Omega}^k F_\tau\Phi_\tau^k-\boldsymbol{\varepsilon}_{pn}^k\boldsymbol{D}_{en}^k F_\tau\Phi_\tau^k\big)-\left(-\boldsymbol{D}_{en}^k\delta\Phi_s^k\right)^T F_s\big(\boldsymbol{e}_{np}^k(\boldsymbol{D}_p^k+\boldsymbol{A}_p^k)F_\tau\boldsymbol{u}_\tau^k+\\
&\boldsymbol{e}_{nn}^k(\boldsymbol{D}_{n\Omega}^k+\boldsymbol{D}_{nz}^k-\boldsymbol{A}_n^k)F_\tau\boldsymbol{u}_\tau^k-\boldsymbol{\varepsilon}_{np}^k\boldsymbol{D}_{e\Omega}^k F_\tau\Phi_\tau^k-\boldsymbol{\varepsilon}_{nn}^k\boldsymbol{D}_{en}^k F_\tau\Phi_\tau^k\big)\}d\Omega_k dz_k\}\\
&=\sum_{k=1}^{N_l}(\delta L_{in}^k+\delta L_e^k)\,.
\end{aligned}
\tag{76}
$$

In order to obtain a strong form of differential equations on the domain Ω_k, as well as the correspondence boundary conditions on edge Γ_k, the integration by parts must be employed. For a generic variable $\boldsymbol{a}^k$, the integration by parts states as in Eq.(60), the additional arrays introduced to perform integration by parts in the case of shell geometry change with respect to the plate case (see Eq.(61)):

$$
\mathbf{I}_p^k=\begin{bmatrix}\frac{1}{H_\alpha^k} & 0 & 0\\ 0 & \frac{1}{H_\beta^k} & 0\\ \frac{1}{H_\beta^k} & \frac{1}{H_\alpha^k} & 0\end{bmatrix};\quad \mathbf{I}_{n\Omega}^k=\begin{bmatrix}0 & 0 & \frac{1}{H_\alpha^k}\\ 0 & 0 & \frac{1}{H_\beta^k}\\ 0 & 0 & 0\end{bmatrix};\quad \mathbf{I}_{e\Omega}^k=\begin{bmatrix}\frac{1}{H_\alpha^k}\\ \frac{1}{H_\beta^k}\end{bmatrix}. \tag{77}
$$

After the integration by parts, the PVD assumes the following form:

$$
\begin{aligned}
&\sum_{k=1}^{N_l}\{\int_{\Omega_k}\int_{A_k}\{\delta \boldsymbol{u}_s^{kT}[(-\boldsymbol{D}_p^k+\boldsymbol{A}_p^k)^T F_s(\boldsymbol{C}_{pp}^k(\boldsymbol{D}_p^k+\boldsymbol{A}_p^k)F_\tau \boldsymbol{u}_\tau^k+\\
&\boldsymbol{C}_{pn}^k(\boldsymbol{D}_{n\Omega}^k+\boldsymbol{D}_{nz}^k-\boldsymbol{A}_n^k)F_\tau \boldsymbol{u}_\tau^k+\boldsymbol{e}_{pp}^{kT}\boldsymbol{D}_{e\Omega}^k F_\tau \Phi_\tau^k+\boldsymbol{e}_{np}^{kT}\boldsymbol{D}_{en}^k F_\tau \Phi_\tau^k)]+\\
&\delta \boldsymbol{u}_s^{kT}[(-\boldsymbol{D}_{n\Omega}^k+\boldsymbol{D}_{nz}^k-\boldsymbol{A}_n^k)^T F_s(\boldsymbol{C}_{np}^k(\boldsymbol{D}_p^k+\boldsymbol{A}_p^k)F_\tau \boldsymbol{u}_\tau^k+\\
&\boldsymbol{C}_{nn}^k(\boldsymbol{D}_{n\Omega}^k+\boldsymbol{D}_{nz}^k-\boldsymbol{A}_n^k)F_\tau \boldsymbol{u}_\tau^k+\boldsymbol{e}_{pn}^{kT}\boldsymbol{D}_{e\Omega}^k F_\tau \Phi_\tau^k+\boldsymbol{e}_{nn}^{kT}\boldsymbol{D}_{en}^k F_\tau \Phi_\tau^k)]+\\
&\delta \Phi_s^{kT}[(-\boldsymbol{D}_{e\Omega}^k)^T F_s(\boldsymbol{e}_{pp}^k(\boldsymbol{D}_p^k+\boldsymbol{A}_p^k)F_\tau \boldsymbol{u}_\tau^k+\boldsymbol{e}_{pn}^k(\boldsymbol{D}_{n\Omega}^k+\boldsymbol{D}_{nz}^k-\boldsymbol{A}_n^k)F_\tau \boldsymbol{u}_\tau^k-\\
&\boldsymbol{\varepsilon}_{pp}^k\boldsymbol{D}_{e\Omega}^k F_\tau \Phi_\tau^k-\boldsymbol{\varepsilon}_{pn}^k\boldsymbol{D}_{en}^k F_\tau \Phi_\tau^k)]+\delta \Phi_s^{kT}[(\boldsymbol{D}_{en}^k)^T F_s(\boldsymbol{e}_{np}^k(\boldsymbol{D}_p^k+\boldsymbol{A}_p^k)F_\tau \boldsymbol{u}_\tau^k+\\
&\boldsymbol{e}_{nn}^k(\boldsymbol{D}_{n\Omega}^k+\boldsymbol{D}_{nz}^k-\boldsymbol{A}_n^k)F_\tau \boldsymbol{u}_\tau^k-\boldsymbol{\varepsilon}_{np}^k\boldsymbol{D}_{e\Omega}^k F_\tau \Phi_\tau^k-\boldsymbol{\varepsilon}_{nn}^k\boldsymbol{D}_{en}^k F_\tau \Phi_\tau^k)]\}d\Omega_k dz_k\}\\
&+\sum_{k=1}^{N_l}\{\int_{\Gamma_k}\int_{A_k}\{\delta \boldsymbol{u}_s^{kT}[\boldsymbol{I}_p^{kT}F_s(\boldsymbol{C}_{pp}^k(\boldsymbol{D}_p^k+\boldsymbol{A}_p^k)F_\tau \boldsymbol{u}_\tau^k+\\
&\boldsymbol{C}_{pn}^k(\boldsymbol{D}_{n\Omega}^k+\boldsymbol{D}_{nz}^k-\boldsymbol{A}_n^k)F_\tau \boldsymbol{u}_\tau^k+\boldsymbol{e}_{pp}^{kT}\boldsymbol{D}_{e\Omega}^k F_\tau \Phi_\tau^k+\boldsymbol{e}_{np}^{kT}\boldsymbol{D}_{en}^k F_\tau \Phi_\tau^k)]+\\
&\delta \boldsymbol{u}_s^{kT}[\boldsymbol{I}_{n\Omega}^{kT}F_s(\boldsymbol{C}_{np}^k(\boldsymbol{D}_p^k+\boldsymbol{A}_p^k)F_\tau \boldsymbol{u}_\tau^k+\\
&\boldsymbol{C}_{nn}^k(\boldsymbol{D}_{n\Omega}^k+\boldsymbol{D}_{nz}^k-\boldsymbol{A}_n^k)F_\tau \boldsymbol{u}_\tau^k+\boldsymbol{e}_{pn}^{kT}\boldsymbol{D}_{e\Omega}^k F_\tau \Phi_\tau+\boldsymbol{e}_{nn}^{kT}\boldsymbol{D}_{en}^k F_\tau \Phi_\tau^k)]+\\
&\delta \Phi_s^{kT}[\boldsymbol{I}_{e\Omega}^{kT}F_s(\boldsymbol{e}_{pp}^k(\boldsymbol{D}_p^k+\boldsymbol{A}_p^k)F_\tau \boldsymbol{u}_\tau^k+\boldsymbol{e}_{pn}^k(\boldsymbol{D}_{n\Omega}^k+\boldsymbol{D}_{nz}^k-\boldsymbol{A}_n^k)F_\tau \boldsymbol{u}_\tau^k-\\
&\boldsymbol{\varepsilon}_{pp}^k\boldsymbol{D}_{e\Omega}^k F_\tau \Phi_\tau^k-\boldsymbol{\varepsilon}_{pn}^k\boldsymbol{D}_{en}^k F_\tau \Phi_\tau^k)]\}d\Gamma_k dz_k\}\\
&=-\sum_{k=1}^{N_l}\{\int_{\Omega_k}\int_{A_k}(\delta \boldsymbol{u}_s^{kT}\rho^k F_s F_\tau \ddot{\boldsymbol{u}}_\tau^k)d\Omega_k dz_k\}+\\
&\sum_{k=1}^{N_l}\{\int_{\Omega_k}\delta \boldsymbol{u}_s^{kT}F_s \boldsymbol{p}_u^k+\delta \Phi_s^{kT}F_s \boldsymbol{p}_\Phi^k)d\Omega_k\}\ .
\end{aligned}
\tag{78}
$$

The governing equations on the domain Ω^k and the relative boundary conditions are the same proposed in Eqs.(63)-(65) for plate geometry. The form of the fundamental nuclei changes as:

$$
\begin{aligned}
\boldsymbol{K}_{uu}^{k\tau s}=\int_{A_k}\Big[&[-\boldsymbol{D}_p^k+\boldsymbol{A}_p^k]^T\,\boldsymbol{C}_{pp}^k[\boldsymbol{D}_p^k+\boldsymbol{A}_p^k]+[-\boldsymbol{D}_p^k+\boldsymbol{A}_p^k]^T\,\boldsymbol{C}_{pn}^k[\boldsymbol{D}_{n\Omega}^k+\boldsymbol{D}_{nz}^k-\boldsymbol{A}_n^k]+\\
&[-\boldsymbol{D}_{n\Omega}^k+\boldsymbol{D}_{nz}^k-\boldsymbol{A}_n^k]^T\,\boldsymbol{C}_{np}^k[\boldsymbol{D}_p^k+\boldsymbol{A}_p^k]+[-\boldsymbol{D}_{n\Omega}^k+\boldsymbol{D}_{nz}^k-\boldsymbol{A}_n^k]^T\,\boldsymbol{C}_{nn}^k[\boldsymbol{D}_{n\Omega}^k+\boldsymbol{D}_{nz}^k-\boldsymbol{A}_n^k]\Big]\\
&F_\tau F_s H_\alpha^k H_\beta^k\ dz,
\end{aligned}
\tag{79}
$$

$$
\boldsymbol{K}_{u\Phi}^{k\tau s}=\int_{A_k}\Big[[-\boldsymbol{D}_p^k+\boldsymbol{A}_p^k]^T\,\boldsymbol{e}_{pp}^{kT}\boldsymbol{D}_{e\Omega}^k+[-\boldsymbol{D}_p^k+\boldsymbol{A}_p^k]^T\,\boldsymbol{e}_{np}^{kT}\boldsymbol{D}_{en}^k+
\tag{80}
$$

$$[-\boldsymbol{D}^k_{n\Omega}+\boldsymbol{D}^k_{nz}-\boldsymbol{A}^k_n]^T\ \boldsymbol{e}^{kT}_{pn}\boldsymbol{D}^k_{e\Omega}+[-\boldsymbol{D}^k_{n\Omega}+\boldsymbol{D}^k_{nz}-\boldsymbol{A}^k_n]^T\ \boldsymbol{e}^{kT}_{nn}\boldsymbol{D}^k_{en}\Big]F_\tau F_s H^k_\alpha H^k_\beta\ dz\,,$$

$$\boldsymbol{K}^{k\tau s}_{\Phi u}=\int_{A_k}\Big[[-\boldsymbol{D}^k_{e\Omega}]^T\ (\boldsymbol{e}^k_{pp}[\boldsymbol{D}^k_p+\boldsymbol{A}^k_p]+\boldsymbol{e}^k_{pn}[\boldsymbol{D}^k_{n\Omega}+\boldsymbol{D}^k_{nz}-\boldsymbol{A}^k_n]+[\boldsymbol{D}^k_{en}]^T\ (\boldsymbol{e}^k_{np}[\boldsymbol{D}^k_p+\boldsymbol{A}^k_p]+$$

$$\boldsymbol{e}^k_{nn}[\boldsymbol{D}^k_{n\Omega}+\boldsymbol{D}^k_{nz}-\boldsymbol{A}^k_n])\Big]F_\tau F_s H^k_\alpha H^k_\beta\ dz\,,$$

$$\boldsymbol{K}^{k\tau s}_{\Phi\Phi}=\int_{A_k}\Big[[-\boldsymbol{D}^k_{e\Omega}]^T\ (-\boldsymbol{\varepsilon}^k_{pp}\boldsymbol{D}^k_{e\Omega})+[-\boldsymbol{D}^k_{e\Omega}]^T\ (-\boldsymbol{\varepsilon}^k_{pn}\boldsymbol{D}^k_{en})+ \tag{81}$$

$$[\boldsymbol{D}^k_{en}]^T\ (-\boldsymbol{\varepsilon}^k_{np}\boldsymbol{D}^k_{e\Omega})+[\boldsymbol{D}^k_{en}]^T\ (-\boldsymbol{\varepsilon}^k_{nn}\boldsymbol{D}^k_{en})\Big]F_\tau F_s H^k_\alpha H^k_\beta\ dz\,.$$

The inertial array is:

$$\boldsymbol{M}^{k\tau s}=\int_{A_k}\boldsymbol{I}\,\rho^k F_\tau F_s H^k_\alpha H^k_\beta\ dz\,, \tag{82}$$

where ρ^k is the mass density for each layer k, and $\boldsymbol{I}$ is the identity matrix of dimension [3×3].

The *nuclei* for the boundary conditions are:

$$\boldsymbol{\Pi}^{k\tau s}_{uu}=\int_{A_k}\Big[\boldsymbol{I}^{kT}_p\ \boldsymbol{C}^k_{pp}[\boldsymbol{D}^k_p+\boldsymbol{A}^k_p]+\boldsymbol{I}^{kT}_p\ \boldsymbol{C}^k_{pn}[\boldsymbol{D}^k_{n\Omega}+\boldsymbol{D}^k_{nz}-\boldsymbol{A}^k_n]+$$

$$\boldsymbol{I}^{kT}_{n\Omega}\boldsymbol{C}^k_{np}[\boldsymbol{D}^k_p+\boldsymbol{A}^k_p]+\boldsymbol{I}^{kT}_{n\Omega}\ \boldsymbol{C}^k_{nn}[\boldsymbol{D}^k_{n\Omega}+\boldsymbol{D}^k_{nz}-\boldsymbol{A}^k_n]\Big]F_\tau F_s H^k_\alpha H^k_\beta\ dz\,, \tag{83}$$

$$\boldsymbol{\Pi}^{k\tau s}_{u\Phi}=\int_{A_k}\Big[\boldsymbol{I}^{kT}_p\,\boldsymbol{e}^{kT}_{pp}\boldsymbol{D}^k_{e\Omega}+\boldsymbol{I}^{kT}_p\,\boldsymbol{e}^{kT}_{np}\boldsymbol{D}^k_{en}+\boldsymbol{I}^{kT}_{n\Omega}\boldsymbol{e}^{kT}_{pn}\boldsymbol{D}^k_{e\Omega}+\boldsymbol{I}^{kT}_{n\Omega}\boldsymbol{e}^{kT}_{nn}\boldsymbol{D}^k_{en}\Big]F_\tau F_s H^k_\alpha H^k_\beta\ dz\,, \tag{84}$$

$$\boldsymbol{\Pi}^{k\tau s}_{\Phi u}=\int_{A_k}\Big[\boldsymbol{I}^{kT}_{e\Omega}(\boldsymbol{e}^k_{pp}[\boldsymbol{D}^k_p+\boldsymbol{A}^k_p]+\boldsymbol{e}^k_{pn}[\boldsymbol{D}^k_{n\Omega}+\boldsymbol{D}^k_{nz}-\boldsymbol{A}^k_n])\Big]F_\tau F_s H^k_\alpha H^k_\beta\ dz\,, \tag{85}$$

$$\boldsymbol{\Pi}^{k\tau s}_{\Phi\Phi}=\int_{A_k}\Big[\boldsymbol{I}^{kT}_{e\Omega}(-\boldsymbol{\varepsilon}^k_{pp}\boldsymbol{D}^k_{e\Omega})+\boldsymbol{I}^{kT}_{e\Omega}(-\boldsymbol{\varepsilon}^k_{pn}\boldsymbol{D}^k_{en})\Big]F_\tau F_s H^k_\alpha H^k_\beta\ dz\,. \tag{86}$$

5.2 The advanced RMVT($\boldsymbol{u},\Phi,\boldsymbol{\sigma}_n$) case

The steps to obtain the governing equations for the partial extension of RMVT to electro-mechanical case are the same illustrated in Section 5.1 (see D'Ottavio and Kröplin (2006) and Carrera and Brischetto (2007a)). The proposed variational statement considers as primary variables the displacements $\boldsymbol{u}$, the electric potential Φ and the transverse shear/normal stresses $\boldsymbol{\sigma}_n$. Eq.(16) written for a multilayered structure is:

$$\mathrm{R}MVT(\boldsymbol{u},\Phi,\boldsymbol{\sigma}_n):\sum_{k=1}^{N_l}\{\int_{\Omega_k}\int_{A_k}\{\delta\boldsymbol{\varepsilon}^{kT}_{pG}\boldsymbol{\sigma}^k_{pC}+\delta\boldsymbol{\varepsilon}^{kT}_{nG}\boldsymbol{\sigma}^k_{nM}-\delta\boldsymbol{\mathscr{E}}^{kT}_{pG}\boldsymbol{\mathscr{D}}^k_{pC} \tag{87}$$

$$- \delta \mathscr{E}_{nG}^{kT} \mathscr{D}_{nC}^{k} + \delta \boldsymbol{\sigma}_{nM}^{kT} (\boldsymbol{\varepsilon}_{nG}^{k} - \boldsymbol{\varepsilon}_{nC}^{k}) \} d\Omega_k dz_k \} = \sum_{k=1}^{N_l} (\delta L_{in}^{k} + \delta L_{e}^{k}) \, .$$

The governing equations on the domain Ω^k are:

$$\begin{aligned}
\delta \boldsymbol{u}_s^k &: \boldsymbol{K}_{uu}^{k\tau s} \boldsymbol{u}_\tau^k + \boldsymbol{K}_{u\sigma}^{k\tau s} \boldsymbol{\sigma}_{n\tau}^k + \boldsymbol{K}_{u\Phi}^{k\tau s} \Phi_\tau^k = \boldsymbol{P}_{us}^k - \boldsymbol{M}^{k\tau s} \ddot{\boldsymbol{u}}_\tau^k \, , \\
\delta \boldsymbol{\sigma}_{ns}^k &: \boldsymbol{K}_{\sigma u}^{k\tau s} \boldsymbol{u}_\tau^k + \boldsymbol{K}_{\sigma\sigma}^{k\tau s} \boldsymbol{\sigma}_{n\tau}^k + \boldsymbol{K}_{\sigma\Phi}^{k\tau s} \Phi_\tau^k = 0 \, , \\
\delta \Phi_s^k &: \boldsymbol{K}_{\Phi u}^{k\tau s} \boldsymbol{u}_\tau^k + \boldsymbol{K}_{\Phi\sigma}^{k\tau s} \boldsymbol{\sigma}_{n\tau}^k + \boldsymbol{K}_{\Phi\Phi}^{k\tau s} \Phi_\tau^k = \boldsymbol{P}_{\Phi s}^k \, ,
\end{aligned} \tag{88}$$

nine fundamental nuclei are obtained which are completely different from those obtained in Section 5.1.

Corresponding boundary conditions of Dirichlet type are:

$$\begin{aligned}
\boldsymbol{u}_\tau^k &= \bar{\boldsymbol{u}}_\tau^k \\
\Phi_\tau^k &= \bar{\Phi}_\tau^k \, ,
\end{aligned} \tag{89}$$

while the Neumann ones are:

$$\begin{aligned}
\boldsymbol{\Pi}_{uu}^{k\tau s} \boldsymbol{u}_\tau^k + \boldsymbol{\Pi}_{u\sigma}^{k\tau s} \boldsymbol{\sigma}_{n\tau}^k + \boldsymbol{\Pi}_{u\Phi}^{k\tau s} \Phi_\tau^k &= \boldsymbol{\Pi}_{uu}^{k\tau s} \bar{\boldsymbol{u}}_\tau^k + \boldsymbol{\Pi}_{u\sigma}^{k\tau s} \bar{\boldsymbol{\sigma}}_{n\tau}^k + \boldsymbol{\Pi}_{u\Phi}^{k\tau s} \bar{\Phi}_\tau^k \, , \\
\boldsymbol{\Pi}_{\Phi u}^{k\tau s} \boldsymbol{u}_\tau^k + \boldsymbol{\Pi}_{\Phi\sigma}^{k\tau s} \boldsymbol{\sigma}_{n\tau}^k + \boldsymbol{\Pi}_{\Phi\Phi}^{k\tau s} \Phi_\tau^k &= \boldsymbol{\Pi}_{\Phi u}^{k\tau s} \bar{\boldsymbol{u}}_\tau^k + \boldsymbol{\Pi}_{\Phi\sigma}^{k\tau s} \bar{\boldsymbol{\sigma}}_{n\tau}^k + \boldsymbol{\Pi}_{\Phi\Phi}^{k\tau s} \bar{\Phi}_\tau^k \, .
\end{aligned} \tag{90}$$

5.2.1 Plate geometry

Fundamental nuclei on domain Ω_k, after integration by parts for plates (see Eqs.(60) and (61)), are:

$$\boldsymbol{K}_{uu}^{k\tau s} = \int_{A_k} \left[[-\boldsymbol{D}_p]^T \hat{\boldsymbol{C}}_{\sigma_p \varepsilon_p}^k \boldsymbol{D}_p \right] F_s F_\tau dz \, , \tag{91}$$

$$\boldsymbol{K}_{u\sigma}^{k\tau s} = \int_{A_k} \left[-\boldsymbol{D}_p]^T \hat{\boldsymbol{C}}_{\sigma_p \sigma_n}^k + [-\boldsymbol{D}_{n\Omega} + \boldsymbol{D}_{nz}]^T \right] F_s F_\tau dz \, , \tag{92}$$

$$\boldsymbol{K}_{u\Phi}^{k\tau s} = \int_{A_k} \left[[-\boldsymbol{D}_p]^T (-\hat{\boldsymbol{C}}_{\sigma_p \mathscr{E}_p}^k \boldsymbol{D}_{e\Omega} - \hat{\boldsymbol{C}}_{\sigma_p \mathscr{E}_n}^k \boldsymbol{D}_{en}) \right] F_s F_\tau dz \, , \tag{93}$$

$$\boldsymbol{K}_{\sigma u}^{k\tau s} = \int_{A_k} \left[[\boldsymbol{D}_{n\Omega} + \boldsymbol{D}_{nz}] - \hat{\boldsymbol{C}}_{\varepsilon_n \varepsilon_p}^k \boldsymbol{D}_p \right] F_s F_\tau dz \, , \tag{94}$$

$$\boldsymbol{K}_{\sigma\sigma}^{k\tau s} = \int_{A_k} \left[-\hat{\boldsymbol{C}}_{\varepsilon_n \sigma_n}^k \right] F_s F_\tau dz \, , \tag{95}$$

$$\boldsymbol{K}_{\sigma\Phi}^{k\tau s} = \int_{A_k} \left[\hat{\boldsymbol{C}}_{\varepsilon_n \mathscr{E}_p}^k \boldsymbol{D}_{e\Omega} + \hat{\boldsymbol{C}}_{\varepsilon_n \mathscr{E}_n}^k \boldsymbol{D}_{en} \right] F_s F_\tau dz \, , \tag{96}$$

$$\boldsymbol{K}^{k\tau s}_{\Phi u} = \int_{A_k} \left[[-\boldsymbol{D}_{e\Omega}]^T \hat{\boldsymbol{C}}^k_{\mathscr{D}_p\varepsilon_p} + [\boldsymbol{D}_{en}]^T \hat{\boldsymbol{C}}^k_{\mathscr{D}_n\varepsilon_p}) \boldsymbol{D}_p \right] F_s F_\tau dz \,, \tag{97}$$

$$\boldsymbol{K}^{k\tau s}_{\Phi\sigma} = \int_{A_k} \left[[-\boldsymbol{D}_{e\Omega}]^T \hat{\boldsymbol{C}}^k_{\mathscr{D}_p\sigma_n} + [\boldsymbol{D}_{en}]^T \hat{\boldsymbol{C}}^k_{\mathscr{D}_n\sigma_n} \right] F_s F_\tau dz \,, \tag{98}$$

$$\begin{aligned} \boldsymbol{K}^{k\tau s}_{\Phi\Phi} = \int_{A_k} \Big[& [-\boldsymbol{D}_{e\Omega}]^T (-\hat{\boldsymbol{C}}^k_{\mathscr{D}_p\mathscr{E}_p} \boldsymbol{D}_{e\Omega} - \hat{\boldsymbol{C}}^k_{\mathscr{D}_p\mathscr{E}_n} \boldsymbol{D}_{en}) + [\boldsymbol{D}_{en}]^T \\ & (-\hat{\boldsymbol{C}}^k_{\mathscr{D}_n\mathscr{E}_p} \boldsymbol{D}_{e\Omega} - \hat{\boldsymbol{C}}^k_{\mathscr{D}_n\mathscr{E}_n} \boldsymbol{D}_{en}) \Big] F_s F_\tau dz \,. \end{aligned} \tag{99}$$

The inertial array does not change with respect to the Section 5.1.

The *nuclei* for the boundary conditions are:

$$\boldsymbol{\Pi}^{k\tau s}_{uu} = \int_{A_k} \left[\boldsymbol{I}_p^T \hat{\boldsymbol{C}}^k_{\sigma_p\varepsilon_p} \boldsymbol{D}_p \right] F_s F_\tau dz \,, \tag{100}$$

$$\boldsymbol{\Pi}^{k\tau s}_{u\sigma} = \int_{A_k} \left[\boldsymbol{I}_p^T \hat{\boldsymbol{C}}^k_{\sigma_p\sigma_n} + \boldsymbol{I}^T_{n\Omega} \right] F_s F_\tau dz \,, \tag{101}$$

$$\boldsymbol{\Pi}^{k\tau s}_{u\Phi} = \int_{A_k} \left[\boldsymbol{I}_p^T (-\hat{\boldsymbol{C}}^k_{\sigma_p\mathscr{E}_p} \boldsymbol{D}_{e\Omega} - \hat{\boldsymbol{C}}^k_{\sigma_p\mathscr{E}_n} \boldsymbol{D}_{en}) \right] F_s F_\tau dz \,, \tag{102}$$

$$\boldsymbol{\Pi}^{k\tau s}_{\Phi u} = \int_{A_k} \left[\boldsymbol{I}^T_{e\Omega} (\hat{\boldsymbol{C}}^k_{\mathscr{D}_p\varepsilon_p} \boldsymbol{D}_p) \right] F_s F_\tau dz \,, \tag{103}$$

$$\boldsymbol{\Pi}^{k\tau s}_{\Phi\sigma} = \int_{A_k} \left[\boldsymbol{I}^T_{e\Omega} \hat{\boldsymbol{C}}^k_{\mathscr{D}_p\sigma_n} \right] F_s F_\tau dz \,, \tag{104}$$

$$\boldsymbol{\Pi}^{k\tau s}_{\Phi\Phi} = \int_{A_k} \left[\boldsymbol{I}^T_{e\Omega} (-\hat{\boldsymbol{C}}^k_{\mathscr{D}_p\mathscr{E}_p} \boldsymbol{D}_{e\Omega} - \hat{\boldsymbol{C}}^k_{\mathscr{D}_p\mathscr{E}_n} \boldsymbol{D}_{en}) \right] F_s F_\tau dz \,. \tag{105}$$

5.2.2 Shell geometry

Fundamental nuclei on domain Ω_k, after integration by parts for shells (see Eqs.(60) and (77)), are:

$$\boldsymbol{K}^{k\tau s}_{uu} = \int_{A_k} \left[[-\boldsymbol{D}^k_p + \boldsymbol{A}^k_p]^T \hat{\boldsymbol{C}}^k_{\sigma_p\varepsilon_p} [\boldsymbol{D}^k_p + \boldsymbol{A}^k_p] \right] F_s F_\tau H^k_\alpha H^k_\beta \, dz \,, \tag{106}$$

$$\boldsymbol{K}^{k\tau s}_{u\sigma} = \int_{A_k} \left[-\boldsymbol{D}^k_p + \boldsymbol{A}^k_p]^T \hat{\boldsymbol{C}}^k_{\sigma_p\sigma_n} + [-\boldsymbol{D}^k_{n\Omega} + \boldsymbol{D}^k_{nz} - \boldsymbol{A}^k_n]^T \right] F_s F_\tau H^k_\alpha H^k_\beta \, dz \,, \tag{107}$$

$$\boldsymbol{K}^{k\tau s}_{u\Phi} = \int_{A_k} \left[[-\boldsymbol{D}^k_p + \boldsymbol{A}^k_p]^T (-\hat{\boldsymbol{C}}^k_{\sigma_p\mathscr{E}_p} \boldsymbol{D}^k_{e\Omega} - \hat{\boldsymbol{C}}^k_{\sigma_p\mathscr{E}_n} \boldsymbol{D}^k_{en}) \right] F_s F_\tau H^k_\alpha H^k_\beta \, dz \,, \tag{108}$$

$$\boldsymbol{K}^{k\tau s}_{\sigma u} = \int_{A_k} \Big[[\boldsymbol{D}^k_{n\Omega} + \boldsymbol{D}^k_{nz} - \boldsymbol{A}^k_n] - \hat{\boldsymbol{C}}^k_{\varepsilon_n \varepsilon_p} [\boldsymbol{D}^k_p + \boldsymbol{A}^k_p] \Big] F_s F_\tau H^k_\alpha H^k_\beta \, dz \,, \tag{109}$$

$$\boldsymbol{K}^{k\tau s}_{\sigma\sigma} = \int_{A_k} \Big[-\hat{\boldsymbol{C}}^k_{\varepsilon_n \sigma_n} \Big] F_s F_\tau H^k_\alpha H^k_\beta \, dz \,, \tag{110}$$

$$\boldsymbol{K}^{k\tau s}_{\sigma\Phi} = \int_{A_k} \Big[\hat{\boldsymbol{C}}^k_{\varepsilon_n \mathscr{E}_p} \boldsymbol{D}^k_{e\Omega} + \hat{\boldsymbol{C}}^k_{\varepsilon_n \mathscr{E}_n} \boldsymbol{D}^k_{en} \Big] F_s F_\tau H^k_\alpha H^k_\beta \, dz \,, \tag{111}$$

$$\boldsymbol{K}^{k\tau s}_{\Phi u} = \int_{A_k} \Big[([-\boldsymbol{D}^k_{e\Omega}]^T \hat{\boldsymbol{C}}^k_{\mathscr{D}_p \varepsilon_p} + [\boldsymbol{D}^k_{en}]^T \hat{\boldsymbol{C}}^k_{\mathscr{D}^k_n \varepsilon_p}) [\boldsymbol{D}^k_p + \boldsymbol{A}^k_p] \Big] F_s F_\tau H^k_\alpha H^k_\beta \, dz \,, \tag{112}$$

$$\boldsymbol{K}^{k\tau s}_{\Phi\sigma} = \int_{A_k} \Big[[-\boldsymbol{D}^k_{e\Omega}]^T \hat{\boldsymbol{C}}^k_{\mathscr{D}_p \sigma_n} + [\boldsymbol{D}^k_{en}]^T \hat{\boldsymbol{C}}^k_{\mathscr{D}_n \sigma_n} \Big] F_s F_\tau H^k_\alpha H^k_\beta \, dz \,, \tag{113}$$

$$\begin{aligned} \boldsymbol{K}^{k\tau s}_{\Phi\Phi} = \int_{A_k} \Big[& [-\boldsymbol{D}^k_{e\Omega}]^T (-\hat{\boldsymbol{C}}^k_{\mathscr{D}_p \mathscr{E}_p} \boldsymbol{D}^k_{e\Omega} - \hat{\boldsymbol{C}}^k_{\mathscr{D}_p \mathscr{E}_n} \boldsymbol{D}^k_{en}) + [\boldsymbol{D}^k_{en}]^T \\ & (-\hat{\boldsymbol{C}}^k_{\mathscr{D}_n \mathscr{E}_p} \boldsymbol{D}^k_{e\Omega} - \hat{\boldsymbol{C}}^k_{\mathscr{D}_n \mathscr{E}_n} \boldsymbol{D}^k_{en}) \Big] F_s F_\tau H^k_\alpha H^k_\beta \, dz \,. \end{aligned} \tag{114}$$

The inertial array does not change with respect to the section 5.1.
The *nuclei* for the boundary conditions are:

$$\boldsymbol{\Pi}^{k\tau s}_{uu} = \int_{A_k} \Big[\boldsymbol{I}^{kT}_p \hat{\boldsymbol{C}}^k_{\sigma_p \varepsilon_p} [\boldsymbol{D}^k_p + \boldsymbol{A}^k_p] \Big] F_s F_\tau H^k_\alpha H^k_\beta \, dz \,, \tag{115}$$

$$\boldsymbol{\Pi}^{k\tau s}_{u\sigma} = \int_{A_k} \Big[\boldsymbol{I}^{kT}_p \hat{\boldsymbol{C}}^k_{\sigma_p \sigma_n} + \boldsymbol{I}^{kT}_{n\Omega} \Big] F_s F_\tau H^k_\alpha H^k_\beta \, dz \,, \tag{116}$$

$$\boldsymbol{\Pi}^{k\tau s}_{u\Phi} = \int_{A_k} \Big[\boldsymbol{I}^{kT}_p (-\hat{\boldsymbol{C}}^k_{\sigma_p \mathscr{E}_p} \boldsymbol{D}^k_{e\Omega} - \hat{\boldsymbol{C}}^k_{\sigma_p \mathscr{E}_n} \boldsymbol{D}^k_{en}) \Big] F_s F_\tau H^k_\alpha H^k_\beta \, dz \,, \tag{117}$$

$$\boldsymbol{\Pi}^{k\tau s}_{\Phi u} = \int_{A_k} \Big[\boldsymbol{I}^{kT}_{e\Omega} (\hat{\boldsymbol{C}}^k_{\mathscr{D}_p \varepsilon_p} [\boldsymbol{D}^k_p + \boldsymbol{A}^k_p]) \Big] F_s F_\tau H^k_\alpha H^k_\beta \, dz \,, \tag{118}$$

$$\boldsymbol{\Pi}^{k\tau s}_{\Phi\sigma} = \int_{A_k} \Big[\boldsymbol{I}^{kT}_{e\Omega} \hat{\boldsymbol{C}}^k_{\mathscr{D}_p \sigma_n} \Big] F_s F_\tau H^k_\alpha H^k_\beta \, dz \,, \tag{119}$$

$$\boldsymbol{\Pi}^{k\tau s}_{\Phi\Phi} = \int_{A_k} \Big[\boldsymbol{I}^{kT}_{e\Omega} (-\hat{\boldsymbol{C}}^k_{\mathscr{D}_p \mathscr{E}_p} \boldsymbol{D}^k_{e\Omega} - \hat{\boldsymbol{C}}^k_{\mathscr{D}_p \mathscr{E}_n} \boldsymbol{D}^k_{en}) \Big] F_s F_\tau H^k_\alpha H^k_\beta \, dz \,. \tag{120}$$

5.3 The advanced RMVT($u,\Phi,\mathscr{D}_n$) case

Variational statement here illustrated considers as primary variables the displacement $\boldsymbol{u}$, the electric potential Φ and the transverse normal electric displacement $\mathscr{D}_n$. Eq.(24) in case of multilayered structures states [Carrera and Nali (2009)]:

$$\mathrm{R}MVT(\boldsymbol{u},\Phi,\mathscr{D}_n) : \sum_{k=1}^{N_l}\{\int_{\Omega_k}\int_{A_k}\{\delta\boldsymbol{\varepsilon}_{pG}^{kT}\boldsymbol{\sigma}_{pC}^{k}+\delta\boldsymbol{\varepsilon}_{nG}^{kT}\boldsymbol{\sigma}_{nM}^{k}-\delta\mathscr{E}_{pG}^{kT}\mathscr{D}_{pC}^{k}- \tag{121}$$
$$-\delta\mathscr{E}_{nG}^{kT}\mathscr{D}_{nM}^{k}-\delta\boldsymbol{D}_{nM}^{kT}(\mathscr{E}_{nG}^{k}-\mathscr{E}_{nC}^{k})\}d\Omega_k dz_k\} = \sum_{k=1}^{N_l}(\delta L_{in}^{k}+\delta L_{e}^{k})\,.$$

Upon substitution of constitutive equations (symbol C), geometrical relations (symbol G) and CUF, as well as via integration by parts, governing equations are derived:

$$\begin{aligned}
\delta\boldsymbol{u}_s^k &: \boldsymbol{K}_{uu}^{k\tau s}\boldsymbol{u}_\tau^k+\boldsymbol{K}_{u\mathscr{D}}^{k\tau s}\mathscr{D}_{n\tau}^{k}+\boldsymbol{K}_{u\Phi}^{k\tau s}\Phi_\tau^k=\boldsymbol{P}_{us}^{k}-\boldsymbol{M}^{k\tau s}\ddot{\boldsymbol{u}}_\tau^k\,,\\
\delta\mathscr{D}_{ns}^k &: \boldsymbol{K}_{\mathscr{D}u}^{k\tau s}\boldsymbol{u}_\tau^k+\boldsymbol{K}_{\mathscr{D}\mathscr{D}}^{k\tau s}\mathscr{D}_{n\tau}^{k}+\boldsymbol{K}_{\mathscr{D}\Phi}^{k\tau s}\Phi_\tau^k=0\,,\\
\delta\Phi_s^k &: \boldsymbol{K}_{\Phi u}^{k\tau s}\boldsymbol{u}_\tau^k+\boldsymbol{K}_{\Phi\mathscr{D}}^{k\tau s}\mathscr{D}_{n\tau}^{k}+\boldsymbol{K}_{\Phi\Phi}^{k\tau s}\Phi_\tau^k=\boldsymbol{P}_{\Phi s}^{k}\,.
\end{aligned} \tag{122}$$

Corresponding boundary conditions of Dirichlet type are:

$$\begin{aligned}
\boldsymbol{u}_\tau^k &= \bar{\boldsymbol{u}}_\tau^k\,,\\
\Phi_\tau^k &= \bar{\Phi}_\tau^k\,,
\end{aligned} \tag{123}$$

the corresponding Neumann ones are:

$$\begin{aligned}
\boldsymbol{\Pi}_{uu}^{k\tau s}\boldsymbol{u}_\tau^k+\boldsymbol{\Pi}_{u\mathscr{D}}^{k\tau s}\mathscr{D}_{n\tau}^{k}+\boldsymbol{\Pi}_{u\Phi}^{k\tau s}\Phi_\tau^k &= \boldsymbol{\Pi}_{uu}^{k\tau s}\bar{\boldsymbol{u}}_\tau^k+\boldsymbol{\Pi}_{u\mathscr{D}}^{k\tau s}\bar{\mathscr{D}}_{n\tau}^{k}+\boldsymbol{\Pi}_{u\Phi}^{k\tau s}\bar{\Phi}_\tau^k\,,\\
\boldsymbol{\Pi}_{\Phi u}^{k\tau s}\boldsymbol{u}_\tau^k+\boldsymbol{\Pi}_{\Phi\mathscr{D}}^{k\tau s}\mathscr{D}_{n\tau}^{k}+\boldsymbol{\Pi}_{\Phi\Phi}^{k\tau s}\Phi_\tau^k &= \boldsymbol{\Pi}_{\Phi u}^{k\tau s}\bar{\boldsymbol{u}}_\tau^k+\boldsymbol{\Pi}_{\Phi\mathscr{D}}^{k\tau s}\bar{\mathscr{D}}_{n\tau}^{k}+\boldsymbol{\Pi}_{\Phi\Phi}^{k\tau s}\bar{\Phi}_\tau^k\,.
\end{aligned} \tag{124}$$

5.3.1 Plate geometry

Fundamental nuclei on domain Ω_k, after integration by parts for plates (see Eqs.(60) and (61)), are:

$$\begin{aligned}
\boldsymbol{K}_{uu}^{k\tau s} = \int_{A_k}\Big[&[-\boldsymbol{D}_p]^T\,(\bar{\boldsymbol{C}}_{\sigma_p\varepsilon_p}^{k}\,\boldsymbol{D}_p+\bar{\boldsymbol{C}}_{\sigma_p\varepsilon_n}^{k}\,[\boldsymbol{D}_{n\Omega}+\boldsymbol{D}_{nz}])+\\
&[\boldsymbol{D}_{nz}-\boldsymbol{D}_{n\Omega}]^T(\bar{\boldsymbol{C}}_{\sigma_n\varepsilon_p}^{k}\,\boldsymbol{D}_p+\bar{\boldsymbol{C}}_{\sigma_n\varepsilon_n}^{k}\,[\boldsymbol{D}_{n\Omega}+\boldsymbol{D}_{nz}])\Big]F_\tau F_s\,dz\,,
\end{aligned} \tag{125}$$

$$\boldsymbol{K}_{u\mathscr{D}}^{k\tau s} = \int_{A_k}\Big[[\boldsymbol{D}_p]^T\bar{\boldsymbol{C}}_{\sigma_p\mathscr{D}_n}^{k}+[\boldsymbol{D}_{nz}-\boldsymbol{D}_{n\Omega}]^T\bar{\boldsymbol{C}}_{\sigma_n\mathscr{D}_n}^{k}\Big]F_\tau F_s\,dz\,, \tag{126}$$

$$\boldsymbol{K}_{u\Phi}^{k\tau s} = \int_{A_k}\Big[[-\boldsymbol{D}_p]^T(-\bar{\boldsymbol{C}}_{\sigma_p\mathscr{E}_n}^{k}\,\boldsymbol{D}_{e\Omega})+[\boldsymbol{D}_{nz}-\boldsymbol{D}_{n\Omega}]^T(-\bar{\boldsymbol{C}}_{\sigma_n\mathscr{E}_n}^{k}\,\boldsymbol{D}_{e\Omega})\Big]F_\tau F_s\,dz\,, \tag{127}$$

$$\boldsymbol{K}^{k\tau s}_{\mathscr{D}u} = \int_{A_k} \left[\bar{\boldsymbol{C}}^k_{\mathscr{E}_n\varepsilon_p}\, \boldsymbol{D}_p + \bar{\boldsymbol{C}}^k_{\mathscr{E}_n\varepsilon_n}\, [\boldsymbol{D}_{n\Omega} + \boldsymbol{D}_{nz}] \right] F_\tau F_s\, dz\,, \tag{128}$$

$$\boldsymbol{K}^{k\tau s}_{\mathscr{D}\mathscr{D}} = \int_{A_k} \left[\bar{\boldsymbol{C}}^k_{\mathscr{E}_n\mathscr{D}_n} \right] F_\tau F_s\, dz\,, \tag{129}$$

$$\boldsymbol{K}^{k\tau s}_{\mathscr{D}\Phi} = \int_{A_k} \left[\boldsymbol{D}_{en} - \bar{\boldsymbol{C}}^k_{\mathscr{E}_n\mathscr{E}_p}\, \boldsymbol{D}_{e\Omega} \right] F_\tau F_s\, dz\,, \tag{130}$$

$$\boldsymbol{K}^{k\tau s}_{\Phi u} = \int_{A_k} \left[-[\boldsymbol{D}_{e\Omega}]^T (\bar{\boldsymbol{C}}^k_{\mathscr{D}_p\varepsilon_p}\, \boldsymbol{D}_p + \bar{\boldsymbol{C}}^k_{\mathscr{D}_p\varepsilon_n}\, [\boldsymbol{D}_{n\Omega} + \boldsymbol{D}_{nz}]) \right] F_\tau F_s\, dz\,, \tag{131}$$

$$\boldsymbol{K}^{k\tau s}_{\Phi\mathscr{D}} = \int_{A_k} \left[[-\boldsymbol{D}_{e\Omega}]^T \bar{\boldsymbol{C}}^k_{\mathscr{D}_p\mathscr{D}_n} + [\boldsymbol{D}_{en}]^T \right] F_\tau F_s\, dz\,, \tag{132}$$

$$\boldsymbol{K}^{k\tau s}_{\Phi\Phi} = \int_{A_k} \left[[-\boldsymbol{D}_{e\Omega})]^T (-\bar{\boldsymbol{C}}^k_{\mathscr{D}_p\mathscr{E}_p}\, \boldsymbol{D}_{e\Omega}) \right] F_\tau F_s\, dz\,. \tag{133}$$

The inertial array does not change with respect to previous sections.
The *nuclei* for the boundary conditions are:

$$\begin{aligned} \boldsymbol{\Pi}^{k\tau s}_{uu} = \int_{A_k} \Big[& \boldsymbol{I}_p^T\, (\bar{\boldsymbol{C}}^k_{\sigma_p\varepsilon_p}\, \boldsymbol{D}_p + \bar{\boldsymbol{C}}^k_{\sigma_p\varepsilon_n}\, [\boldsymbol{D}_{n\Omega} + \boldsymbol{D}_{nz}]) + \\ & \boldsymbol{I}^T_{n\Omega}\, (\bar{\boldsymbol{C}}^k_{\sigma_n\varepsilon_p}\, \boldsymbol{D}_p + \bar{\boldsymbol{C}}^k_{\sigma_n\varepsilon_n}\, [\boldsymbol{D}_{n\Omega} + \boldsymbol{D}_{nz}]) \Big] F_\tau F_s\, dz\,, \end{aligned} \tag{134}$$

$$\boldsymbol{\Pi}^{k\tau s}_{u\mathscr{D}} = \int_{A_k} \left[\boldsymbol{I}_p^T\, \bar{\boldsymbol{C}}^k_{\sigma_p\mathscr{D}_n} + \boldsymbol{I}^T_{n\Omega}\, \bar{\boldsymbol{C}}^k_{\sigma_n\mathscr{D}_n} \right] F_\tau F_s\, dz\,, \tag{135}$$

$$\boldsymbol{\Pi}^{k\tau s}_{u\Phi} = \int_{A_k} \left[\boldsymbol{I}_p^T\, (-\bar{\boldsymbol{C}}^k_{\sigma_p\mathscr{E}_n}\, \boldsymbol{D}_{e\Omega}) + \boldsymbol{I}^T_{n\Omega}\, (-\bar{\boldsymbol{C}}^k_{\sigma_n\mathscr{E}_n}\, \boldsymbol{D}_{e\Omega}) \right] F_\tau F_s\, dz\,, \tag{136}$$

$$\boldsymbol{\Pi}^{k\tau s}_{\Phi u} = \int_{A_k} \left[\boldsymbol{I}^T_{e\Omega}\, (\bar{\boldsymbol{C}}^k_{\mathscr{D}_p\varepsilon_p}\, \boldsymbol{D}_p + \bar{\boldsymbol{C}}^k_{\mathscr{D}_p\varepsilon_n}\, [\boldsymbol{D}_{n\Omega} + \boldsymbol{D}_{nz}]) \right] F_\tau F_s\, dz\,, \tag{137}$$

$$\boldsymbol{\Pi}^{k\tau s}_{\Phi\mathscr{D}} = \int_{A_k} \left[\boldsymbol{I}^T_{e\Omega}\, \bar{\boldsymbol{C}}^k_{\mathscr{D}_p\mathscr{D}_n} \right] F_\tau F_s\, dz\,, \tag{138}$$

$$\boldsymbol{\Pi}^{k\tau s}_{\Phi\Phi} = \int_{A_k} \left[\boldsymbol{I}^T_{e\Omega}\, (-\bar{\boldsymbol{C}}^k_{\mathscr{D}_p\mathscr{E}_p}\, \boldsymbol{D}_{e\Omega}) \right] F_\tau F_s\, dz\,. \tag{139}$$

5.3.2 Shell geometry

Fundamental nuclei on domain Ω_k, after integration by parts for shells (see Eqs.(60) and (77)), are:

$$\begin{aligned} \boldsymbol{K}^{k\tau s}_{uu} = \int_{A_k} \Big[& [-\boldsymbol{D}^k_p + \boldsymbol{A}^k_p]^T\, (\bar{\boldsymbol{C}}^k_{\sigma_p\varepsilon_p}\, [\boldsymbol{D}^k_p + \boldsymbol{A}^k_p] + \bar{\boldsymbol{C}}^k_{\sigma_p\varepsilon_n}\, [\boldsymbol{D}^k_{n\Omega} + \boldsymbol{D}^k_{nz} - \boldsymbol{A}^k_n]) + \\ & [\boldsymbol{D}^k_{nz} - \boldsymbol{D}^k_{n\Omega} - \boldsymbol{A}^k_n]^T (\bar{\boldsymbol{C}}^k_{\sigma_n\varepsilon_p}\, [\boldsymbol{D}^k_p + \boldsymbol{A}^k_p] + \bar{\boldsymbol{C}}^k_{\sigma_n\varepsilon_n}\, [\boldsymbol{D}^k_{n\Omega} + \boldsymbol{D}^k_{nz} - \boldsymbol{A}^k_n]) \Big] F_\tau F_s H^k_\alpha H^k_\beta\, dz\,, \end{aligned} \tag{140}$$

$$\boldsymbol{K}^{k\tau s}_{u\mathscr{D}} = \int_{A_k} \left[[-\boldsymbol{D}^k_p + \boldsymbol{A}^k_p]^T \bar{\boldsymbol{C}}^k_{\sigma_p \mathscr{D}_n} + [\boldsymbol{D}^k_{nz} - \boldsymbol{D}^k_{n\Omega} - \boldsymbol{A}^k_n]^T \bar{\boldsymbol{C}}^k_{\sigma_n \mathscr{D}_n} \right] F_\tau F_s H^k_\alpha H^k_\beta \, dz \,, \quad (141)$$

$$\boldsymbol{K}^{k\tau s}_{u\Phi} = \int_{A_k} \left[[-\boldsymbol{D}^k_p + \boldsymbol{A}^k_p]^T (-\bar{\boldsymbol{C}}^k_{\sigma_p \mathscr{E}_n} \boldsymbol{D}^k_{e\Omega}) + [\boldsymbol{D}^k_{nz} - \boldsymbol{D}^k_{n\Omega} - \boldsymbol{A}^k_n]^T (-\bar{\boldsymbol{C}}^k_{\sigma_n \mathscr{E}_n} \boldsymbol{D}^k_{e\Omega}) \right] F_\tau F_s H^k_\alpha H^k_\beta \, dz \,, \quad (142)$$

$$\boldsymbol{K}^{k\tau s}_{\mathscr{D}u} = \int_{A_k} \left[\bar{\boldsymbol{C}}^k_{\mathscr{E}_n \varepsilon_p} [\boldsymbol{D}^k_p + \boldsymbol{A}^k_p] + \bar{\boldsymbol{C}}^k_{\mathscr{E}_n \varepsilon_n} [\boldsymbol{D}^k_{n\Omega} + \boldsymbol{D}^k_{nz} - \boldsymbol{A}^k_n] \right] F_\tau F_s H^k_\alpha H^k_\beta \, dz \,, \quad (143)$$

$$\boldsymbol{K}^{k\tau s}_{\mathscr{D}\mathscr{D}} = \int_{A_k} \left[\bar{\boldsymbol{C}}^k_{\mathscr{E}_n \mathscr{D}_n} \right] F_\tau F_s H^k_\alpha H^k_\beta \, dz \,, \quad (144)$$

$$\boldsymbol{K}^{k\tau s}_{\mathscr{D}\Phi} = \int_{A_k} \left[\boldsymbol{D}^k_{en} - \bar{\boldsymbol{C}}^k_{\mathscr{E}_n \mathscr{E}_p} \boldsymbol{D}^k_{e\Omega} \right] F_\tau F_s H^k_\alpha H^k_\beta \, dz \,, \quad (145)$$

$$\boldsymbol{K}^{k\tau s}_{\Phi u} = \int_{A_k} \left[-[\boldsymbol{D}^k_{e\Omega}]^T (\bar{\boldsymbol{C}}^k_{\mathscr{D}_p \varepsilon_p} [\boldsymbol{D}^k_p + \boldsymbol{A}^k_p] + \bar{\boldsymbol{C}}^k_{\mathscr{D}_p \varepsilon_n} [\boldsymbol{D}^k_{n\Omega} + \boldsymbol{D}^k_{nz} - \boldsymbol{A}^k_n]) \right] F_\tau F_s H^k_\alpha H^k_\beta \, dz \,, \quad (146)$$

$$\boldsymbol{K}^{k\tau s}_{\Phi\mathscr{D}} = \int_{A_k} \left[[-\boldsymbol{D}^k_{e\Omega}]^T \bar{\boldsymbol{C}}^k_{\mathscr{D}_p \mathscr{D}_n} + [\boldsymbol{D}^k_{en}]^T \right] F_\tau F_s H^k_\alpha H^k_\beta \, dz \,, \quad (147)$$

$$\boldsymbol{K}^{k\tau s}_{\Phi\Phi} = \int_{A_k} \left[[-\boldsymbol{D}^k_{e\Omega}]^T (-\bar{\boldsymbol{C}}^k_{\mathscr{D}_p \mathscr{E}_p} \boldsymbol{D}^k_{e\Omega}) \right] F_\tau F_s H^k_\alpha H^k_\beta \, dz \,. \quad (148)$$

The inertial array does not change with respect to previous sections.
The *nuclei* for the boundary conditions are:

$$\boldsymbol{\Pi}^{k\tau s}_{uu} = \int_{A_k} \left[\boldsymbol{I}^{kT}_p (\bar{\boldsymbol{C}}^k_{\sigma_p \varepsilon_p} [\boldsymbol{D}^k_p + \boldsymbol{A}^k_p] + \bar{\boldsymbol{C}}^k_{\sigma_p \varepsilon_n} [\boldsymbol{D}^k_{n\Omega} + \boldsymbol{D}^k_{nz} - \boldsymbol{A}^k_n]) + \boldsymbol{I}^{kT}_{n\Omega} (\bar{\boldsymbol{C}}^k_{\sigma_n \varepsilon_p} [\boldsymbol{D}^k_p + \boldsymbol{A}^k_p] + \bar{\boldsymbol{C}}^k_{\sigma_n \varepsilon_n} [\boldsymbol{D}^k_{n\Omega} + \boldsymbol{D}^k_{nz} - \boldsymbol{A}^k_n]) \right] F_\tau F_s H^k_\alpha H^k_\beta \, dz \,, \quad (149)$$

$$\boldsymbol{\Pi}^{k\tau s}_{u\mathscr{D}} = \int_{A_k} \left[\boldsymbol{I}^{kT}_p \bar{\boldsymbol{C}}^k_{\sigma_p \mathscr{D}_n} + \boldsymbol{I}^{kT}_{n\Omega} \bar{\boldsymbol{C}}^k_{\sigma_n \mathscr{D}_n} \right] F_\tau F_s H^k_\alpha H^k_\beta \, dz \,, \quad (150)$$

$$\boldsymbol{\Pi}^{k\tau s}_{u\Phi} = \int_{A_k} \left[\boldsymbol{I}^{kT}_p (-\bar{\boldsymbol{C}}^k_{\sigma_p \mathscr{E}_n} \boldsymbol{D}^k_{e\Omega}) + \boldsymbol{I}^{kT}_{n\Omega} (-\bar{\boldsymbol{C}}^k_{\sigma_n \mathscr{E}_n} \boldsymbol{D}^k_{e\Omega}) \right] F_\tau F_s H^k_\alpha H^k_\beta \, dz \,, \quad (151)$$

$$\boldsymbol{\Pi}^{k\tau s}_{\Phi u} = \int_{A_k} \left[\boldsymbol{I}^{kT}_{e\Omega} (\bar{\boldsymbol{C}}^k_{\mathscr{D}_p \varepsilon_p} [\boldsymbol{D}^k_p + \boldsymbol{A}^k_p] + \bar{\boldsymbol{C}}^k_{\mathscr{D}_p \varepsilon_n} [\boldsymbol{D}^k_{n\Omega} + \boldsymbol{D}^k_{nz} - \boldsymbol{A}^k_n]) \right] F_\tau F_s H^k_\alpha H^k_\beta \, dz \,, \quad (152)$$

$$\boldsymbol{\Pi}^{k\tau s}_{\Phi\mathscr{D}} = \int_{A_k} \left[\boldsymbol{I}^{kT}_{e\Omega} \bar{\boldsymbol{C}}^k_{\mathscr{D}_p \mathscr{D}_n} \right] F_\tau F_s H^k_\alpha H^k_\beta \, dz \,, \quad (153)$$

$$\boldsymbol{\Pi}^{k\tau s}_{\Phi\Phi} = \int_{A_k} \left[\boldsymbol{I}^{kT}_{e\Omega} (-\bar{\boldsymbol{C}}^k_{\mathscr{D}_p \mathscr{E}_p} \boldsymbol{D}^k_{e\Omega}) \right] F_\tau F_s H^k_\alpha H^k_\beta \, dz \,. \quad (154)$$

5.4 The advanced RMVT($\boldsymbol{u},\Phi,\boldsymbol{\sigma}_n,\mathscr{D}_n$) case

Governing equations, boundary conditions and fundamental nuclei for the full extension of RMTV are presented in this section. Displacement $\boldsymbol{u}$, transverse shear/normal stresses $\boldsymbol{\sigma}_n$, electric potential Φ and transverse normal electric displacement $\mathscr{D}_n$ are the chosen primary variables (see Carrera and Brischetto (2007b)). The Eq.(30) states:

$$\mathrm{R}MVT(\boldsymbol{u},\Phi,\boldsymbol{\sigma}_n,\mathscr{D}_n):\sum_{k=1}^{N_l}\{\int_{\Omega_k}\int_{A_k}\{\delta\boldsymbol{\varepsilon}_{pG}^{kT}\boldsymbol{\sigma}_{pC}^{k}+\delta\boldsymbol{\varepsilon}_{nG}^{kT}\boldsymbol{\sigma}_{nM}^{k}-\delta\mathscr{E}_{pG}^{kT}\mathscr{D}_{pC}^{k}-\delta\mathscr{E}_{nG}^{kT}\mathscr{D}_{nM}^{k}$$
$$+\delta\boldsymbol{\sigma}_{nM}^{kT}(\boldsymbol{\varepsilon}_{nG}^{k}-\boldsymbol{\varepsilon}_{nC}^{k})-\delta\mathscr{D}_{nM}^{kT}(\mathscr{E}_{nG}^{k}-\mathscr{E}_{nC}^{k})\}d\Omega_k dz_k\}=\sum_{k=1}^{N_l}(\delta L_{in}^{k}+\delta L_{e}^{k})\,. \quad (155)$$

Governing equations on domain Ω_k are:

$$\begin{aligned}
\delta\boldsymbol{u}_s^k &: \boldsymbol{K}_{uu}^{k\tau s}\boldsymbol{u}_\tau^k+\boldsymbol{K}_{u\sigma}^{k\tau s}\boldsymbol{\sigma}_{n\tau}^k+\boldsymbol{K}_{u\Phi}^{k\tau s}\Phi_\tau^k+\boldsymbol{K}_{u\mathscr{D}}^{k\tau s}\mathscr{D}_{n\tau}^k=\boldsymbol{P}_{us}^k-\boldsymbol{M}^{k\tau s}\ddot{\boldsymbol{u}}_\tau^k\,,\\
\delta\boldsymbol{\sigma}_{ns}^k &: \boldsymbol{K}_{\sigma u}^{k\tau s}\boldsymbol{u}_\tau^k+\boldsymbol{K}_{\sigma\sigma}^{k\tau s}\boldsymbol{\sigma}_{n\tau}^k+\boldsymbol{K}_{\sigma\Phi}^{k\tau s}\Phi_\tau^k+\boldsymbol{K}_{\sigma\mathscr{D}}^{k\tau s}\mathscr{D}_{n\tau}^k=0\,,\\
\delta\boldsymbol{\Phi}_s^k &: \boldsymbol{K}_{\Phi u}^{k\tau s}\boldsymbol{u}_\tau^k+\boldsymbol{K}_{\Phi\sigma}^{k\tau s}\boldsymbol{\sigma}_{n\tau}^k+\boldsymbol{K}_{\Phi\Phi}^{k\tau s}\Phi_\tau^k+\boldsymbol{K}_{\Phi\mathscr{D}}^{k\tau s}\mathscr{D}_{n\tau}^k=\boldsymbol{P}_{\Phi s}^k\,,\\
\delta\mathscr{D}_{ns}^k &: \boldsymbol{K}_{\mathscr{D}u}^{k\tau s}\boldsymbol{u}_\tau^k+\boldsymbol{K}_{\mathscr{D}\sigma}^{k\tau s}\boldsymbol{\sigma}_{n\tau}^k+\boldsymbol{K}_{\mathscr{D}\Phi}^{k\tau s}\Phi_\tau^k+\boldsymbol{K}_{\mathscr{D}\mathscr{D}}^{k\tau s}\mathscr{D}_{n\tau}^k=0\,,
\end{aligned} \quad (156)$$

Dirichlet type boundary conditions are:

$$\begin{aligned}
\boldsymbol{u}_\tau^k&=\bar{\boldsymbol{u}}_\tau^k\\
\Phi_\tau^k&=\bar{\Phi}_\tau^k
\end{aligned} \quad (157)$$

the Neumann ones are:

$$\begin{aligned}
&\boldsymbol{\Pi}_{uu}^{k\tau s}\,\boldsymbol{u}_\tau^k+\boldsymbol{\Pi}_{u\sigma}^{k\tau s}\,\boldsymbol{\sigma}_{nM\tau}^k+\boldsymbol{\Pi}_{u\Phi}^{k\tau s}\,\Phi_\tau^k+\boldsymbol{\Pi}_{u\mathscr{D}}^{k\tau s}\,\mathscr{D}_{nM\tau}^k=\boldsymbol{\Pi}_{uu}^{k\tau s}\,\bar{\boldsymbol{u}}_\tau^k+\boldsymbol{\Pi}_{u\sigma}^{k\tau s}\,\bar{\boldsymbol{\sigma}}_{nM\tau}^k\\
&+\boldsymbol{\Pi}_{u\Phi}^{k\tau s}\,\bar{\Phi}_\tau^k+\boldsymbol{\Pi}_{u\mathscr{D}}^{k\tau s}\,\bar{\mathscr{D}}_{nM\tau}^k\,,\\
&\boldsymbol{\Pi}_{\Phi u}^{k\tau s}\,\boldsymbol{u}_\tau^k+\boldsymbol{\Pi}_{\Phi\sigma}^{k\tau s}\,\boldsymbol{\sigma}_{nM\tau}^k+\boldsymbol{\Pi}_{\Phi\Phi}^{k\tau s}\,\Phi_\tau^k+\boldsymbol{\Pi}_{\Phi\mathscr{D}}^{k\tau s}\,\mathscr{D}_{nM\tau}^k=\boldsymbol{\Pi}_{\Phi u}^{k\tau s}\,\bar{\boldsymbol{u}}_\tau^k+\boldsymbol{\Pi}_{\Phi\sigma}^{k\tau s}\,\bar{\boldsymbol{\sigma}}_{nM\tau}^k\\
&+\boldsymbol{\Pi}_{\Phi\Phi}^{k\tau s}\,\bar{\Phi}_\tau^k+\boldsymbol{\Pi}_{\Phi\mathscr{D}}^{k\tau s}\,\bar{\mathscr{D}}_{nM\tau}^k\,.
\end{aligned} \quad (158)$$

5.4.1 Plate geometry

Explicit forms of the fundamental *nuclei* on the domain Ω^k, after integration by parts for plates (see Eqs.(60) and (61)), are:

$$\boldsymbol{K}_{uu}^{k\tau s}=\int_{A_k}\left[(-\boldsymbol{D}_p)^T(\tilde{\boldsymbol{C}}_{\sigma_p\varepsilon_p}^{k}\boldsymbol{D}_p)\right]F_sF_\tau dz\,, \quad (159)$$

$$\boldsymbol{K}_{u\sigma}^{k\tau s} = \int_{A_k} \left[(-\boldsymbol{D}_p)^T (\tilde{\boldsymbol{C}}^k_{\sigma_p\sigma_n}) + (-\boldsymbol{D}_{n\Omega} + \boldsymbol{D}_{nz})^T \right] F_s F_\tau dz \,, \tag{160}$$

$$\boldsymbol{K}_{u\Phi}^{k\tau s} = \int_{A_k} \left[(-\boldsymbol{D}_p)^T (-\tilde{\boldsymbol{C}}^k_{\sigma_p\mathscr{E}_p} \boldsymbol{D}_{e\Omega}) \right] F_s F_\tau dz \,, \tag{161}$$

$$\boldsymbol{K}_{u\mathscr{D}}^{k\tau s} = \int_{A_k} \left[(-\boldsymbol{D}_p)^T (\tilde{\boldsymbol{C}}^k_{\sigma_p\mathscr{D}_n}) \right] F_s F_\tau dz \,, \tag{162}$$

$$\boldsymbol{K}_{\sigma u}^{k\tau s} = \int_{A_k} \left[(\boldsymbol{D}_{n\Omega} + \boldsymbol{D}_{nz}) - (\tilde{\boldsymbol{C}}^k_{\varepsilon_n\varepsilon_p} \boldsymbol{D}_p) \right] F_s F_\tau dz \,, \tag{163}$$

$$\boldsymbol{K}_{\sigma\sigma}^{k\tau s} = \int_{A_k} \left[-\tilde{\boldsymbol{C}}^k_{\varepsilon_n\sigma_n} \right] F_s F_\tau dz \,, \tag{164}$$

$$\boldsymbol{K}_{\sigma\Phi}^{k\tau s} = \int_{A_k} \left[\tilde{\boldsymbol{C}}^k_{\varepsilon_n\mathscr{E}_p} \boldsymbol{D}_{e\Omega} \right] F_s F_\tau dz \,, \tag{165}$$

$$\boldsymbol{K}_{\sigma\mathscr{D}}^{k\tau s} = \int_{A_k} \left[-\tilde{\boldsymbol{C}}^k_{\varepsilon_n\mathscr{D}_n} \right] F_s F_\tau dz \,, \tag{166}$$

$$\boldsymbol{K}_{\Phi u}^{k\tau s} = \int_{A_k} \left[-\boldsymbol{D}^T_{e\Omega} \tilde{\boldsymbol{C}}^k_{\mathscr{D}_p\varepsilon_p} \boldsymbol{D}_p \right] F_s F_\tau dz \,, \tag{167}$$

$$\boldsymbol{K}_{\Phi\sigma}^{k\tau s} = \int_{A_k} \left[-\boldsymbol{D}^T_{e\Omega} \tilde{\boldsymbol{C}}^k_{\mathscr{D}_p\sigma_n} \right] F_s F_\tau dz \,, \tag{168}$$

$$\boldsymbol{K}_{\Phi\Phi}^{k\tau s} = \int_{A_k} \left[\boldsymbol{D}^T_{e\Omega} \tilde{\boldsymbol{C}}^k_{\mathscr{D}_p\mathscr{E}_p} \boldsymbol{D}_{e\Omega} \right] F_s F_\tau dz \,, \tag{169}$$

$$\boldsymbol{K}_{\Phi\mathscr{D}}^{k\tau s} = \int_{A_k} \left[-\boldsymbol{D}^T_{e\Omega} \tilde{\boldsymbol{C}}^k_{\mathscr{D}_p\mathscr{D}_n} + \boldsymbol{D}^T_{en} \right] F_s F_\tau dz \,, \tag{170}$$

$$\boldsymbol{K}_{\mathscr{D}u}^{k\tau s} = \int_{A_k} \left[\tilde{\boldsymbol{C}}^k_{\mathscr{E}_n\varepsilon_p} \boldsymbol{D}^T_p \right] F_s F_\tau dz \,, \tag{171}$$

$$\boldsymbol{K}_{\mathscr{D}\sigma}^{k\tau s} = \int_{A_k} \left[\tilde{\boldsymbol{C}}^k_{\mathscr{E}_n\sigma_n} \right] F_s F_\tau dz \,, \tag{172}$$

$$\boldsymbol{K}_{\mathscr{D}\Phi}^{k\tau s} = \int_{A_k} \left[\boldsymbol{D}_{en} - \tilde{\boldsymbol{C}}^k_{\mathscr{E}_n\mathscr{E}_p} \boldsymbol{D}_{e\Omega} \right] F_s F_\tau dz \,, \tag{173}$$

$$\boldsymbol{K}_{\mathscr{D}\mathscr{D}}^{k\tau s} = \int_{A_k} \left[\tilde{\boldsymbol{C}}^k_{\mathscr{E}_n\mathscr{D}_n} \right] F_s F_\tau dz \,. \tag{174}$$

The expression of the inertial matrix is the same of the other PVD and RMVT variational statements.

The fundamental *nuclei* on the boundary Γ^k are:

$$\mathbf{\Pi}^{k\tau s}_{uu} = \int_{A_k} \left[\boldsymbol{I}_p^T \tilde{\boldsymbol{C}}^k_{\sigma_p \varepsilon_p} \boldsymbol{D}_p \right] F_s F_\tau dz \,, \tag{175}$$

$$\mathbf{\Pi}^{k\tau s}_{u\sigma} = \int_{A_k} \left[\boldsymbol{I}_p^T \tilde{\boldsymbol{C}}^k_{\sigma_p \sigma_n} + \boldsymbol{I}^T_{n\Omega} \right] F_s F_\tau dz \,, \tag{176}$$

$$\mathbf{\Pi}^{k\tau s}_{u\Phi} = \int_{A_k} \left[-\boldsymbol{I}_p^T \tilde{\boldsymbol{C}}^k_{\sigma_p \mathscr{E}_p} \boldsymbol{D}_{e\Omega} \right] F_s F_\tau dz \,, \tag{177}$$

$$\mathbf{\Pi}^{k\tau s}_{u\mathscr{D}} = \int_{A_k} \left[\boldsymbol{I}_p^T \tilde{\boldsymbol{C}}^k_{\sigma_p \mathscr{D}_n} \right] F_s F_\tau dz \,, \tag{178}$$

$$\mathbf{\Pi}^{k\tau s}_{\Phi u} = \int_{A_k} \left[\boldsymbol{I}^T_{e\Omega} \tilde{\boldsymbol{C}}^k_{\mathscr{D}_p \varepsilon_p} \boldsymbol{D}_p \right] F_s F_\tau dz \,, \tag{179}$$

$$\mathbf{\Pi}^{k\tau s}_{\Phi\sigma} = \int_{A_k} \left[\boldsymbol{I}^T_{e\Omega} \tilde{\boldsymbol{C}}^k_{\mathscr{D}_p \sigma_n} \right] F_s F_\tau dz \,, \tag{180}$$

$$\mathbf{\Pi}^{k\tau s}_{\Phi\Phi} = \int_{A_k} \left[-\boldsymbol{I}^T_{e\Omega} \tilde{\boldsymbol{C}}^k_{\mathscr{D}_p \mathscr{E}_p} \boldsymbol{D}_{e\Omega} \right] F_s F_\tau dz \,, \tag{181}$$

$$\mathbf{\Pi}^{k\tau s}_{\Phi\mathscr{D}} = \int_{A_k} \left[\boldsymbol{I}^T_{e\Omega} \tilde{\boldsymbol{C}}^k_{\mathscr{D}_p \mathscr{D}_n} \right] F_s F_\tau dz \,. \tag{182}$$

5.4.2 Shell geometry

Fundamental nuclei on domain Ω_k, after integration by parts for shells (see Eqs.(60) and (77)), are:

$$\boldsymbol{K}^{k\tau s}_{uu} = \int_{A_k} \left[[-\boldsymbol{D}^k_p + \boldsymbol{A}^k_p]^T \, \tilde{\boldsymbol{C}}^k_{\sigma_p \varepsilon_p} [\boldsymbol{D}^k_p + \boldsymbol{A}^k_p] \right] F_s F_\tau H^k_\alpha H^k_\beta \, dz \,, \tag{183}$$

$$\boldsymbol{K}^{k\tau s}_{u\sigma} = \int_{A_k} \left[[-\boldsymbol{D}^k_p + \boldsymbol{A}^k_p]^T \, \tilde{\boldsymbol{C}}^k_{\sigma_p \sigma_n} + [-\boldsymbol{D}^k_{n\Omega} + \boldsymbol{D}^k_{nz} - \boldsymbol{A}^k_n]^T \right] F_s F_\tau H^k_\alpha H^k_\beta \, dz \,, \tag{184}$$

$$\boldsymbol{K}^{k\tau s}_{u\Phi} = \int_{A_k} \left[[-\boldsymbol{D}^k_p + \boldsymbol{A}^k_p]^T \, (-\tilde{\boldsymbol{C}}^k_{\sigma_p \mathscr{E}_p} \boldsymbol{D}^k_{e\Omega}) \right] F_s F_\tau H^k_\alpha H^k_\beta \, dz \,, \tag{185}$$

$$\boldsymbol{K}^{k\tau s}_{u\mathscr{D}} = \int_{A_k} \left[[-\boldsymbol{D}^k_p + \boldsymbol{A}^k_p]^T \, \tilde{\boldsymbol{C}}^k_{\sigma_p \mathscr{D}_n} \right] F_s F_\tau H^k_\alpha H^k_\beta \, dz \,, \tag{186}$$

$$\boldsymbol{K}^{k\tau s}_{\sigma u} = \int_{A_k} \left[[\boldsymbol{D}^k_{n\Omega} + \boldsymbol{D}^k_{nz} - \boldsymbol{A}^k_n] - (\tilde{\boldsymbol{C}}^k_{\varepsilon_n\varepsilon_p} [\boldsymbol{D}^k_p + \boldsymbol{A}^k_p]) \right] F_s F_\tau H^k_\alpha H^k_\beta \, dz \,, \tag{187}$$

$$\boldsymbol{K}^{k\tau s}_{\sigma\sigma} = \int_{A_k} \left[-\tilde{\boldsymbol{C}}^k_{\varepsilon_n\sigma_n} \right] F_s F_\tau H^k_\alpha H^k_\beta \, dz \,, \tag{188}$$

$$\boldsymbol{K}^{k\tau s}_{\sigma\Phi} = \int_{A_k} \left[\tilde{\boldsymbol{C}}^k_{\varepsilon_n\mathscr{E}_p} \boldsymbol{D}^k_{e\Omega} \right] F_s F_\tau H^k_\alpha H^k_\beta \, dz \,, \tag{189}$$

$$\boldsymbol{K}^{k\tau s}_{\sigma\mathscr{D}} = \int_{A_k} \left[-\tilde{\boldsymbol{C}}^k_{\varepsilon_n\mathscr{D}_n} \right] F_s F_\tau H^k_\alpha H^k_\beta \, dz \,, \tag{190}$$

$$\boldsymbol{K}^{k\tau s}_{\Phi u} = \int_{A_k} \left[-\boldsymbol{D}^{kT}_{e\Omega} \tilde{\boldsymbol{C}}^k_{\mathscr{D}_p\varepsilon_p} [\boldsymbol{D}^k_p + \boldsymbol{A}^k_p] \right] F_s F_\tau H^k_\alpha H^k_\beta \, dz \,, \tag{191}$$

$$\boldsymbol{K}^{k\tau s}_{\Phi\sigma} = \int_{A_k} \left[-\boldsymbol{D}^{kT}_{e\Omega} \tilde{\boldsymbol{C}}^k_{\mathscr{D}_p\sigma_n} \right] F_s F_\tau H^k_\alpha H^k_\beta \, dz \,, \tag{192}$$

$$\boldsymbol{K}^{k\tau s}_{\Phi\Phi} = \int_{A_k} \left[\boldsymbol{D}^{kT}_{e\Omega} \tilde{\boldsymbol{C}}^k_{\mathscr{D}_p\mathscr{E}_p} \boldsymbol{D}^k_{e\Omega} \right] F_s F_\tau H^k_\alpha H^k_\beta \, dz \,, \tag{193}$$

$$\boldsymbol{K}^{k\tau s}_{\Phi\mathscr{D}} = \int_{A_k} \left[-\boldsymbol{D}^{kT}_{e\Omega} \tilde{\boldsymbol{C}}^k_{\mathscr{D}_p\mathscr{D}_n} + \boldsymbol{D}^{kT}_{en} \right] F_s F_\tau H^k_\alpha H^k_\beta \, dz \,, \tag{194}$$

$$\boldsymbol{K}^{k\tau s}_{\mathscr{D}u} = \int_{A_k} \left[\tilde{\boldsymbol{C}}^k_{\mathscr{E}_n\varepsilon_p} [\boldsymbol{D}^k_p + \boldsymbol{A}^k_p]^T \right] F_s F_\tau H^k_\alpha H^k_\beta \, dz \,, \tag{195}$$

$$\boldsymbol{K}^{k\tau s}_{\mathscr{D}\sigma} = \int_{A_k} \left[\tilde{\boldsymbol{C}}^k_{\mathscr{E}_n\sigma_n} \right] F_s F_\tau H^k_\alpha H^k_\beta \, dz \,, \tag{196}$$

$$\boldsymbol{K}^{k\tau s}_{\mathscr{D}\Phi} = \int_{A_k} \left[\boldsymbol{D}^k_{en} - \tilde{\boldsymbol{C}}^k_{\mathscr{E}_n\mathscr{E}_p} \boldsymbol{D}^k_{e\Omega} \right] F_s F_\tau H^k_\alpha H^k_\beta \, dz \,, \tag{197}$$

$$\boldsymbol{K}^{k\tau s}_{\mathscr{D}\mathscr{D}} = \int_{A_k} \left[\tilde{\boldsymbol{C}}^k_{\mathscr{E}_n\mathscr{D}_n} \right] F_s F_\tau H^k_\alpha H^k_\beta \, dz \,. \tag{198}$$

The expression of the inertial array is the same of the other PVD and RMVT variational statements.

The fundamental *nuclei* on the boundary Γ^k are:

$$\boldsymbol{\Pi}^{k\tau s}_{uu} = \int_{A_k} \left[\boldsymbol{I}^{kT}_p \tilde{\boldsymbol{C}}^k_{\sigma_p\varepsilon_p} [\boldsymbol{D}^k_p + \boldsymbol{A}^k_p] \right] F_s F_\tau H^k_\alpha H^k_\beta \, dz \,, \tag{199}$$

$$\mathbf{\Pi}^{k\tau s}_{u\sigma} = \int\limits_{A_k} \left[\boldsymbol{I}^{kT}_{p} \tilde{\boldsymbol{C}}^{k}_{\sigma_p \sigma_n} + \boldsymbol{I}^{kT}_{n\Omega} \right] F_s F_\tau H^k_\alpha H^k_\beta \, dz \,, \tag{200}$$

$$\mathbf{\Pi}^{k\tau s}_{u\Phi} = \int\limits_{A_k} \left[-\boldsymbol{I}^{kT}_{p} \tilde{\boldsymbol{C}}^{k}_{\sigma_p \mathscr{E}_p} \boldsymbol{D}^{k}_{e\Omega} \right] F_s F_\tau H^k_\alpha H^k_\beta \, dz \,, \tag{201}$$

$$\mathbf{\Pi}^{k\tau s}_{u\mathscr{D}} = \int\limits_{A_k} \left[\boldsymbol{I}^{kT}_{p} \tilde{\boldsymbol{C}}^{k}_{\sigma_p \mathscr{D}_n} \right] F_s F_\tau H^k_\alpha H^k_\beta \, dz \,, \tag{202}$$

$$\mathbf{\Pi}^{k\tau s}_{\Phi u} = \int\limits_{A_k} \left[\boldsymbol{I}^{kT}_{e\Omega} \tilde{\boldsymbol{C}}^{k}_{\mathscr{D}_p \varepsilon_p} [\boldsymbol{D}^{k}_{p} + \boldsymbol{A}^{k}_{p}] \right] F_s F_\tau H^k_\alpha H^k_\beta \, dz \,, \tag{203}$$

$$\mathbf{\Pi}^{k\tau s}_{\Phi\sigma} = \int\limits_{A_k} \left[\boldsymbol{I}^{kT}_{e\Omega} \tilde{\boldsymbol{C}}^{k}_{\mathscr{D}_p \sigma_n} \right] F_s F_\tau H^k_\alpha H^k_\beta \, dz \,, \tag{204}$$

$$\mathbf{\Pi}^{k\tau s}_{\Phi\Phi} = \int\limits_{A_k} \left[-\boldsymbol{I}^{kT}_{e\Omega} \tilde{\boldsymbol{C}}^{k}_{\mathscr{D}_p \mathscr{E}_p} \boldsymbol{D}^{k}_{e\Omega} \right] F_s F_\tau H^k_\alpha H^k_\beta \, dz \,, \tag{205}$$

$$\mathbf{\Pi}^{k\tau s}_{\Phi\mathscr{D}} = \int\limits_{A_k} \left[\boldsymbol{I}^{kT}_{e\Omega} \tilde{\boldsymbol{C}}^{k}_{\mathscr{D}_p \mathscr{D}_n} \right] F_s F_\tau H^k_\alpha H^k_\beta \, dz \,. \tag{206}$$

6 Closed form solution

Navier-type closed form solutions are applied to the proposed governing equations if the considered materials fulfill the following conditions:

$$\begin{aligned} &C_{16} = C_{26} = C_{36} = C_{45} = 0 \,, \\ &e_{25} = e_{14} = e_{36} = 0 \,, \\ &\varepsilon_{12} = \varepsilon_{21} = 0 \,. \end{aligned} \tag{207}$$

The following harmonic assumptions can be made for the field variables in the case of plate geometry:

$$\begin{aligned} (u^k_{x_\tau}, \sigma^k_{xz_\tau}) &= \sum_{m,n} (\hat{U}^k_{x_\tau}, \hat{\sigma}^k_{xz_\tau}) \cos\frac{m\pi x_k}{a_k} \, \sin\frac{n\pi y_k}{b_k} \, e^{i\omega_{mn}t} \,, \; k = 1, N_l \,, \\ (u^k_{y_\tau}, \sigma^k_{yz_\tau}) &= \sum_{m,n} (\hat{U}^k_{y_\tau}, \hat{\sigma}^k_{yz_\tau}) \sin\frac{m\pi x_k}{a_k} \, \cos\frac{n\pi y_k}{b_k} \, e^{i\omega_{mn}t} \,, \; \tau = t, b, r \,, \\ (u^k_{z_\tau}, \sigma^k_{zz_\tau}, \Phi^k_\tau, \mathscr{D}^k_{z_\tau}) &= \sum_{m,n} (\hat{U}^k_{z_\tau}, \hat{\sigma}^k_{zz_\tau}, \hat{\Phi}^k_\tau, \hat{\mathscr{D}}^k_{z_\tau}) \sin\frac{m\pi x_k}{a_k} \, \sin\frac{n\pi y_k}{b_k} \, e^{i\omega_{mn}t} \,, \; r = 2, N \,, \end{aligned} \tag{208}$$

in which a_k and b_k are the plate lengths in the x_k and y_k directions, respectively; m and n are the corresponding waves numbers; $i = \sqrt{-1}$, t is the time and ω_{mn} is the circular frequency. The quantities with $\hat{}$ indicate the amplitudes.

The following assumptions for the field variables in the case of shell geometry consider the curvilinear coordinates (α, β, z):

$$
\begin{aligned}
(u^k_{\alpha_\tau}, \sigma^k_{\alpha z_\tau}) &= \sum_{m,n} (\hat{U}^k_{\alpha_\tau}, \hat{\sigma}^k_{\alpha z_\tau}) \cos\frac{m\pi\alpha_k}{a_k} \sin\frac{n\pi\beta_k}{b_k} e^{i\omega_{mn}t} \ , k = 1, N_l \\
(u^k_{\beta_\tau}, \sigma^k_{\beta z_\tau}) &= \sum_{m,n} (\hat{U}^k_{\beta_\tau}, \hat{\sigma}^k_{\beta z_\tau}) \sin\frac{m\pi\alpha_k}{a_k} \cos\frac{n\pi\beta_k}{b_k} e^{i\omega_{mn}t} \ , \tau = t, b, r \\
(u^k_{z_\tau}, \sigma^k_{zz_\tau}, \Phi^k_\tau, \mathscr{D}^k_{z_\tau}) &= \sum_{m,n} (\hat{U}^k_{z_\tau}, \hat{\sigma}^k_{zz_\tau}, \hat{\Phi}^k_\tau, \hat{\mathscr{D}}^k_{z_\tau}) \sin\frac{m\pi\alpha_k}{a_k} \sin\frac{n\pi\beta_k}{b_k} e^{i\omega_{mn}t} \ , r = 2, N
\end{aligned}
\tag{209}
$$

in which a_k and b_k are the shell lengths in the α_k and β_k directions, respectively.

These assumptions correspond to the simply-supported boundary conditions. Upon substitution of Eqs.(207) and Eqs.(208) or (209), the governing equations on Ω^k assume the form of a linear system of algebraic equations in the domain, while the boundary conditions are exactly fulfilled.

Examples of fundamental nuclei for plates in explicit and in closed-algebraic form are given in Appendix A.1 and A.2, respectively, for the case of the Principle of Virtual Displacements. Appendix B.1 and B.2 are for the shell geometry (both open spherical and cylindrical geometry).

7 Free vibration analysis

The free vibration analysis leads to an eigenvalue problem. Upon substitution of Eqs.(207) and Eqs.(208) for plate geometry or Eqs.(209) for shell geometry, the governing equations assume the form of a linear system of algebraic equations in the Ω_k domain:

$$
\boldsymbol{K^*}\hat{\boldsymbol{U}} = \omega^2_{mn}\boldsymbol{M}\hat{\boldsymbol{U}} \ , \tag{210}
$$

where $\boldsymbol{K^*}$ is the equivalent stiffness matrix obtained by means of static condensation (for further details see Carrera et al. (2005) and D'Ottavio et al. (2006)), $\boldsymbol{M}$ is the inertial matrix and $\hat{\boldsymbol{U}}$ is the vector of unknown variables. Only the free vibration analysis is investigated in this article, and the external loadings (mechanical and electrical) are therefore set to zero and the relative boundary conditions are exactly fulfilled. By defining $\lambda_{mn} = \omega^2_{mn}$, the solution of the associated eigenvalue problem becomes:

$$
||\boldsymbol{K^*} - \lambda_{mn}\hat{\boldsymbol{M}}|| = 0 \ . \tag{211}
$$

The eigenvectors $\hat{\boldsymbol{U}}$ associated to the eigenvalues λ_{mn} (or to circular frequencies ω_{mn}) define the vibration modes of the structure in terms of primary variables. Once

the waves number (m,n) has been defined in the in-plane directions, the number of obtained frequencies becomes equal to the degrees of freedom of the employed two-dimensional model. It is possible to obtain the relative eigenvector, in terms of primary variables, for each value of frequency, in order to display the modes plotted in the thickness direction.

8 Results

The proposed results consider a square plate geometry in closed circuit configuration in the first part of the section. The second part of the section investigates shell geometries (both ring and cylindrical panels).

8.1 Plate geometry

The free vibrations problem for multilayered plates including piezoelectric layers has been investigated. By imposing the waves number in the in-plane directions, the corresponding vibration modes are obtained. The number of frequencies is equal to the number of degrees of freedom through the thickness according to the considered kinematics.

A five-layered plate is considered (see Figure 6). The two external layers are made of piezoelectric material with a thickness $h_1 = h_5 = \frac{h}{10}$, the three internal ones consist of reinforced carbon fiber layers with lamination sequence $0^\circ/90^\circ/0^\circ$ and thickness $h_2 = h_3 = h_4 = \frac{4}{15}h$. The elastic and electrical properties of the multilayered plate are given in Table 1. The three-dimensional solution was proposed by Heyliger and Saravanos (1995). The considered plate has a square geometry ($a = b$) in a closed circuit configuration (electric potential applied at the top and bottom equal to zero, as indicated in Figure 6). In order to obtain the reference solution, Heyliger and Saravanos (1995) employed a mass density $\rho = 1 kg/m^3$ for both materials; this operation does not have a physical sense but it is however acceptable for the proposed preliminary assessment. The results are given as the first three fundamental circular frequencies $\overline{\omega} = \omega/100 = 2\pi f/100$ (for waves number $m = n = 1$). Two thickness ratios are investigated: a thick plate ($a/h = 4$ with $h = 0.01\ m$) and a moderately thin plate ($a/h = 50$ with $h = 0.01\ m$).

Table 2 gives the first three circular frequencies for the thick and thin plates in the case of CLT and FSDT. Tables 3 and 4 consider the ESL models and the ESL models with the Murakami zigzag function in the case of PVD extended to an electro-mechanical problem (PVD($\boldsymbol{u}, \Phi$)). LW theories are investigated in Table 5 using the same variational statement (PVD($\boldsymbol{u}, \Phi$)). Tables 6-11 give the results of the first three circular frequencies in the case of the three possible extensions of RMVT to the electro-mechanical case; the same kinematics models introduced for

Table 1: Elastic and electric properties of the considered multilayered plate and cylindrical panel.

Properties	$PZT-4$	Gr/EP
$E_1[GPa]$	81.3	132.38
$E_2[GPa]$	81.3	10.756
$E_3[GPa]$	64.5	10.756
$\nu_{12}[-]$	0.329	0.24
$\nu_{13}[-]$	0.432	0.24
$\nu_{23}[-]$	0.432	0.49
$G_{23}[GPa]$	25.6	3.606
$G_{13}[GPa]$	25.6	5.6537
$G_{12}[GPa]$	30.6	5.6537
$e_{15}[C/m^2]$	12.72	0
$e_{24}[C/m^2]$	12.72	0
$e_{31}[C/m^2]$	-5.20	0
$e_{32}[C/m^2]$	-5.20	0
$e_{33}[C/m^2]$	15.08	0
$\varepsilon_{11}[pC/Vm]$	1.306×10^4	30.9897
$\varepsilon_{22}[pC/Vm]$	1.306×10^4	26.563
$\varepsilon_{33}[pC/Vm]$	1.151×10^4	26.563
$\rho[kg/m^3]$(3D solution plate)	1	1
$\rho[kg/m^3]$(real case plate)	7600	1578
$\rho[kg/m^3]$(cylindrical panel)	1	1
$h_1=h_5[m]$	$h/10$	–
$h_2=h_3=h_4[m]$	–	$\frac{4}{15}h$
$\theta[deg]$	–	$0^\circ/90^\circ/0^\circ$

the PVD case are considered.

The results show that the 3D solution for the thick plate [Heyliger and Saravanos (1995)] can be obtained using Layer Wise kinematics and higher orders of expansion, whereas for the thin plate, an order of expansion equal to 2 is sufficient. The use of Equivalent Single Layer models, even though higher orders are considered, gives a larger error than 2% in the case of the thick plate for the first frequency. The error is smaller for the thin plate (less than 1%), but the exact solution is not achieved. Table 2 shows that classical theories, such as FSDT and CLT, are totally inappropriate for such cases; in fact, CLT gives a larger error than 50% for the first

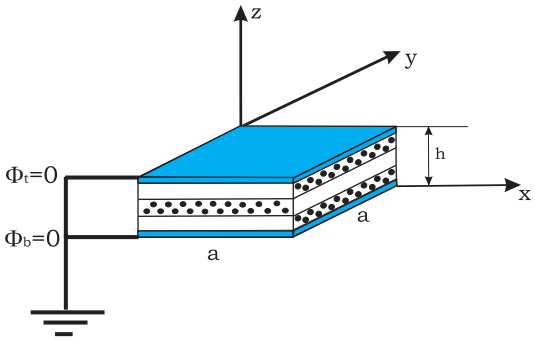

Figure 6: Geometry for vibrations problem in case of a multilayered piezoelectric plate: closed circuit configuration.

Table 2: Plate: 3D results vs CLT and FSDT analysis. 3D solution by Heyliger and Saravanos (1995). $m = n = 1$, first three modes.

	$a/h = 4$			$a/h = 50$		
	Mode 1	*Mode* 2	*Mode* 3	*Mode* 1	*Mode* 2	*Mode* 3
3D	57074.5	191301	250769	618.118	15681.6	21492.8
			$PVD(\boldsymbol{u}, \Phi)$			
CLT	88173.4	195086	262887	592.439	15607.0	21031.4
$Err(\%)$	(54.49)	(1.98)	(4.83)	(-4.15)	(-0.48)	(-2.15)
FSDT	67878.5	195086	262887	590.917	15607.0	21031.4
$Err(\%)$	(18.93)	(1.98)	(4.83)	(-4.40)	(-0.48)	(-2.15)

frequency (thick plate). The zig-zag theories provide better results with respect to ESL models; however they do not provide the 3D solution.

The use of mixed models does not appear mandatory to obtain the frequencies: the kinematic based PVD leads to a quasi-3D evaluation of the first three frequencies for $m = m = 1$. The use of mixed models instead appears mandatory to obtain the correct evaluation of modes through the thickness in terms of displacements, stresses, electric potential and electric displacement. This fact is illustrated in the following analysis.

The mode through the thickness for the first frequency is given in Figures 7-10 in

Table 3: Plate: 3D results vs Equivalent Single Layer (ESL) theories. 3D solution by Heyliger and Saravanos (1995). $m = n = 1$, first three modes.

	$a/h = 4$			$a/h = 50$		
	Mode 1	*Mode* 2	*Mode* 3	*Mode* 1	*Mode* 2	*Mode* 3
3D	57074.5	191301	250769	618.118	15681.6	21492.8
			$PVD(\boldsymbol{u}, \Phi)$			
$ED1$	74105.9	196021	266337	689.867	15694.9	21507.4
$Err(\%)$	(29.84)	(2.47)	(6.21)	(11.61)	(0.08)	(0.07)
$ED2$	69413.8	195860	262204	620.300	15694.9	21505.2
$Err(\%)$	(21.62)	(2.38)	(4.56)	(0.35)	(0.08)	(0.06)
$ED3$	58818.6	195825	259586	618.551	15694.2	21500.1
$Err(\%)$	(3.06)	(2.36)	(3.52)	(0.07)	(0.08)	(0.03)
$ED4$	58713.8	194592	254740	618.465	15693.5	21497.8
$Err(\%)$	(2.87)	(1.72)	(1.58)	(0.06)	(0.08)	(0.02)

Table 4: Plate: 3D results vs ESL zig-zag theories. 3D solution by Heyliger and Saravanos (1995). $m = n = 1$, first three modes.

	$a/h = 4$			$a/h = 50$		
	Mode 1	*Mode* 2	*Mode* 3	*Mode* 1	*Mode* 2	*Mode* 3
3D	57074.5	191301	250769	618.118	15681.6	21492.8
			$PVD(\boldsymbol{u}, \Phi)$			
$EDZ1$	63204.7	195965	266196	688.082	15693.6	21498.5
$Err(\%)$	(10.74)	(2.44)	(6.15)	(11.32)	(0.08)	(0.03)
$EDZ2$	60605.5	195721	260861	619.047	15693.5	21496.5
$Err(\%)$	(6.19)	(2.31)	(4.02)	(0.15)	(0.08)	(0.02)
$EDZ3$	57656.8	195711	259570	618.382	15687.0	21496.5
$Err(\%)$	(1.02)	(2.30)	(3.51)	(0.04)	(0.03)	(0.02)

Table 5: Plate: 3D results vs Layer Wise (LW) theories. 3D solution by Heyliger and Saravanos (1995). $m = n = 1$, first three modes.

	$a/h = 4$			$a/h = 50$		
	Mode 1	*Mode* 2	*Mode* 3	*Mode* 1	*Mode* 2	*Mode* 3
3D	57074.5	191301	250769	618.118	15681.6	21492.8
			$PVD(\boldsymbol{u}, \Phi)$			
*LD*1	57252.5	194840	255646	619.023	15683.4	21494.4
$Err(\%)$	(0.31)	(1.85)	(1.94)	(0.15)	(0.01)	(0.01)
*LD*2	57081.9	191311	250786	618.106	15681.6	21492.6
$Err(\%)$	(0.01)	(0.00)	(0.01)	(0.00)	(0.00)	(0.00)
*LD*3	57074.0	191301	250768	618.105	15681.6	21492.6
$Err(\%)$	(0.00)	(0.00)	(0.00)	(0.00)	(0.00)	(0.00)
*LD*4	57074.0	191301	250768	618.106	15681.6	21492.6
$Err(\%)$	(0.00)	(0.00)	(0.00)	(0.00)	(0.00)	(0.00)

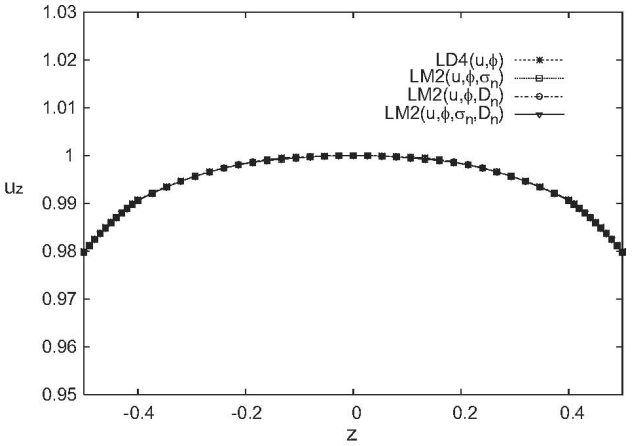

Figure 7: Plate proposed by Heyligher and Saravanos (1995): mechanical transverse displacement u_z vs z. $a/h = 4$, first mode for $m = n = 1$.

Table 6: Plate: 3D results vs mixed ESL theories with Interlaminar Continuous transverse stress components. 3D solution by Heyliger and Saravanos (1995). $m = n = 1$, first three modes.

	$a/h = 4$			$a/h = 50$		
	Mode 1	*Mode* 2	*Mode* 3	*Mode* 1	*Mode* 2	*Mode* 3
3D	57074.5	191301	250769	618.118	15681.6	21492.8
			$RMVT(\boldsymbol{u}, \Phi, \boldsymbol{\sigma}_n)$			
$EM1$	71619.2	195939	266276	679.117	15689.3	21505.5
$Err(\%)$	(25.48)	(2.42)	(6.18)	(9.87)	(0.05)	(0.06)
$EM2$	68710.5	195835	262092	620.214	15693.3	21504.6
$Err(\%)$	(20.39)	(2.37)	(4.51)	(0.34)	(0.07)	(0.05)
$EM3$	58576.0	195807	259495	618.504	15693.0	21499.7
$Err(\%)$	(2.63)	(2.35)	(3.48)	(0.06)	(0.07)	(0.03)
$EM4$	58568.2	194571	254601	618.432	15692.9	21497.5
$Err(\%)$	(2.62)	(1.71)	(1.53)	(0.05)	(0.07)	(0.02)

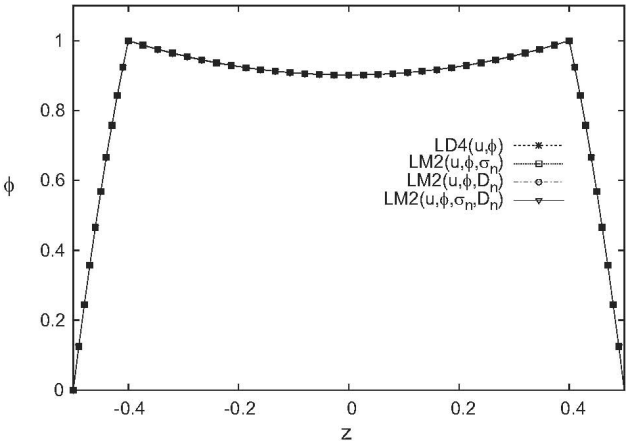

Figure 8: Plate proposed by Heyligher and Saravanos (1995): electric potential Φ vs z. $a/h = 4$, first mode for $m = n = 1$.

Table 7: Plate: 3D results vs mixed LW theories with Interlaminar Continuous transverse stress components. 3D solution by Heyliger and Saravanos (1995). $m = n = 1$, first three modes.

	$a/h = 4$			$a/h = 50$		
	Mode 1	*Mode* 2	*Mode* 3	*Mode* 1	*Mode* 2	*Mode* 3
3D	57074.5	191301	250769	618.118	15681.6	21492.8
			$RMVT(\boldsymbol{u}, \Phi, \boldsymbol{\sigma}_n)$			
*LM*1	57056.6	194696	253955	617.996	15683.3	21493.9
$Err(\%)$	(-0.03)	(1.77)	(1.27)	(-0.02)	(0.01)	(0.01)
*LM*2	57078.3	191301	250779	618.106	15681.6	21492.6
$Err(\%)$	(0.01)	(0.00)	(0.01)	(0.00)	(0.00)	(0.00)
*LM*3	57074.0	191301	250768	618.105	15681.6	21492.6
$Err(\%)$	(0.00)	(0.00)	(0.00)	(0.00)	(0.00)	(0.00)
*LM*4	57074.0	191301	250768	618.105	15681.6	21492.6
$Err(\%)$	(0.00)	(0.00)	(0.00)	(0.00)	(0.00)	(0.00)

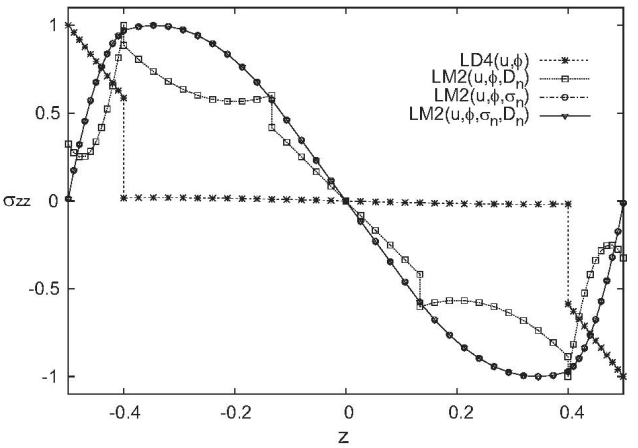

Figure 9: Plate proposed by Heyligher and Saravanos (1995): transverse normal stress σ_{zz} vs z. $a/h = 4$, first mode for $m = n = 1$.

Table 8: Plate: 3D results vs mixed ESL theories with Interlaminar Continuous transverse normal electrical displacement. 3D solution by Heyliger and Saravanos (1995). $m = n = 1$, first three modes.

	$a/h = 4$			$a/h = 50$		
	Mode 1	*Mode* 2	*Mode* 3	*Mode* 1	*Mode* 2	*Mode* 3
3D	57074.5	191301	250769	618.118	15681.6	21492.8
			$RMVT(\boldsymbol{u}, \Phi, \mathscr{D}_n)$			
$EM1$	74117.2	196021	266338	689.885	15694.9	21507.4
$Err(\%)$	(29.86)	(2.47)	(6.21)	(11.61)	(0.08)	(0.07)
$EM2$	69413.8	195860	262204	620.300	15694.9	21505.2
$Err(\%)$	(21.62)	(2.38)	(4.56)	(0.35)	(0.08)	(0.06)
$EM3$	58818.6	195825	259586	618.551	15694.2	21500.1
$Err(\%)$	(3.06)	(2.36)	(3.52)	(0.07)	(0.08)	(0.03)
$EM4$	58713.8	194592	254740	618.465	15693.5	21497.8
$Err(\%)$	(2.87)	(1.72)	(1.58)	(0.06)	(0.08)	(0.02)

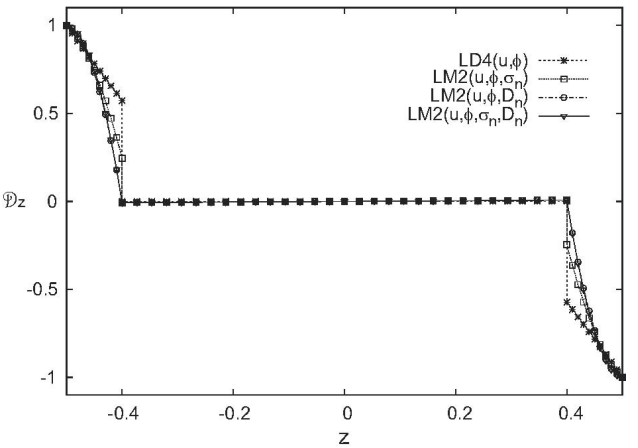

Figure 10: Plate proposed by Heyligher and Saravanos (1995): transverse normal electric displacement $\mathscr{D}_z$ vs z. $a/h = 4$, first mode for $m = n = 1$.

Table 9: Plate: 3D results vs mixed LW theories with Interlaminar Continuous transverse normal electrical displacement. 3D solution by Heyliger and Saravanos (1995). $m = n = 1$, first three modes.

	$a/h = 4$			$a/h = 50$		
	Mode 1	*Mode* 2	*Mode* 3	*Mode* 1	*Mode* 2	*Mode* 3
3D	57074.5	191301	250769	618.118	15681.6	21492.8
			$RMVT(\boldsymbol{u}, \Phi, \mathscr{D}_n)$			
$LM1$	57257.9	194840	255646	619.043	15683.4	21494.4
$Err(\%)$	(0.32)	(1.85)	(1.94)	(0.15)	(0.01)	(0.01)
$LM2$	57081.9	191311	250786	618.106	15681.5	21492.6
$Err(\%)$	(0.01)	(0.00)	(0.01)	(0.00)	(0.00)	(0.00)
$LM3$	57074.0	191301	250768	618.105	15681.5	21492.6
$Err(\%)$	(0.00)	(0.00)	(0.00)	(0.00)	(0.00)	(0.00)
$LM4$	57074.0	191301	250768	618.105	15681.5	21492.6
$Err(\%)$	(0.00)	(0.00)	(0.00)	(0.00)	(0.00)	(0.00)

terms of displacements, electric potential, stresses and electric displacement. The distribution of the transverse displacement u_z through the thickness is given in Figure 7; in this case, there are no differences for the considered variational statements because the displacement is a primary variable in all them. The mode is given in Figure 8 in terms of electric potential. The potential Φ consists of a primary variable in each considered model; as a consequence, the same considerations made for the displacements are confirmed: the electric potential is continuous and satisfies the closed-circuit boundary conditions. In order to give the mode through the thickness in terms of stress σ_{zz}, the use of mixed models in which σ_{zz} is a primary variable is mandatory: these models permit the interlaminar continuity and the correct boundary homogeneous conditions to be obtained, even if low orders of expansion are employed (see Figure 9). Finally, Figure 10 gives the modes in terms of transverse normal electric displacement $\mathscr{D}_z$. As in the case of stress σ_{zz}, mixed models, where normal electric displacement is a primary variable, are necessary in order to achieve the interlaminar continuity of $\mathscr{D}_z$ at the interfaces.

The frequencies calculated using a pure mechanical model are quoted in Table 12. In order to estimate the piezoelectric effect, the following parameter is evaluated:

Table 10: Plate: 3D results vs mixed ESL theories with Interlaminar Continuous transverse stresses and transverse normal electrical displacement. 3D solution by Heyliger and Saravanos (1995). $m = n = 1$, first three modes.

	$a/h = 4$			$a/h = 50$		
	Mode 1	*Mode* 2	*Mode* 3	*Mode* 1	*Mode* 2	*Mode* 3
3D	57074.5	191301	250769	618.118	15681.6	21492.8
			$RMVT(\boldsymbol{u}, \Phi, \boldsymbol{\sigma}_n, \mathscr{D}_n)$			
$EM1$	71645.9	195940	266276	679.982	15689.3	21505.7
$Err(\%)$	(25.53)	(2.42)	(6.18)	(10.00)	(0.05)	(0.06)
$EM2$	68710.5	195835	262094	620.214	15693.3	21504.6
$Err(\%)$	(20.39)	(2.37)	(4.52)	(0.34)	(0.07)	(0.05)
$EM3$	58576.0	195807	259498	618.504	15693.0	21499.7
$Err(\%)$	(2.63)	(2.35)	(3.48)	(0.06)	(0.07)	(0.03)
$EM4$	58568.2	194571	254603	618.432	15692.9	21497.5
$Err(\%)$	(2.62)	(1.71)	(1.53)	(0.05)	(0.07)	(0.02)

$$\Delta^p[\%] = \sqrt{\frac{\omega^2 - \omega_{el}^2}{\omega^2}} \cdot 100 \tag{212}$$

where the eigenfrequency ω is obtained by considering the electric effect, whereas ω_{el} is computed neglecting the electric part (only the elastic properties of the piezoelectric layers are considered). Due to the employed high orders, each model gives the exact solution according to the solution proposed by Heyliger and Saravanos (1995) for both thick and thin laminates. Figure 11 and Table 12 confirm that the effect produced by the electro-mechanical interaction is not predictable and the dependence on the thickness ratio a/h (see Figure 11a) and on the considered mode (see Figure 11b) cannot be a priori estimated.

Effect of the real mass on the electro-mechanical coupling

The case proposed in Heyliger and Saravanos (1995) is a well-known three-dimensional benchmark which has been employed to validate the proposed variational statements and variable kinematics models, the electro-mechanical coupling has

Table 11: Plate: 3D results vs mixed LW theories with Interlaminar Continuous transverse stresses and transverse normal electrical displacement. 3D solution by Heyliger and Saravanos (1995). $m = n = 1$, first three modes.

	$a/h = 4$			$a/h = 50$		
	Mode 1	*Mode* 2	*Mode* 3	*Mode* 1	*Mode* 2	*Mode* 3
3D	57074.5	191301	250769	618.118	15681.6	21492.8
			$RMVT(\boldsymbol{u}, \Phi, \boldsymbol{\sigma}_n, \mathscr{D}_n)$			
$LM1$	57094.0	194697	253958	618.143	15683.3	21493.9
$Err(\%)$	(0.03)	(1.77)	(1.27)	(0.00)	(0.01)	(0.01)
$LM2$	57078.3	191301	250779	618.106	15681.6	21492.6
$Err(\%)$	(0.01)	(0.00)	(-0.01)	(0.00)	(0.00)	(0.00)
$LM3$	57074.0	191301	250768	618.105	15681.6	21492.6
$Err(\%)$	(0.00)	(0.00)	(0.00)	(0.00)	(0.00)	(0.00)
$LM4$	57074.0	191301	250768	618.106	15681.6	21492.6
$Err(\%)$	(0.00)	(0.00)	(0.00)	(0.00)	(0.00)	(0.00)

been also investigated. However, in Heyliger and Saravanos (1995) a mass density $\rho = 1\ kg/m^3$ has been assumed for both piezoelectric and composite materials. This assumption does not have a physical meaning, therefore in this section we suppose a real mass density $\rho = 7600\ kg/m^3$ and $\rho = 1578\ kg/m^3$ for $PZT-4$ and Gr/EP materials, respectively. The first three circular frequencies $\overline{\omega} = \omega/100$ for $m = n = 1$ are considered.

The most refined theory proposed in this paper is the layer wise model with fourth order of expansion in the thickness direction for each modelled variable ($LM4(\boldsymbol{u}, \Phi, \boldsymbol{\sigma}_n, \mathscr{D}_n)$). This theory has been validated in the previous section by using the three-dimensional solution proposed by Heyliger and Saravanos (1995): it gives 0% of error for the three first modes and for thin and thick plates. In Table 13 $LM4(\boldsymbol{u}, \Phi, \boldsymbol{\sigma}_n, \mathscr{D}_n)$ is used as reference solution for the case of real mass density for the embedded layers. Several classical and refined models are compared and no further comments are obtained by the introduction of mass densities different from $1\ kg/m^3$. In Table 14 and in Figure 12, the electro-mechanical coupling has been analyzed in the case of real mass density, the piezoelectric effect does not change with respect to the case proposed in Heyliger and Saravanos (1995). The mass density influences the frequency values, but it does not add new effects in the

Table 12: Plate: comparison between frequency response of pure mechanical problem and electro-mechanical problem for the case proposed by Heyliger and Saravanos (1995). $m = n = 1$, first three modes.

	$a/h = 4$			$a/h = 50$		
	Mode 1	*Mode* 2	*Mode* 3	*Mode* 1	*Mode* 2	*Mode* 3
$LD4(\boldsymbol{u})$	55514.8	189939	246834	584.085	15590.0	20948.1
$LD4(\boldsymbol{u},\Phi)$	57074.0	191301	250768	618.105	15681.5	21492.6
$LM4(\boldsymbol{u},\Phi,\mathscr{D}_n)$	57074.0	191301	250768	618.105	15681.5	21492.6
$\Delta^p[\%]$	(23.21)	(11.91)	(17.64)	(32.72)	(10.79)	(22.37)
$LM4(\boldsymbol{u},\boldsymbol{\sigma}_n)$	55514.8	189939	246834	584.085	15590.0	20948.1
$LM4(\boldsymbol{u},\Phi,\boldsymbol{\sigma}_n)$	57074.0	191301	250768	618.105	15681.6	21492.6
$LM4(\boldsymbol{u},\Phi,\boldsymbol{\sigma}_n,\mathscr{D}_n)$	57074.0	191301	250768	618.105	15681.6	21492.6
$\Delta^p[\%]$	(23.21)	(11.91)	(17.64)	(32.72)	(10.79)	(22.37)

electro-mechanical coupling behavior.

8.2 Shell geometry

The free vibration problem of multilayered shells including thickness polarized piezoelectric layers has been investigated. As in the plate case, by imposing the waves number in the in-plane directions, the corresponding vibration modes have been obtained. The number of frequencies is equal to the number of degrees of freedom through the thickness of the considered kinematics model.

A two-layered ring shell and a multilayered cylindrical panel have been considered. The geometry of these shells are given in Figure 13. The free vibration problem has been investigated in closed circuit configuration: the electric potential is zero at the top and bottom of the shell ($\Phi_t = \Phi_b = 0$). The elastic and piezoelectric properties of the embedded materials, and the geometrical parameters are given in Table 15 (ring shell) and in Table 1 (cylindrical panel).

The cylindrical ring shell has two layers, the internal layer in Titanium and the external one in piezoelectric PZT-4. The 3D solution was given by Heyliger et

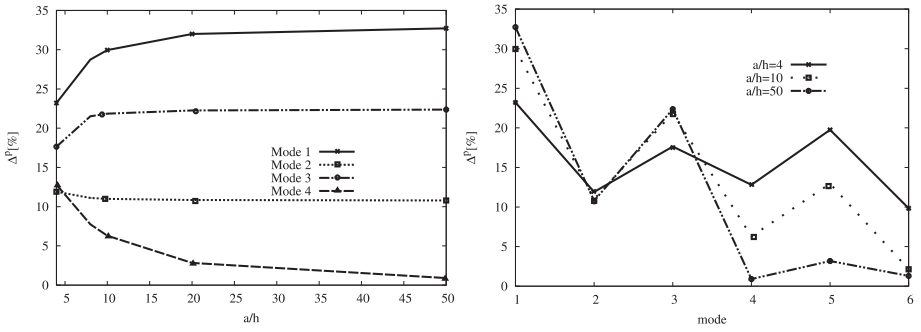

a) *b)*

Figure 11: Plate: $\Delta^p[\%]$ calculated for LD4($\boldsymbol{u}$) vs. LD4($\boldsymbol{u}, \Phi$). Variation of $\Delta^p[\%]$ depending on the thickness ratio a/h (a). Variation of $\Delta^p[\%]$ depending on the considered mode (b). Case proposed by Heyligher and Saravanos (1995).

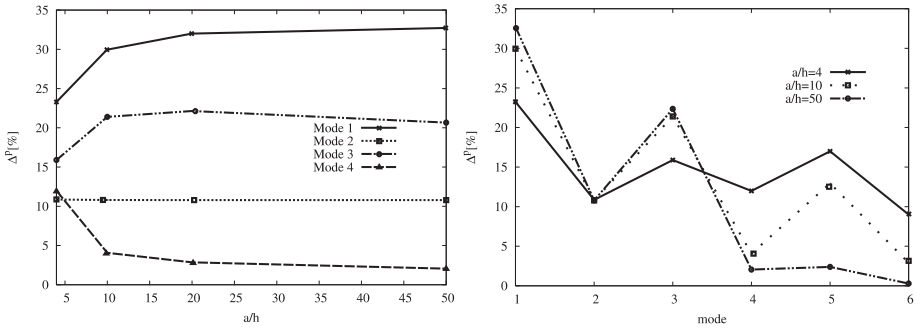

a) *b)*

Figure 12: Plate: $\Delta^p[\%]$ calculated for LD4($\boldsymbol{u}$) vs. LD4($\boldsymbol{u}, \Phi$). Variation of $\Delta^p[\%]$ depending on the thickness ratio a/h (a). Variation of $\Delta^p[\%]$ depending on the considered mode (b). Case of real mass for the embedded layers.

Table 13: Plate: refined results vs classical theories for the case of real mass of the embedded layers. The error in percentage of each theory is calculated as $\frac{theory-LM4(\boldsymbol{u},\Phi,\boldsymbol{\sigma}_n,\mathscr{D}_n)}{LM4(\boldsymbol{u},\Phi,\boldsymbol{\sigma}_n,\mathscr{D}_n)} \times 100$. $m = n = 1$, first three modes.

	$a/h = 4$			$a/h = 50$		
	Mode 1	*Mode* 2	*Mode* 3	*Mode* 1	*Mode* 2	*Mode* 3
$LM4(\boldsymbol{u},\Phi,\boldsymbol{\sigma}_n,\mathscr{D}_n)$	714.106	2390.66	3027.73	7.72934	196.087	268.669
			CUF theories			
$CLT(\boldsymbol{u},\Phi)$	1116.75	2439.42	3287.22	7.40869	195.154	262.982
$Err(\%)$	(56.4)	(2.04)	(8.57)	(−4.15)	(−0.48)	(−2.12)
$FSDT(\boldsymbol{u},\Phi)$	852.682	2439.42	3287.22	7.38966	195.154	262.982
$Err(\%)$	(19.4)	(2.04)	(8.57)	(−4.39)	(−0.48)	(−2.12)
$ED3(\boldsymbol{u},\Phi)$	735.673	2446.70	3206.23	7.73489	196.244	268.817
$Err(\%)$	(3.02)	(2.34)	(5.89)	(0.07)	(0.08)	(0.05)
$EDZ3(\boldsymbol{u},\Phi)$	720.900	2445.41	3206.22	7.73278	196.155	268.772
$Err(\%)$	(0.95)	(2.29)	(5.89)	(0.04)	(0.03)	(0.04)
$LD2(\boldsymbol{u},\Phi)$	714.201	2390.81	3028.05	7.72936	196.087	268.669
$Err(\%)$	(0.01)	(0.01)	(0.01)	(0.00)	(0.00)	(0.00)
$LD4(\boldsymbol{u},\Phi)$	714.106	2390.66	3027.73	7.72934	196.087	268.669
$Err(\%)$	(0.00)	(0.00)	(0.00)	(0.00)	(0.00)	(0.00)
$EM3(\boldsymbol{u},\Phi,\boldsymbol{\sigma}_n)$	732.612	2446.42	3204.46	7.73430	196.229	268.811
$Err(\%)$	(2.59)	(2.33)	(5.84)	(0.06)	(0.07)	(0.05)
$LM2(\boldsymbol{u},\Phi,\mathscr{D}_n)$	714.201	2390.81	3028.05	7.72936	196.087	268.669
$Err(\%)$	(0.01)	(0.01)	(0.01)	(0.00)	(0.00)	(0.00)
$LM4(\boldsymbol{u},\Phi,\boldsymbol{\sigma}_n)$	714.106	2390.66	3027.73	7.72934	196.087	268.669
$Err(\%)$	(0.00)	(0.00)	(0.00)	(0.00)	(0.00)	(0.00)

al. (1996): the first fundamental frequency in Hz is given by imposing $m = 0$ and $n = 4, 8, 12, 16, 20$. The thickness ratio R_β/h is equal to 72.75 (where the total thickness is $h = 0.004\ m$, and the radii of curvature at the midsurface are $R_\alpha = \infty$ and $R_\beta = 0.291\ m$). The dimensions are $a = 0.3048\ m$ and $b = 2\pi R_\beta = 1.82841\ m$.

Table 16 gives the first fundamental frequency in the case of CLT and FSDT models. Tables 17 and 18 consider the ESL models and the ESL models with the Murakami zigzag function, respectively: the PVD extended to an electro-mechanical problem (PVD($\boldsymbol{u}$,Φ)) has been considered. LW theories are investigated in Table

Table 14: Plate: comparison between frequency response of pure mechanical problem and electro-mechanical problem for the case of real mass of the embedded layers. $m = n = 1$, first three modes.

	$a/h = 4$			$a/h = 50$		
	Mode 1	*Mode* 2	*Mode* 3	*Mode* 1	*Mode* 2	*Mode* 3
$LD4(\boldsymbol{u})$	694.561	2376.51	2989.28	7.30390	194.944	261.874
$LD4(\boldsymbol{u},\Phi)$	714.106	2390.66	3027.73	7.72934	196.087	268.669
$LM4(\boldsymbol{u},\Phi,\mathscr{D}_n)$	714.106	2390.66	3027.73	7.72934	196.087	268.669
$\Delta^p[\%]$	(23.24)	(10.86)	(15.89)	(32.72)	(10.78)	(22.35)
$LM4(\boldsymbol{u},\boldsymbol{\sigma}_n)$	694.561	2376.51	2989.28	7.30390	194.944	261.874
$LM4(\boldsymbol{u},\Phi,\boldsymbol{\sigma}_n)$	714.106	2390.66	3027.73	7.72934	196.087	268.669
$LM4(\boldsymbol{u},\Phi,\boldsymbol{\sigma}_n,\mathscr{D}_n)$	714.106	2390.66	3027.73	7.72934	196.087	268.669
$\Delta^p[\%]$	(23.24)	(10.86)	(15.89)	(32.72)	(10.78)	(22.35)

19 using the same variational statement (PVD($\boldsymbol{u}$,Φ)). Tables 20-25 give the results of the first fundamental frequency in the case of the three possible extensions of RMVT to the electro-mechanical case: the same kinematics models introduced for the PVD case are considered.

The results obtained in each case (ESL or LW, and PVD or RMVT model) are very close to the 3D solution if higher orders of expansion are used ($N = 4$), the maximum error is 2.68% for imposed waves number $m = 0$ and $n = 20$. The use of LW theories is not mandatory because in the considered two-layered ring the largest part is in Titanium (isotropic material) with a very thin layer in PZT-4: the ZZ effect is not so evident. Table 16 shows that classical theories, such as CLT and FSDT, give larger errors with respect to the refined and advanced 2D models based on CUF, the same happens for ED1 theories: a good 2D theory for the electro-mechanical problems must have an electric potential at least quadratically varying in the thickness direction.

The use of mixed models does not appear mandatory to obtain the frequencies: the kinematic based on PVD leads to a quasi-3D evaluation of the first fundamental frequency for each waves number n. The use of mixed models, based on RMVT,

Table 15: Elastic and electric properties of the ring in PZT-4 and Titanium.

Properties	$PZT-4$	$Titanium$
$E_1[GPa]$	81.3	114
$E_2[GPa]$	81.3	114
$E_3[GPa]$	64.5	114
$\nu_{12}[-]$	0.329	0.3
$\nu_{13}[-]$	0.432	0.3
$\nu_{23}[-]$	0.432	0.3
$G_{23}[GPa]$	25.6	43.85
$G_{13}[GPa]$	25.6	43.85
$G_{12}[GPa]$	30.6	43.85
$e_{15}[C/m^2]$	12.72	0
$e_{24}[C/m^2]$	12.72	0
$e_{31}[C/m^2]$	-5.20	0
$e_{32}[C/m^2]$	-5.20	0
$e_{33}[C/m^2]$	15.08	0
$\varepsilon_{11}[pC/Vm]$	1.306×10^4	8.850
$\varepsilon_{22}[pC/Vm]$	1.306×10^4	8.850
$\varepsilon_{33}[pC/Vm]$	1.151×10^4	8.850
$\rho[kg/m^3]$	7600	2768
$h_{PZT4}[m]$	0.001	–
$h_T[m]$	–	0.003

is mandatory to obtain the correct evaluation of modes through the thickness in terms of displacements, electric potential, stresses and electric displacement. This fact is clearly explained in Figures 14-17 where the mode through the thickness for the fundamental frequency is given in terms of displacements, electric potential, stresses and electric displacement. The distribution of the transverse displacement u_z through the thickness is given in Figure 14; in this case, there are no differences because the displacement is a primary variable in each proposed variational statement. The mode in Figure 15 is given in terms of electric potential. The electric potential Φ is a primary variable in each considered variational statement; this feature permits a continuous electric potential through the thickness which satisfies the closed-circuit boundary conditions. In order to give the mode through the thickness in terms of stress σ_{zz}, the use of mixed models in which σ_{zz} is a primary variable is mandatory: these models permit the interlaminar continuity and the correct bound-

Table 16: Ring in PZT-4 and Titanium, closed circuit configuration. 3D results vs CLT and FSDT analysis, fundamental mode for $m = 0$. 3D solution by Heyliger et al. (1996).

	$n=4$	$n=8$	$n=12$	$n=16$	$n=20$
3D	31.27	170.42	407.29	745.21	1190.48
			$PVD(\boldsymbol{u},\Phi)$		
CLT	30.71	166.63	395.29	715.59	1127.24
$Err(\%)$	(-1.79)	(-2.22)	(-2.95)	(-3.97)	(-5.31)
$FSDT$	30.71	166.57	394.98	714.60	1124.79
$Err(\%)$	(-1.79)	(-2.26)	(-3.02)	(-4.11)	(-5.52)

ary homogeneous conditions to be obtained (see Figure 16). Finally, Figure 17 gives the modes in terms of transverse normal electric displacement $\mathscr{D}_z$. As in the case of stress σ_{zz}, mixed models, where normal electric displacement is a primary variable, are mandatory in order to achieve the interlaminar continuity of $\mathscr{D}_z$ at the interfaces.

The frequencies calculated using a pure mechanical model are shown in Table 26. In order to estimate the piezoelectric effect, the parameter $\Delta^p[\%]$ as defined in Eq.(212) is employed. Due to the considered higher orders of expansion, each model gives the same value of the parameter Δ^p, this last is quite large, so the piezoelectric effect cannot be neglected. In addition to the conclusions already given for the plate (the effect produced by the electromechanical interaction is not predictable for variations of the thickness ratio and for the order of the considered mode), it is possible to note that in the proposed case the parameter Δ^p does not depend on the waves number n because of the particular geometry and vibration modes (closed cylinder, axisymmetric modes with $m = 0$).

The cylindrical panel has two external layers in piezoelectric material PTZ-4 with thickness $h_1 = h_5 = \frac{h_{TOT}}{10}$ and three internal layers in graphite-epoxy with lamination sequence $0^\circ/90^\circ/0^\circ$ and thickness $h_2 = h_3 = h_4 = \frac{4}{15}h_{TOT}$. The dimensions are $a = 1\ m$ and $b = \frac{\pi}{3}R_\beta = 10.47197\ m$ (radii of curvature $R_\alpha = \infty$ and $R_\beta = 10\ m$). This assessment is a sort of extension of the plate case proposed in the previous section to the shell geometry. In this case, the reference solution (Ref) in Tables 27-30 is the $LM4(\boldsymbol{u},\Phi,\boldsymbol{\sigma}_n,\boldsymbol{\mathscr{D}}_n)$ theory. The results are given as the first fundamental

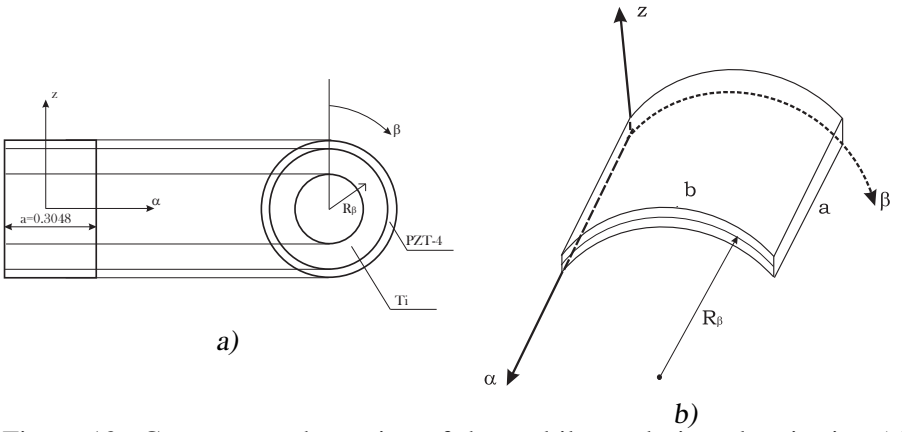

Figure 13: Geometry and notation of the multilayered piezoelectric ring (a) and multilayered piezoelectric cylindrical panel (b).

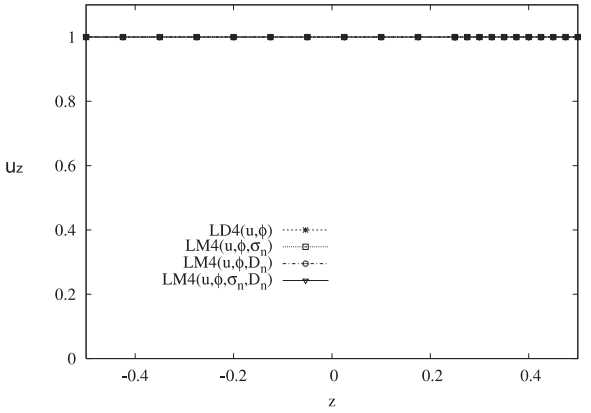

Figure 14: Ring in PZT-4 and Titanium: mechanical transverse displacement u_z vs z. First mode for $m = 0$ and $n = 4$.

circular frequency $\overline{\omega} = \omega\sqrt{\frac{R_\beta(\rho)_{PTZ-4}}{(E_3)_{PTZ-4}h_{TOT}^2}}$. Four thickness ratios are investigated: $R_\beta/h = 2,4,10,100$ (where the values of the total thickness are $h = 5,2.5,1,0.1\ m$). Tables 27 and 28 give the fundamental frequencies of the shell for different thickness ratios and for both PVD and RMVT theories, the waves number are $m = n = 1$. Tables 29 and 30 are for waves number $m = n = 10$. The results show that in case of thick shell, Layer Wise kinematics and an order of expansion equal to 4 are mandatory to obtain the reference solution, whereas for thin shells lower order of

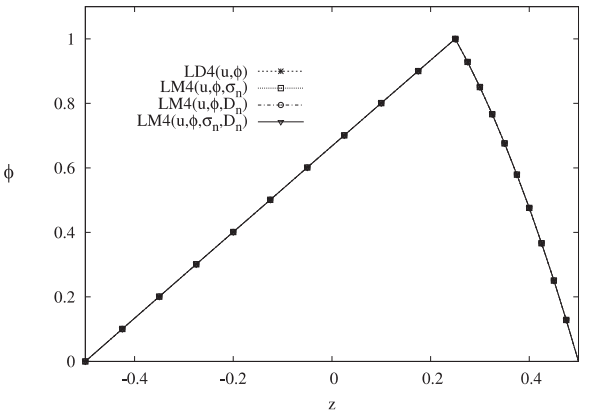

Figure 15: Ring in PZT-4 and Titanium: electric potential Φ vs z. First mode for $m = 0$ and $n = 4$.

Table 17: Ring in PZT-4 and Titanium, closed circuit configuration. 3D results vs Equivalent Single Layer (ESL) theories, fundamental mode for $m = 0$. 3D solution by Heyliger et al. (1996).

	$n=4$	$n=8$	$n=12$	$n=16$	$n=20$
3D	31.27	170.42	407.29	745.21	1190.48
			$PVD(\boldsymbol{u},\Phi)$		
$ED1$	30.65	166.28	394.29	713.35	1122.85
$Err(\%)$	(-1.98)	(-2.43)	(-3.19)	(-4.27)	(-5.68)
$ED2$	31.65	171.67	407.05	736.45	1159.21
$Err(\%)$	(1.21)	(0.73)	(-0.06)	(-1.17)	(-2.63)
$ED3$	31.64	171.62	406.93	736.18	1158.70
$Err(\%)$	(1.18)	(0.70)	(-0.09)	(-1.21)	(-2.67)
$ED4$	31.64	171.61	406.91	736.14	1158.64
$Err(\%)$	(1.18)	(0.70)	(-0.09)	(-1.22)	(-2.67)

Table 18: Ring in PZT-4 and Titanium, closed circuit configuration. 3D results vs ESL zig-zag theories, fundamental mode for $m = 0$. 3D solution by Heyliger et al. (1996).

	$n=4$	$n=8$	$n=12$	$n=16$	$n=20$
3D	31.27	170.42	407.29	745.21	1190.48
			$PVD(\boldsymbol{u},\Phi)$		
$EDZ1$	33.28	180.53	428.05	774.35	1218.71
$Err(\%)$	(6.43)	(5.93)	(5.10)	(3.91)	(2.37)
$EDZ2$	31.64	171.60	406.90	736.16	1158.73
$Err(\%)$	(1.18)	(0.69)	(-0.10)	(-1.21)	(-2.67)
$EDZ3$	31.64	171.60	406.88	736.08	1158.55
$Err(\%)$	(1.18)	(0.69)	(-0.10)	(-1.22)	(-2.68)

expansion could be considered. The reference solution is not achieved by using Equivalent Single Layer models, even if high orders of expansion and thin shells are considered. This happens because in this case the transverse anisotropy of the shell is much bigger than the ring case. Classical theories give a larger error, so they are totally inappropriate. The zig-zag theories provide little better results with respect to ESL models but the error does not become zero even if the shell is thin. As above, the use of mixed models appears mandatory only to obtain the correct evaluation of modes through the thickness in terms of transverse shear/normal stresses and normal electric displacement.

The frequencies calculated using a pure mechanical model are given in Table 31. The parameter Δ^p increases with the thickness ratio if the fundamental frequency is investigated for waves number $m = n = 1$. It is evident that the effect produced by the electromechanical interaction becomes more important when the total thickness of the shell decreases, even if the percentage of piezoelectric material is the same. Figure 18 confirms that the effect of the electromechanical interaction is very hard to predict if several parameters are involved in the investigation (thickness ratio, higher modes and waves number m and n in the plane directions).

Table 19: Ring in PZT-4 and Titanium, closed circuit configuration. 3D results vs Layer Wise (LW) theories, fundamental mode for $m = 0$. 3D solution by Heyliger et al. (1996).

	$n=4$	$n=8$	$n=12$	$n=16$	$n=20$
3D	31.27	170.42	407.29	745.21	1190.48
			$PVD(\boldsymbol{u},\Phi)$		
$LD1$	33.28	180.51	427.99	774.24	1218.54
$Err(\%)$	(6.43)	(5.92)	(5.08)	(3.89)	(2.36)
$LD2$	31.64	171.60	406.88	736.11	1158.61
$Err(\%)$	(1.18)	(0.69)	(−0.10)	(−1.22)	(−2.68)
$LD3$	31.64	171.59	406.87	736.07	1158.51
$Err(\%)$	(1.18)	(0.69)	(−0.10)	(−1.23)	(−2.68)
$LD4$	31.64	171.59	406.87	736.07	1158.51
$Err(\%)$	(1.18)	(0.69)	(−0.10)	(−1.23)	(−2.68)

Table 20: Ring in PZT-4 and Titanium, closed circuit configuration. 3D results vs mixed ESL theories with Interlaminar Continuous transverse stress components, fundamental mode for $m = 0$. 3D solution by Heyliger et al. (1996).

	$n=4$	$n=8$	$n=12$	$n=16$	$n=20$
3D	31.27	170.42	407.29	745.21	1190.48
			$RMVT(\boldsymbol{u},\Phi,\boldsymbol{\sigma}_n)$		
$EM1$	35.53	192.70	456.86	826.39	1300.41
$Err(\%)$	(13.62)	(13.07)	(12.17)	(10.89)	(9.23)
$EM2$	31.65	171.65	407.03	736.40	1159.13
$Err(\%)$	(1.21)	(0.72)	(−0.06)	(−1.18)	(−2.63)
$EM3$	31.64	171.61	406.91	736.15	1158.65
$Err(\%)$	(1.18)	(0.70)	(−0.10)	(−1.22)	(−2.67)
$EM4$	31.64	171.61	406.90	736.13	1158.62
$Err(\%)$	(1.18)	(0.70)	(−0.10)	(−1.22)	(−2.68)

Table 21: Ring in PZT-4 and Titanium, closed circuit configuration. 3D results vs mixed LW theories with Interlaminar Continuous transverse stress components, fundamental mode for $m = 0$. 3D solution by Heyliger et al. (1996).

	$n=4$	$n=8$	$n=12$	$n=16$	$n=20$
3D	31.27	170.42	407.29	745.21	1190.48
			$RMVT(\boldsymbol{u},\Phi,\boldsymbol{\sigma}_n)$		
$LM1$	32.39	175.66	416.50	753.47	1185.87
$Err(\%)$	(3.58)	(3.07)	(2.26)	(1.11)	(−0.39)
$LM2$	31.64	171.60	406.88	736.10	1158.58
$Err(\%)$	(1.18)	(0.69)	(−0.10)	(−1.22)	(−2.68)
$LM3$	31.64	171.59	406.87	736.07	1158.51
$Err(\%)$	(1.18)	(0.69)	(−0.10)	(−1.23)	(−2.68)
$LM4$	31.64	171.59	406.87	736.07	1158.51
$Err(\%)$	(1.18)	(0.69)	(−0.10)	(−1.23)	(−2.68)

Table 22: Ring in PZT-4 and Titanium, closed circuit configuration. 3D results vs mixed ESL theories with Interlaminar Continuous transverse normal electrical displacement, fundamental mode for $m = 0$. 3D solution by Heyliger et al. (1996).

	$n=4$	$n=8$	$n=12$	$n=16$	$n=20$
3D	31.27	170.42	407.29	745.21	1190.48
			$RMVT(\boldsymbol{u},\Phi,\mathscr{D}_n)$		
$EM1$	35.54	192.73	456.93	826.51	1300.61
$Err(\%)$	(13.65)	(13.09)	(12.19)	(10.91)	(9.25)
$EM2$	31.65	171.67	407.05	736.45	1159.21
$Err(\%)$	(1.21)	(0.73)	(−0.06)	(−1.17)	(−2.63)
$EM3$	31.64	171.62	406.93	736.18	1158.70
$Err(\%)$	(1.18)	(0.70)	(−0.09)	(−1.21)	(−2.67)
$EM4$	31.64	171.62	406.91	736.14	1158.64
$Err(\%)$	(1.18)	(0.70)	(−0.09)	(−1.22)	(−2.67)

Table 23: Ring in PZT-4 and Titanium, closed circuit configuration. 3D results vs mixed LW theories with Interlaminar Continuous transverse normal electrical displacement, fundamental mode for $m = 0$. 3D solution by Heyliger et al. (1996).

	$n=4$	$n=8$	$n=12$	$n=16$	$n=20$
3D	31.27	170.42	407.29	745.21	1190.48
			$RMVT(\boldsymbol{u},\Phi,\mathscr{D}_n)$		
$LM1$	33.28	180.53	428.05	774.35	1218.71
$Err(\%)$	(6.43)	(5.93)	(5.10)	(3.91)	(2.37)
$LM2$	31.64	171.60	406.88	736.11	1158.61
$Err(\%)$	(1.18)	(0.69)	(-0.10)	(-1.22)	(-2.68)
$LM3$	31.64	171.59	406.87	736.07	1158.51
$Err(\%)$	(1.18)	(0.69)	(-0.10)	(-1.23)	(-2.68)
$LM4$	31.64	171.59	406.87	736.07	1158.51
$Err(\%)$	(1.18)	(0.69)	(-0.10)	(-1.23)	(-2.68)

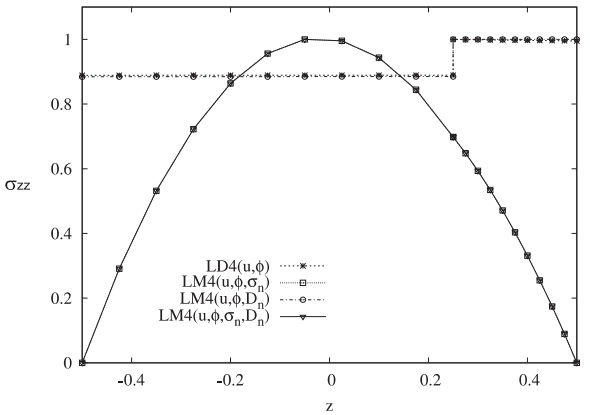

Figure 16: Ring in PZT-4 and Titanium: transverse normal stress σ_{zz} vs z. First mode for $m = 0$ and $n = 4$.

Table 24: Ring in PZT-4 and Titanium, closed circuit configuration. 3D results vs mixed ESL theories with Interlaminar Continuous transverse stresses and transverse normal electrical displacement, fundamental mode for $m = 0$. 3D solution by Heyliger et al. (1996).

	$n=4$	$n=8$	$n=12$	$n=16$	$n=20$
3D	31.27	170.42	407.29	745.21	1190.48
			$RMVT(\boldsymbol{u},\Phi,\boldsymbol{\sigma}_n,\mathscr{D}_n)$		
$EM1$	35.54	192.73	456.92	826.49	1300.57
$Err(\%)$	(13.65)	(13.09)	(12.18)	(10.91)	(9.25)
$EM2$	31.65	171.66	407.03	736.40	1159.13
$Err(\%)$	(1.21)	(0.73)	(-0.06)	(-1.18)	(-2.63)
$EM3$	31.64	171.61	406.91	736.15	1158.65
$Err(\%)$	(1.18)	(0.70)	(-0.09)	(-1.22)	(-2.67)
$EM4$	31.64	171.61	406.90	736.13	1158.62
$Err(\%)$	(1.18)	(0.70)	(-0.10)	(-1.22)	(-2.68)

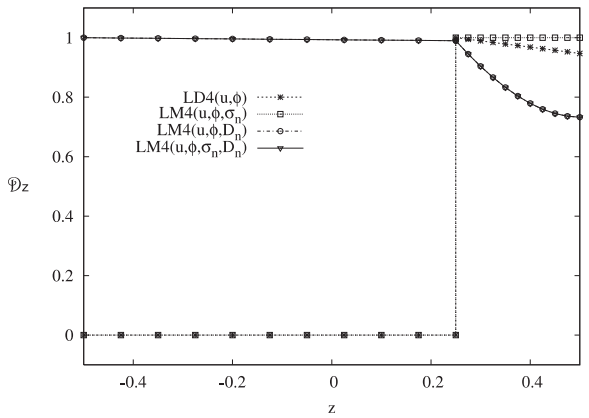

Figure 17: Ring in PZT-4 and Titanium: transverse normal electric displacement $\mathscr{D}_z$ vs z. First mode for $m = 0$ and $n = 4$.

Table 25: Ring in PZT-4 and Titanium, closed circuit configuration. 3D results vs mixed LW theories with Interlaminar Continuous transverse stresses and transverse normal electrical displacement, fundamental mode for $m = 0$. 3D solution by Heyliger et al. (1996).

	$n=4$	$n=8$	$n=12$	$n=16$	$n=20$
3D	31.27	170.42	407.29	745.21	1190.48
			$RMVT(\boldsymbol{u},\Phi,\boldsymbol{\sigma}_n,\mathscr{D}_n)$		
$LM1$	32.53	176.42	418.30	756.73	1191.00
$Err(\%)$	(4.03)	(3.52)	(2.70)	(1.55)	(0.04)
$LM2$	31.64	171.60	406.88	736.09	1158.58
$Err(\%)$	(1.18)	(0.69)	(-0.10)	(-1.22)	(-2.68)
$LM3$	31.64	171.59	406.87	736.07	1158.51
$Err(\%)$	(1.18)	(0.69)	(-0.10)	(-1.23)	(-2.68)
$LM4$	31.64	171.59	406.87	736.07	1158.51
$Err(\%)$	(1.18)	(0.69)	(-0.10)	(-1.23)	(-2.68)

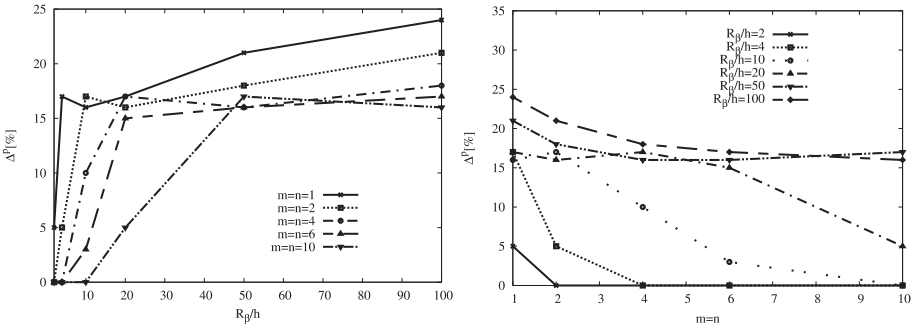

a) *b)*

Figure 18: Multilayered piezoelectric cylindrical panel: $\Delta^p[\%]$ calculated for LD4($\boldsymbol{u}$) vs. LD4($\boldsymbol{u},\Phi$). Variation of $\Delta^p[\%]$ depending on the thickness ratio R_β/h (a). Variation of $\Delta^p[\%]$ depending on the waves number m,n (b).

Table 26: Ring in PZT-4 and Titanium, closed circuit configuration. Comparison between frequency response of pure mechanical problem and electro-mechanical problem.

	$n=4$	$n=8$	$n=12$	$n=16$	$n=20$
$LD4(\boldsymbol{u})$	30.55	165.69	392.87	710.78	1118.77
$LD4(\boldsymbol{u},\Phi)$	31.64	171.59	406.87	736.07	1158.51
$LM4(\boldsymbol{u},\Phi,\mathscr{D}_n)$	31.64	171.59	406.87	736.07	1158.51
$\Delta^p[\%]$	(26.02)	(26.00)	(26.00)	(26.00)	(26.00)
$LM4(\boldsymbol{u},\boldsymbol{\sigma}_n)$	30.55	165.69	392.87	710.78	1118.77
$LM4(\boldsymbol{u},\Phi,\boldsymbol{\sigma}_n)$	31.64	171.59	406.87	736.07	1158.51
$LM4(\boldsymbol{u},\Phi,\boldsymbol{\sigma}_n,\mathscr{D}_n)$	31.64	171.59	406.87	736.07	1158.51
$\Delta^p[\%]$	(26.02)	(26.00)	(26.00)	(26.00)	(26.00)

9 Conclusions

This paper has provided governing equations for the electro-mechanical problem according to the Principle of Virtual Displacements (PVD) and Reissner's Mixed Variational Theorem (RMVT). Various forms of RMVT are discussed in which the transverse shear/normal stresses and/or the transverse normal electric displacement are assumed variables. Governing differential equations are derived according to Carrera's Unified Formulation (CUF) for multilayered plates and shells. Closed-form solutions are given for the free vibration problem of simply supported, orthotropic piezoelectric laminates in closed circuit configurations (electric potential imposed to zero at the top and bottom). Assessments have been provided in which the obtained frequencies have been compared with available three-dimensional solutions proposed for plates [Heyliger and Saravanos (1995)] and shells [Heyliger et al. (1996)]. Further benchmarks has been also performed in the case of both plate and shell geometries. From an analysis of the results, the following main conclusions can be drawn:

1. The use of Layer Wise models is mandatory to achieve a 3D solution, whereas Equivalent Single Layer models could give erroneous results in particular for

Table 27: Closed circuit vibration problem for multilayered piezoelectric cylindrical panel, fundamental frequency $\overline{\omega} = \omega\sqrt{\frac{{R_\beta}^4(\rho)_{PZT4}}{(E_3)_{PZT4}h^2_{TOT}}}$ obtained by using PVD theories. $m = n = 1$.

R_β/h	2	4	10	100
(Ref)	17.584	37.351	83.816	357.27
		$PVD(\boldsymbol{u}, \Phi)$		
CLT	26.575	52.481	130.70	385.82
$Err(\%)$	(51.12)	(40.50)	(55.94)	(7.99)
$FSDT$	24.829	48.060	113.49	369.14
$Err(\%)$	(41.19)	(28.66)	(35.40)	(3.32)
$ED3$	20.529	41.907	88.193	359.47
$Err(\%)$	(16.74)	(12.19)	(5.22)	(0.62)
$ED4$	18.229	40.442	87.869	359.30
$Err(\%)$	(3.66)	(8.27)	(4.83)	(0.57)
$EDZ3$	20.234	39.527	85.849	359.31
$Err(\%)$	(15.06)	(5.82)	(2.42)	(0.57)
$LD3$	17.620	37.416	83.818	357.27
$Err(\%)$	(0.20)	(0.17)	(0.00)	(0.00)
$LD4$	17.585	37.353	83.816	357.27
$Err(\%)$	(0.00)	(0.00)	(0.00)	(0.00)

Table 28: Closed circuit vibration problem for multilayered piezoelectric cylindrical panel, fundamental frequency $\overline{\omega} = \omega\sqrt{\frac{{R_\beta}^4(\rho)_{PZT4}}{(E_3)_{PZT4}h_{TOT}^2}}$ obtained by using RMVT theories. $m = n = 1$.

R_β/h	2	4	10	100
(Ref)	17.584	37.351	83.816	357.27
		$RMVT(\boldsymbol{u}, \Phi, \boldsymbol{\sigma}_n)$		
$EM3$	20.283	41.436	87.646	359.12
$Err(\%)$	(15.34)	(10.94)	(4.57)	(0.52)
$EM4$	18.143	40.178	87.510	359.08
$Err(\%)$	(3.18)	(7.57)	(4.41)	(0.51)
$LM3$	17.593	37.369	83.815	357.27
$Err(\%)$	(0.05)	(0.05)	(0.00)	(0.00)
$LM4$	17.584	37.351	83.816	357.27
$Err(\%)$	(0.00)	(0.00)	(0.00)	(0.00)
		$RMVT(\boldsymbol{u}, \Phi, \mathscr{D}_n)$		
$LM3$	17.620	37.416	83.818	357.27
$Err(\%)$	(0.20)	(0.17)	(0.00)	(0.00)
$LM4$	17.585	37.353	83.816	357.27
$Err(\%)$	(0.00)	(0.00)	(0.00)	(0.00)
		$RMVT(\boldsymbol{u}, \Phi, \boldsymbol{\sigma}_n, \mathscr{D}_n)$		
$LM3$	17.593	37.369	83.815	357.27
$Err(\%)$	(0.05)	(0.05)	(0.00)	(0.00)
$LM4$	17.584	37.351	83.816	357.27
$Err(\%)$	(0.00)	(0.00)	(0.00)	(0.00)

Table 29: Closed circuit vibration problem for multilayered piezoelectric cylindrical panel, fundamental frequency $\overline{\omega} = \omega\sqrt{\frac{{R_\beta}^4(\rho)_{PZT4}}{(E_3)_{PZT4}h_{TOT}^2}}$ obtained by using PVD theories. $m = n = 10$.

R_β/h	2	4	10	100
(Ref)	150.09	302.76	796.46	8338.2
		$PVD(\boldsymbol{u}, \Phi)$		
CLT	265.66	524.76	1306.9	13061
$Err(\%)$	(77.00)	(73.32)	(64.08)	(56.64)
$FSDT$	259.58	518.06	1276.3	11321
$Err(\%)$	(72.95)	(71.11)	(60.24)	(35.77)
$ED3$	172.26	348.16	925.26	8776.4
$Err(\%)$	(14.77)	(14.99)	(16.17)	(5.25)
$ED4$	162.86	327.61	843.39	8746.9
$Err(\%)$	(8.51)	(8.20)	(5.89)	(4.90)
$EDZ3$	172.34	348.20	923.51	8539.6
$Err(\%)$	(14.82)	(15.00)	(15.95)	(2.41)
$LD3$	150.34	304.17	802.71	8338.3
$Err(\%)$	(0.17)	(0.46)	(0.78)	(0.00)
$LD4$	150.09	302.77	796.49	8338.2
$Err(\%)$	(0.00)	(0.00)	(0.00)	(0.00)

Table 30: Closed circuit vibration problem for multilayered piezoelectric cylindrical panel, fundamental frequency $\overline{\omega} = \omega\sqrt{\frac{{R_\beta}^4(\rho)_{PZT4}}{(E_3)_{PZT4}h_{TOT}^2}}$ by using RMVT theories. $m = n = 10$.

R_β/h	2	4	10	100
(Ref)	150.09	302.76	796.46	8338.2
		$RMVT(\boldsymbol{u}, \Phi, \boldsymbol{\sigma}_n)$		
$EM3$	171.25	345.78	915.75	8721.4
$Err(\%)$	(14.10)	(14.21)	(15.00)	(4.60)
$EM4$	162.51	326.94	841.08	8710.8
$Err(\%)$	(8.27)	(7.99)	(5.60)	(4.47)
$LM3$	150.13	303.07	798.50	8338.1
$Err(\%)$	(0.03)	(0.10)	(0.26)	(0.00)
$LM4$	150.09	302.76	796.46	8338.2
$Err(\%)$	(0.00)	(0.00)	(0.00)	(0.00)
		$RMVT(\boldsymbol{u}, \Phi, \mathscr{D}_n)$		
$LM3$	150.34	304.17	802.71	8338.3
$Err(\%)$	(0.17)	(0.47)	(0.78)	(0.00)
$LM4$	150.09	302.77	796.49	8338.2
$Err(\%)$	(0.00)	(0.00)	(0.00)	(0.00)
		$RMVT(\boldsymbol{u}, \Phi, \boldsymbol{\sigma}_n, \mathscr{D}_n)$		
$LM3$	150.13	303.07	798.51	8338.1
$Err(\%)$	(0.03)	(0.10)	(0.26)	(0.00)
$LM4$	150.09	302.76	796.46	8338.2
$Err(\%)$	(0.00)	(0.00)	(0.00)	(0.00)

Table 31: Closed circuit vibration problem for multilayered piezoelectric cylindrical panel. Comparison between frequency response of pure mechanical problem and electro-mechanical problem.

	$m=n=1$			
R_β/h	2	4	10	100
$LD4(\boldsymbol{u})$	17.555	36.784	82.658	346.77
$LD4(\boldsymbol{u},\Phi)$	17.585	37.353	83.816	357.27
$LM4(\boldsymbol{u},\Phi,\mathscr{D}_n)$	17.585	37.353	83.816	357.27
$\Delta^p[\%]$	(5.84)	(17.39)	(16.56)	(24.07)
$LM4(\boldsymbol{u},\boldsymbol{\sigma}_n)$	17.554	36.783	82.658	346.77
$LM4(\boldsymbol{u},\Phi,\boldsymbol{\sigma}_n)$	17.584	37.351	83.816	357.27
$LM4(\boldsymbol{u},\Phi,\boldsymbol{\sigma}_n,\mathscr{D}_n)$	17.584	37.351	83.816	357.27
$\Delta^p[\%]$	(5.84)	(17.37)	(16.56)	(24.07)

lower orders of expansion; classical theories such as CLT and FSDT lead to large errors. For higher values of the transverse anisotropy ESL models give erroneous results even if higher orders of expansion are used.

2. Mixed theories do not significantly improve the results in terms of circular frequency parameters; however, their use becomes mandatory to predict the correct 'through the thickness' modes for both transverse mechanical and electrical variables.

3. The effect produced by the electromechanical interaction on the frequency response, is not a priori predictable: several parameters are involved in this effect such as the thickness ratio, the order of the considered frequency and the waves number. As a consequence, the accuracy of various theories cannot be predicted a priori.

4. The introduction of the curvature does not give further comments and CUF description remains also suitable for shell geometry.

The extension of the present findings to FEM applications will be proposed in the future (both plate and shell geometries). In this new work different expansion functions for the involved electro-mechanical variables will be proposed in order to weigh up the different contributions.

Acknowledgement: Financial support from the Regione Piemonte projects E42, E59 and STEPS is gratefully acknowledged.

References

Ballhause, D.; D'Ottavio, M.; Kröplin, B.; Carrera, E. (2005): A unified formulation to assess multilayered theories for piezoelectric plates. *Computers and Structures*, vol. 83, pp. 1217-1235.

Becker, J.; Fein, O.; Maess, M.; Gaul, L. (2006): Finite element-based analysis of shunted piezoelectric structures for vibration damping. *Computers and Structures*, vol. 84, pp. 2340-2350.

Benjeddou, A. (2000): Advances in piezoelectric finite element modelling of adaptive structural elements: a survey. *Computers and Structures*, vol. 76, pp. 347-363.

Benjeddou, A.; Deü, J.-F. (2001): A two-dimensional closed-form solution for the free-vibrations analysis of piezoelectric sandwich plates. *International Journal of Solids and Structures*, vol. 39, pp. 1463-1486.

Benjeddou, A.; Gorge, V.; Ohayon, R. (2001): Use of piezoelectric shear response in adaptive sandwich shells of revolution - Part 1: theoretical formulation.

Journal of Intelligent Material Systems and Structures, vol. 12, pp. 235-245.

Benjeddou, A.; Gorge, V.; Ohayon R. (2001): Use of piezoelectric shear response in adaptive sandwich shells of revolution - Part 2: finite element implementation. *Journal of Intelligent Material Systems and Structures*, vol. 12, pp. 247-257.

Carrera, E. (1995): A class of two-dimensional theories for anisotropic multilayered plates analysis. *Accademia delle Scienze di Torino, Memorie Scienze Fisiche*, vol. 19-20, pp. 1-39.

Carrera, E. (1997): An improved Reissner-Mindlin-type model for the electromechanical analysis of multilayered plates including piezo-layers. *Journal of Intelligent Material Systems and Structures*, vol. 8, pp. 232-248.

Carrera, E. (1997): C_z^0 requirements-models for the two dimensional analysis of multilayered structures. *Composite Structures*, vol. 37, pp. 373-383.

Carrera, E. (2001): Developments, ideas, and evaluations based upon Reissner's Mixed Variational Theorem in the modeling of multilayered plates and shells. *Applied Mechanics Reviews*, vol. 54, pp. 301-329.

Carrera, E. (2002): Theories and finite elements for multilayered anisotropic, composite plates and shells. *Archives of Computational Methods in Engineering*, vol. 9, pp. 87-140.

Carrera, E. (2003): Historical review of zig-zag theories for multilayered plates and shells. *Applied Mechanics Reviews*, vol. 56, pp. 287-309.

Carrera, E. (2004): On the use of Murakami's zig-zag function in the modeling of layered plates and shells. *Computers and Structures*, vol. 82, pp. 541-554.

Carrera, E.; Boscolo, M. (2007): Classical and mixed finite elements for static and dynamic analysis of piezoelectric plates. *International Journal for Numerical Methods in Engineering*, vol. 70, pp. 1135-1181.

Carrera, E.; Brischetto, S. (2007): Reissner mixed theorem applied to static analysis of piezoelectric shells. *Journal of Intelligent Material Systems and Structures*, vol. 18, pp. 1083-1107.

Carrera, E.; Brischetto, S. (2007): Piezoelectric shell theories with a priori continuous transverse electromechanical variables. *Journal of Mechanics of Materials and Structures*, vol. 2, pp. 377-399.

Carrera, E.; Brischetto, S.; D'Ottavio, M. (2005): Vibration of piezo-electric shells by unified formulation and Reissner's mixed theorem. *II ECCOMAS Thematic Conference on Smart Structures and Materials*, Lisbon, Portugal.

Carrera, E.; Brischetto, S.; Nali, P. (2008): Variational statements and computational models for multifield problems and multilayered structures. *Mechanics of Advanced Materials and Structures*, vol. 15, pp. 182-198.

Carrera, E.; Nali, P. (2009): Mixed piezoelectric plate elements with direct evaluation of transverse electric displacement. *International Journal for Numerical Methods in Engineering*, vol. 80, pp. 403-424.

Chen, Y.C.; Hwu, C. (2010): Green's functions for anisotropic/piezoelectric bimaterials and their applications to boundary element analysis. *CMES: Computer Modeling in Engineering & Sciences*, vol. 57, pp. 31-50.

Chopra, I. (1996): Review of current status of smart structures and integrated systems. *Conference on Smart Structures and Materials 1996: Smart Structures and Integrated Systems*, San Diego, California (USA).

Chopra, I. (2002): Review of state of art of smart structures and integrated systems. *AIAA Journal*, vol. 40, pp. 2145-2187.

Crawley, E. (1994): Intelligent structures for aerospace: a technology overview and assessment. *AIAA Journal*, vol. 32, pp. 1689-1699.

Cupial, P. (2005): Three-dimensional natural vibration analysis and energy considerations for a piezoelectric rectangular plate. *Journal of Sound and Vibrations*, vol. 283, pp. 1093-1113.

D'Ottavio, M.; Ballhause, D.; Kröplin, B.; Carrera, E. (2006): Closed-form solutions for the free-vibration problem of multilayered piezoelectric shells. *Computers and Structures*, vol. 84, pp. 1506-1518.

D'Ottavio, M.; Kröplin, B. (2006): An extension of Reissner mixed variational theorem to piezoelectric laminates. *Mechanics of Advanced Materials and Structures*, vol. 13, pp. 139-150.

Du, J.K.; Wang, J.; Zhou, Y.Y. (2006): Thickness vibrations of a piezoelectric plate under biasing fields. *Ultrasonics*, vol. 44, pp. 853-857.

Duan, W.H.; Quek, S.T.; Wang, Q. (2005): Free vibration analysis of piezoelectric coupled thin and thick annular plate. *Journal of Sound and Vibrations*, vol. 281, pp. 119-139.

Dziatkiewicz, G.; Fedelinski, P. (2007): Dynamic analysis of piezoelectric structures by the dual reciprocity boundary element method. *CMES: Computer Modeling in Engineering & Sciences*, vol. 17, pp. 35-46.

Han, X.; Ding, H.; Liu, G.R. (2005): Elastic waves in a hybrid multilayered piezoelectric plate. *CMES: Computer Modeling in Engineering & Sciences*, vol. 9, pp. 49-55.

He, S.Y.; Chen, W.S.; Chen, Z.L. (1998): A uniformizing method for the free vibration analysis of metal-piezoceramic composite thin plate. *Journal of Sound and Vibration*, vol. 217, pp. 261-281.

Heidary, F.; Eslami, M.R. (2006): Piezo-control of forced vibrations of a ther-

moelastic composite plate. *Composite Structures*, vol. 74, pp. 99-105.

Heyliger, P.R.; Pei, K.; Saravanos, D. (1996): Layerwise mechanics and finite element model for laminated piezoelectric shells. *AIAA Journal*, vol. 34, pp. 2353-2360.

Heyliger, P.R.; Saravanos, D.A. (1995): Exact free vibration analysis of laminated plates with embedded piezoelectric layers. *Journal Acoustical Society of America*, vol. 98, pp. 1547-1557.

Ikeda, T. (1990): Fundamentals of Piezoelectricity, Oxford University Press, Oxford (UK).

Im, S.Y.; Atluri, S.N. (1989): Effects of a piezo-actuator on a finitely deformed beam subjected to general loading. *AIAA Journal*, vol. 27, pp. 1801-1807.

Kapuria, S. (2004): A coupled zig-zag third-order theory for piezoelectric hybrid cross-ply plates. *Journal of Applied Mechanics*, vol. 71, pp. 604-614.

Kapuria, S. (2004): Higher order zig-zag theory for fully coupled thermo-electric-mechanical smart composite plates. *International Journal of Solids and Structures*, vol. 41, pp. 1331-1356.

Kapuria, S.; Achary, G.G.S. (2005): A coupled zigzag theory for the dynamics of piezoelectric hybrid cross-ply plates. *Archive of Applied Mechanics*, vol. 75, pp. 42-57.

Kapuria, S.; Achary, G.G.S. (2005): Exact 3D piezoelasticity solution of hybrid cross-ply plates with damping under harmonic electro-mechanical loads. *Journal of Sound and Vibration*, vol. 282, pp. 617-634.

Kapuria, S.; Kulkarni, S.D. (2008): An efficient quadrilateral element based on improved zigzag theory for dynamic analysis of hybrid plates with electroded piezoelectric actuators and sensors. *Journal of Sound and Vibration*, vol. 315, pp. 118-145.

Leissa, A.W. (1973): Vibration of Shells, NASA SP-288, Washington, D.C. (USA).

Mindlin, R.D. (1972): High frequency vibrations of piezoelectric crystal plate. *International Journal of Solids and Structures*, vol. 8, pp. 895-906.

Mitchell, J.A.; Reddy, J.N. (1995): A refined hybrid plate theory for composite laminates with piezoelectric laminae. *International Journal of Solids and Structures*, vol. 32, pp. 2345-2367.

MUL2, (accessed 28/05/2009): Modeling for Multilayered Structures in Multifield Analysis [on line]. *Available: http://www.mul2.com.*

Murakami, H. (1986): Laminated composite plate theory with improved in-plane responses. *Journal of Applied Mechanics*, vol. 53, pp. 661-666.

Ossadzow-David, C.; Touratier, M. (2004): A multilayered piezoelectric shell theory. *International Composites Science and Technology*, vol. 64, pp. 2121-2137.

Pan, E.; Heyliger, P.R. (2002): Free vibration of simply supported and multilayered magneto-electro-elastic plates. *Journal of Sound and Vibrations*, vol. 252, pp. 429-442.

Ramirez, F.; Heyliger, P.R.; Pan, E. (2006): Free vibration response of two-dimensional magneto-electro-elastic laminated plates. *Journal of Sound and Vibrations*, vol. 292, pp. 626-644.

Rao, S.S.; Sunar, M. (1994): Piezoelectricity and its use in disturbance sensing and control of flexible structures: a survey. *Applied Mechanics Reviews*, vol. 47, pp. 113-123.

Reddy, J.N. (2004): Mechanics of Laminated Composite Plates and Shells. Theory and Analysis, CRC Press, New York (USA).

Reissner, E. (1984): On a certain mixed variational theory and a proposed application. *International Journal for Numerical Methods in Engineering*, vol. 20, pp. 1366-1368.

Robbins Jr, D.H.; Chopra, I. (2006): The effect of laminate kinematic assumptions on the global response of actuated plates. *Journal of Intelligent Material Systems and Structures*, vol. 17, pp. 273-299.

Rogacheva, N.N. (1994): The Theory of Piezoelectric Shells and Plates, CRC Press, Boca Raton, Florida (USA).

Shakeri, M.; Eblami, M.R.; Daneshmehr, A. (2006): Dynamic analysis of thick laminated shell panel with piezoelectric layer based on three dimensional elasticity solution. *Computers and Structures*, vol. 84, pp. 1519-1526.

Sunar, M.; Rao, S.S. (1999): Recent advances in sensing and control of flexible structures via piezolecteric materials technology. *Applied Mechanics Reviews*, vol. 52, pp. 1-16.

Tani, J.; Takagi, T.; Qiu, J. (1998): Intelligent materials systems: application of functional materials. *Applied Mechanics Reviews*, vol. 51, pp. 505-521.

Tiersten, H.F. (1969): Linear Piezoelectric Plate Vibrations, Plenum, New York (USA).

Wang, H.M.; Ding, H.J.; Chen, Y.M. (2005): Dynamic solution of a multilayered orthotropic piezoelectric hollow cylinder of axisymmetric plane strain problems. *International Journal of Solids and Structures*, vol. 42, pp. 85-102.

Wu, K.-C.; Chen, S.-H. (2007): Two dimensional dynamic Green's functions for piezoelectric materials. *CMES: Computer Modeling in Engineering & Sciences*, vol. 20, pp. 147-156.

Wu, Y.-C.; Heyliger, P. (2001): Free vibration of layered piezoelctric spherical caps. *Journal of Sound and Vibration*, vol. 245, pp. 527-544.

Yang, J.S. (2006): A review of a few topics in piezoelectricity. *Applied Mechanics Reviews*, vol. 59, pp. 335-345.

Yang, J.S.; Yu, J.D. (1993): Equations for a laminated piezoelectric plate. *Archives of Mechanics*, vol. 45, pp. 653-664.

Zhang, Z.; Feng, C.; Liew, K.M. (2006): Three-dimensional vibration analysis of multilayered piezoelectric composite plates. *International Journal of Engineering Science*, vol. 44, pp. 397-408.

Zheng, S.; Wang, X., Chen, W. (2004): The formulation of a refined hybrid enhanced assumed strain solid shell element and its application to model smart structures containing distributed piezoelectric sensors/actuators. *Smart Materials and Structures*, vol. 13, pp. 43-50.

Zhu, J.-Q.; Chen, C.; Shen, Y.-P. (2003): Three dimensional analysis of dynamic stability of piezoelectric circular cylindrical shells. *European Journal of Mechanics A/Solids*, vol. 22, pp. 401-411.

Appendix A: Fundamental nuclei for plates

After performing the arrays products and introducing the appropriate integrals in the thickness direction z, it is possible to obtain the explicit form of fundamental nuclei: they are arrays which can be expanded in τ and s directions depending on the order of expansion N, and assembled in k index depending on the number of layers and on the multilayer approach (ESL or LW). An example is given for the fundamental nucleus K_{uu} for PVD in case of electro-mechanical problem. In A.1 the explicit components for plates in differential form are proposed. A.2 gives the relative closed form after the introduction of harmonic assumptions.

Appendix A:.1 Explicit form

The following integrals are introduced to perform the explicit form of fundamental nuclei:

$$(J^{k\tau s}, J^{k\tau_z s}, J^{k\tau s_z}, J^{k\tau_z s_z}) = \int_{A_k} (F_\tau F_s, \frac{\partial F_\tau}{\partial z} F_s, F_\tau \frac{\partial F_s}{\partial z}, \frac{\partial F_\tau}{\partial z}\frac{\partial F_s}{\partial z})\, dz\,. \tag{213}$$

Fundamental nucleus K_{uu} for PVD extended to electro-mechanical case for plate geometry is:

$$\left(K^{k\tau s}_{uu}\right)_{11} = -C^k_{11} J^{k\tau s}\partial_{xx} - 2C^k_{16} J^{k\tau s}\partial_{xy} - C^k_{66} J^{k\tau s}\partial_{yy} + C^k_{55} J^{k\tau_z s_z}\,,$$

$$
\begin{aligned}
\left(K_{uu}^{k\tau s}\right)_{12} &= -C_{12}^{k}J^{k\tau s}\partial_{xy} - C_{16}^{k}J^{k\tau s}\partial_{xx} - C_{26}^{k}J_{\alpha}^{k\tau s}\partial_{yy} - C_{66}^{k}J^{k\tau s}\partial_{xy} + C_{45}^{k}J^{k\tau_z s_z} \ , \\
\left(K_{uu}^{k\tau s}\right)_{13} &= -C_{13}^{k}J^{k\tau s_z}\partial_{x} - C_{36}^{k}J^{k\tau s_z}\partial_{y} + C_{45}^{k}J^{k\tau_z s}\partial_{y} + C_{55}^{k}J^{k\tau_z s}\partial_{x} \ , \\
\left(K_{uu}^{k\tau s}\right)_{21} &= -C_{12}^{k}J^{k\tau s}\partial_{xy} - C_{16}^{k}J^{k\tau s}\partial_{xx} - C_{26}^{k}J^{k\tau s}\partial_{yy} - C_{66}^{k}J^{k\tau s}\partial_{xy} + C_{45}^{k}J^{k\tau_z s_z} \ , \\
\left(K_{uu}^{k\tau s}\right)_{22} &= -C_{22}^{k}J^{k\tau s}\partial_{yy} - 2C_{26}^{k}J^{k\tau s}\partial_{xy} - C_{66}^{k}J^{k\tau s}\partial_{xx} + C_{44}^{k}J^{k\tau_z s_z} \ , \\
\left(K_{uu}^{k\tau s}\right)_{23} &= -C_{23}^{k}J^{k\tau s_z}\partial_{y} - C_{36}^{k}J^{k\tau s_z}\partial_{x} + C_{45}^{k}J^{k\tau_z s}\partial_{x} + C_{44}^{k}J^{k\tau_z s}\partial_{y} \ , \\
\left(K_{uu}^{k\tau s}\right)_{31} &= C_{13}^{k}J^{k\tau_z s}\partial_{x} + C_{36}^{k}J^{k\tau_z s}\partial_{y} - C_{45}^{k}J^{k\tau s_z}\partial_{y} - C_{55}^{k}J^{k\tau s_z}\partial_{x} \ , \\
\left(K_{uu}^{k\tau s}\right)_{32} &= C_{23}^{k}J^{k\tau_z s}\partial_{y} + C_{36}^{k}J^{k\tau_z s}\partial_{x} - C_{45}^{k}J^{k\tau s_z}\partial_{x} - C_{44}^{k}J^{k\tau s_z}\partial_{y} \ , \\
\left(K_{uu}^{k\tau s}\right)_{33} &= C_{33}^{k}J^{k\tau_z s_z} - C_{44}^{k}J^{k\tau s}\partial_{yy} - C_{55}^{k}J^{k\tau s}\partial_{xx} - 2C_{45}^{k}J^{k\tau s}\partial_{xy} \ ,
\end{aligned}
\tag{214}
$$

where the symbols ∂_{ij} and ∂_i indicate partial derivatives.

Appendix A:.2 Closed algebraic form

Nuclei presented in A.1 can be written in closed form for the algebraic system if Eqs.(207) and (208) are employed:

$$
\begin{aligned}
\left(K_{uu}^{k\tau s}\right)_{11} &= \bar{\alpha}^2 C_{11}^{k}J^{k\tau s} + \bar{\beta}^2 C_{66}^{k}J^{k\tau s} + C_{55}^{k}J^{k\tau_z s_z} \ , \\
\left(K_{uu}^{k\tau s}\right)_{12} &= \bar{\alpha}\bar{\beta}C_{12}^{k}J^{k\tau s} + \bar{\alpha}\bar{\beta}C_{66}^{k}J^{k\tau s} = \left(K_{uu}^{k\tau s}\right)_{21} \ , \\
\left(K_{uu}^{k\tau s}\right)_{13} &= -\bar{\alpha}C_{13}^{k}J^{k\tau s_z} + \bar{\alpha}C_{55}^{k}J^{k\tau_z s} \ , \\
\left(K_{uu}^{k\tau s}\right)_{22} &= \bar{\beta}^2 C_{22}^{k}J^{k\tau s} + \bar{\alpha}^2 C_{66}^{k}J^{k\tau s} + C_{44}^{k}J^{k\tau_z s_z} \ , \\
\left(K_{uu}^{k\tau s}\right)_{23} &= -C_{23}^{k}J^{k\tau s_z}\bar{\beta} + C_{44}^{k}J^{k\tau_z s}\bar{\beta} \ , \\
\left(K_{uu}^{k\tau s}\right)_{31} &= -\bar{\alpha}C_{13}^{k}J^{k\tau_z s} + \bar{\alpha}C_{55}^{k}J^{k\tau s_z} \ , \\
\left(K_{uu}^{k\tau s}\right)_{32} &= -\bar{\beta}C_{23}^{k}J^{k\tau_z s} + \bar{\beta}C_{44}^{k}J^{k\tau s_z} \ ,
\end{aligned}
\tag{215}
$$

$$\left(K_{uu}^{k\tau s}\right)_{33} = C_{33}^{k} J^{k\tau_z s_z} + \bar{\beta}^2 C_{44}^{k} J^{k\tau s} + \bar{\alpha}^2 C_{55}^{k} J^{k\tau s} \ ,$$

where $\bar{\alpha} = \frac{m\pi}{a}$ and $\bar{\beta} = \frac{n\pi}{b}$, with a and b as plate dimensions, and m and n as waves number in x and y directions, respectively.

Appendix B: Fundamental nuclei for shells

After performing the arrays products and introducing the appropriate integrals in the thickness direction z of the shell, it is possible to obtain the explicit form of fundamental nuclei. An example is given for the fundamental nucleus K_{uu} for PVD in case of electro-mechanical problem. In A.1 the explicit components for shells in differential form are proposed. A.2 gives the relative closed form after the introduction of harmonic assumptions.

Appendix B:.1 Explicit form

The following integrals are introduced to perform the explicit form of fundamental nuclei:

$$(J^{k\tau s}, J_{\alpha}^{k\tau s}, J_{\beta}^{k\tau s}, J_{\alpha/\beta}^{k\tau s}, J_{\beta/\alpha}^{k\tau s}, J_{1/\beta}^{k\tau s}, J_{1/\alpha}^{k\tau s}, J_{\alpha\beta}^{k\tau s})$$
$$= \int_{A_k} F_\tau F_s (1, H_\alpha^k, H_\beta^k, \frac{H_\alpha^k}{H_\beta^k}, \frac{H_\beta^k}{H_\alpha^k}, \frac{1}{H_\beta^k}, \frac{1}{H_\alpha^k}, H_\alpha^k H_\beta^k)\, dz, \quad (216)$$

$$(J^{k\tau_z s}, J_{\alpha}^{k\tau_z s}, J_{\beta}^{k\tau_z s}, J_{\alpha/\beta}^{k\tau_z s}, J_{\beta/\alpha}^{k\tau_z s}, J_{1/\beta}^{k\tau_z s}, J_{1/\alpha}^{k\tau_z s}, J_{\alpha\beta}^{k\tau_z s})$$
$$= \int_{A_k} \frac{\partial F_\tau}{\partial z} F_s (1, H_\alpha^k, H_\beta^k, \frac{H_\alpha^k}{H_\beta^k}, \frac{H_\beta^k}{H_\alpha^k}, \frac{1}{H_\beta^k}, \frac{1}{H_\alpha^k}, H_\alpha^k H_\beta^k)\, dz,$$

$$(J^{k\tau s_z}, J_{\alpha}^{k\tau s_z}, J_{\beta}^{k\tau s_z}, J_{\alpha/\beta}^{k\tau s_z}, J_{\beta/\alpha}^{k\tau s_z}, J_{1/\beta}^{k\tau s_z}, J_{1/\alpha}^{k\tau s_z}, J_{\alpha\beta}^{k\tau s_z})$$
$$= \int_{A_k} F_\tau \frac{\partial F_s}{\partial z} (1, H_\alpha^k, H_\beta^k, \frac{H_\alpha^k}{H_\beta^k}, \frac{H_\beta^k}{H_\alpha^k}, \frac{1}{H_\beta^k}, \frac{1}{H_\alpha^k}, H_\alpha^k H_\beta^k)\, dz,$$

$$(J^{k\tau_z s_z}, J_{\alpha}^{k\tau_z s_z}, J_{\beta}^{k\tau_z s_z}, J_{\alpha/\beta}^{k\tau_z s_z}, J_{\beta/\alpha}^{k\tau_z s_z}, J_{1/\beta}^{k\tau_z s_z}, J_{1/\alpha}^{k\tau_z s_z}, J_{\alpha\beta}^{k\tau_z s_z})$$
$$= \int_{A_k} \frac{\partial F_\tau}{\partial z} \frac{\partial F_s}{\partial z} (1, H_\alpha^k, H_\beta^k, \frac{H_\alpha^k}{H_\beta^k}, \frac{H_\beta^k}{H_\alpha^k}, \frac{1}{H_\beta^k}, \frac{1}{H_\alpha^k}, H_\alpha^k H_\beta^k)\, dz,$$

First, fundamental nucleus K_{uu} related to PVD extended to electro-mechanical case is given for doubly curved shells (radii of curvature in both α and β directions, see Figure 2); the symbols ∂_{ij} and ∂_i indicate partial derivatives:

$$
\begin{aligned}
\left(K_{uu}^{k\tau s}\right)_{11} &= -C_{11}^{k} J_{\beta/\alpha}^{k\tau s}\partial_{\alpha\alpha} - 2C_{16}^{k} J^{k\tau s}\partial_{\alpha\beta} - C_{66}^{k} J_{\alpha/\beta}^{k\tau s}\partial_{\beta\beta} \\
&\quad + C_{55}^{k}\left(J_{\alpha\beta}^{k\tau_z s_z} - \frac{1}{R_\alpha^k} J_{\beta}^{k\tau_z s} - \frac{1}{R_\alpha^k} J_{\beta}^{k\tau s_z} + \frac{1}{R_\alpha^k}\frac{1}{R_\alpha^k} J_{\beta/\alpha}^{k\tau s}\right), \\
\left(K_{uu}^{k\tau s}\right)_{12} &= -C_{12}^{k} J^{k\tau s}\partial_{\alpha\beta} - C_{16}^{k} J_{\beta/\alpha}^{k\tau s}\partial_{\alpha\alpha} - C_{26}^{k} J_{\alpha/\beta}^{k\tau s}\partial_{\beta\beta} - C_{66}^{k} J^{k\tau s}\partial_{\alpha\beta} \\
&\quad + C_{45}^{k}\left(J_{\alpha\beta}^{k\tau_z s_z} - \frac{1}{R_\beta^k} J_{\alpha}^{k\tau_z s} - \frac{1}{R_\alpha^k} J_{\beta}^{k\tau s_z} + \frac{1}{R_\alpha^k}\frac{1}{R_\beta^k} J^{k\tau s}\right), \\
\left(K_{uu}^{k\tau s}\right)_{13} &= -C_{11}^{k}\frac{1}{R_\alpha^k} J_{\beta/\alpha}^{k\tau s}\partial_{\alpha} - C_{12}^{k}\frac{1}{R_\beta^k} J^{k\tau s}\partial_{\alpha} - C_{13}^{k} J_{\beta}^{k\tau s_z}\partial_{\alpha}, \\
&\quad - C_{16}^{k}\frac{1}{R_\alpha^k} J^{k\tau s}\partial_{\beta} - C_{26}^{k}\frac{1}{R_\beta^k} J_{\alpha/\beta}^{k\tau s}\partial_{\beta} - C_{36}^{k} J_{\alpha}^{k\tau s_z}\partial_{\beta} \\
&\quad + C_{45}^{k}\left(J_{\alpha}^{k\tau_z s}\partial_{\beta} - \frac{1}{R_\alpha^k} J^{k\tau s}\partial_{\beta}\right) + C_{55}^{k}\left(J_{\beta}^{k\tau_z s}\partial_{\alpha} - \frac{1}{R_\alpha^k} J_{\beta/\alpha}^{k\tau s}\partial_{\alpha}\right), \\
\left(K_{uu}^{k\tau s}\right)_{21} &= -C_{12}^{k} J^{k\tau s}\partial_{\alpha\beta} - C_{16}^{k} J_{\beta/\alpha}^{k\tau s}\partial_{\alpha\alpha} - C_{26}^{k} J_{\alpha/\beta}^{k\tau s}\partial_{\beta\beta} - C_{66}^{k} J^{k\tau s}\partial_{\alpha\beta} \\
&\quad + C_{45}^{k}\left(J_{\alpha\beta}^{k\tau_z s_z} - \frac{1}{R_\beta^k} J_{\alpha}^{k\tau s_z} - \frac{1}{R_\alpha^k} J_{\beta}^{k\tau_z s} + \frac{1}{R_\alpha^k}\frac{1}{R_\beta^k} J^{k\tau s}\right), \\
\left(K_{uu}^{k\tau s}\right)_{22} &= -C_{22}^{k} J_{\alpha/\beta}^{k\tau s}\partial_{\beta\beta} - 2C_{26}^{k} J^{k\tau s}\partial_{\alpha\beta} - C_{66}^{k} J_{\beta/\alpha}^{k\tau s}\partial_{\alpha\alpha} \\
&\quad + C_{44}^{k}\left(J_{\alpha\beta}^{k\tau_z s_z} - \frac{1}{R_\beta^k} J_{\alpha}^{k\tau_z s} - \frac{1}{R_\beta^k} J_{\alpha}^{k\tau s_z} + \frac{1}{R_\beta^k}\frac{1}{R_\beta^k} J_{\alpha/\beta}^{k\tau s}\right), \\
\left(K_{uu}^{k\tau s}\right)_{23} &= -C_{12}^{k}\frac{1}{R_\alpha^k} J^{k\tau s}\partial_{\beta} - C_{22}^{k}\frac{1}{R_\beta^k} J_{\alpha/\beta}^{k\tau s}\partial_{\beta} - C_{23}^{k} J_{\alpha}^{k\tau s_z}\partial_{\beta} \\
&\quad - C_{16}^{k}\frac{1}{R_\alpha^k} J_{\beta/\alpha}^{k\tau s}\partial_{\alpha} - C_{26}^{k}\frac{1}{R_\beta^k} J^{k\tau s}\partial_{\alpha} - C_{36}^{k} J_{\beta}^{k\tau s_z}\partial_{\alpha} \\
&\quad + C_{45}^{k}\left(J_{\beta}^{k\tau_z s}\partial_{\alpha} - \frac{1}{R_\beta^k} J^{k\tau s}\partial_{\alpha}\right) + C_{44}^{k}\left(J_{\alpha}^{k\tau_z s}\partial_{\beta} - \frac{1}{R_\beta^k} J_{\alpha/\beta}^{k\tau s}\partial_{\beta}\right),
\end{aligned}
\tag{217}
$$

$$\left(K_{uu}^{k\tau s}\right)_{31} = C_{11}^{k}\frac{1}{R_{\alpha}^{k}}J_{\beta/\alpha}^{k\tau s}\partial_{\alpha} + C_{12}^{k}\frac{1}{R_{\beta}^{k}}J^{k\tau s}\partial_{\alpha} + C_{13}^{k}J_{\beta}^{k\tau_{z}s}\partial_{\alpha}$$
$$+ C_{16}^{k}\frac{1}{R_{\alpha}^{k}}J^{k\tau s}\partial_{\beta} + C_{26}^{k}\frac{1}{R_{\beta}^{k}}J_{\alpha/\beta}^{k\tau s}\partial_{\beta} + C_{36}^{k}J_{\alpha}^{k\tau_{z}s}\partial_{\beta}$$
$$- C_{45}^{k}\left(J_{\alpha}^{k\tau s_{z}}\partial_{\beta} - \frac{1}{R_{\alpha}^{k}}J^{k\tau s}\partial_{\beta}\right) - C_{55}^{k}\left(J_{\beta}^{k\tau s_{z}}\partial_{\alpha} - \frac{1}{R_{\alpha}^{k}}J_{\beta/\alpha}^{k\tau s}\partial_{\alpha}\right),$$

$$\left(K_{uu}^{k\tau s}\right)_{32} = C_{12}^{k}\frac{1}{R_{\alpha}^{k}}J^{k\tau s}\partial_{\beta} + C_{22}^{k}\frac{1}{R_{\beta}^{k}}J_{\alpha/\beta}^{k\tau s}\partial_{\beta} + C_{23}^{k}J_{\alpha}^{k\tau_{z}s}\partial_{\beta}$$
$$+ C_{16}^{k}\frac{1}{R_{\alpha}^{k}}J_{\beta/\alpha}^{k\tau s}\partial_{\alpha} + C_{26}^{k}\frac{1}{R_{\beta}^{k}}J^{k\tau s}\partial_{\alpha} + C_{36}^{k}J_{\beta}^{k\tau_{z}s}\partial_{\alpha}$$
$$- C_{45}^{k}\left(J_{\beta}^{k\tau s_{z}}\partial_{\alpha} - \frac{1}{R_{\beta}^{k}}J^{k\tau s}\partial_{\alpha}\right) - C_{44}^{k}\left(J_{\alpha}^{k\tau s_{z}}\partial_{\beta} - \frac{1}{R_{\beta}^{k}}J_{\alpha/\beta}^{k\tau s}\partial_{\beta}\right),$$

$$\left(K_{uu}^{k\tau s}\right)_{33} = C_{11}^{k}\frac{1}{R_{\alpha}^{k}}\frac{1}{R_{\alpha}^{k}}J_{\beta/\alpha}^{k\tau s} + C_{22}^{k}\frac{1}{R_{\beta}^{k}}\frac{1}{R_{\beta}^{k}}J_{\alpha/\beta}^{k\tau s} + C_{33}^{k}J_{\alpha\beta}^{k\tau_{z}s_{z}}$$
$$+ 2C_{12}^{k}\frac{1}{R_{\alpha}^{k}}\frac{1}{R_{\beta}^{k}}J^{k\tau s} + C_{13}^{k}\frac{1}{R_{\alpha}^{k}}\left(J_{\beta}^{k\tau_{z}s} + J_{\beta}^{k\tau s_{z}}\right) + C_{23}^{k}\frac{1}{R_{\beta}^{k}}\left(J_{\alpha}^{k\tau_{z}s} + J_{\alpha}^{k\tau s_{z}}\right)$$
$$- C_{44}^{k}J_{\alpha/\beta}^{k\tau s}\partial_{\beta\beta} - C_{55}^{k}J_{\beta/\alpha}^{k\tau s}\partial_{\alpha\alpha} - 2C_{45}^{k}J^{k\tau s}\partial_{\alpha\beta}.$$

For cylindrical shells, one of the radii of curvature is ∞, we consider the example of $R_{\beta}^{k} = \infty$, so $1/R_{\beta}^{k} = 0$ and $H_{\beta}^{k} = 1$, Eqs.(217) are simplified in:

$$\left(K_{uu}^{k\tau s}\right)_{11} = -C_{11}^{k}J_{1/\alpha}^{k\tau s}\partial_{\alpha\alpha} - 2C_{16}^{k}J^{k\tau s}\partial_{\alpha\beta} - C_{66}^{k}J_{\alpha}^{k\tau s}\partial_{\beta\beta}$$
$$+ C_{55}^{k}\left(J_{\alpha}^{k\tau_{z}s_{z}} - \frac{1}{R_{\alpha}^{k}}J^{k\tau_{z}s} - \frac{1}{R_{\alpha}^{k}}J^{k\tau s_{z}} + \frac{1}{R_{\alpha}^{k}}\frac{1}{R_{\alpha}^{k}}J_{1/\alpha}^{k\tau s}\right),$$

$$\left(K_{uu}^{k\tau s}\right)_{12} = -C_{12}^{k}J^{k\tau s}\partial_{\alpha\beta} - C_{16}^{k}J_{1/\alpha}^{k\tau s}\partial_{\alpha\alpha} - C_{26}^{k}J_{\alpha}^{k\tau s}\partial_{\beta\beta} - C_{66}^{k}J^{k\tau s}\partial_{\alpha\beta}$$
$$+ C_{45}^{k}\left(J_{\alpha}^{k\tau_{z}s_{z}} - \frac{1}{R_{\alpha}^{k}}J^{k\tau s_{z}}\right),$$

$$\left(K_{uu}^{k\tau s}\right)_{13} = -C_{11}^{k}\frac{1}{R_{\alpha}^{k}}J_{1/\alpha}^{k\tau s}\partial_{\alpha} - C_{13}^{k}J^{k\tau s_{z}}\partial_{\alpha} - C_{16}^{k}\frac{1}{R_{\alpha}^{k}}J^{k\tau s}\partial_{\beta} - C_{36}^{k}J_{\alpha}^{k\tau s_{z}}\partial_{\beta}$$
$$+ C_{45}^{k}\left(J_{\alpha}^{k\tau_{z}s}\partial_{\beta} - \frac{1}{R_{\alpha}^{k}}J^{k\tau s}\partial_{\beta}\right) + C_{55}^{k}\left(J^{k\tau_{z}s}\partial_{\alpha} - \frac{1}{R_{\alpha}^{k}}J_{1/\alpha}^{k\tau s}\partial_{\alpha}\right),$$

$$\left(K_{uu}^{k\tau s}\right)_{21} = -C_{12}^{k} J^{k\tau s}\partial_{\alpha\beta} - C_{16}^{k} J_{1/\alpha}^{k\tau s}\partial_{\alpha\alpha} - C_{26}^{k} J_{\alpha}^{k\tau s}\partial_{\beta\beta} - C_{66}^{k} J^{k\tau s}\partial_{\alpha\beta} + C_{45}^{k}\left(J_{\alpha}^{k\tau_z s_z} - \frac{1}{R_{\alpha}^{k}} J^{k\tau_z s}\right),$$

$$\left(K_{uu}^{k\tau s}\right)_{22} = -C_{22}^{k} J_{\alpha}^{k\tau s}\partial_{\beta\beta} - 2C_{26}^{k} J^{k\tau s}\partial_{\alpha\beta} - C_{66}^{k} J_{1/\alpha}^{k\tau s}\partial_{\alpha\alpha} + C_{44}^{k}\left(J_{\alpha}^{k\tau_z s_z}\right), \tag{218}$$

$$\left(K_{uu}^{k\tau s}\right)_{23} = -C_{12}^{k}\frac{1}{R_{\alpha}^{k}} J^{k\tau s}\partial_{\beta} - C_{23}^{k} J_{\alpha}^{k\tau s_z}\partial_{\beta} - C_{16}^{k}\frac{1}{R_{\alpha}^{k}} J_{1/\alpha}^{k\tau s}\partial_{\alpha} - C_{36}^{k} J^{k\tau s_z}\partial_{\alpha} + C_{45}^{k}\left(J^{k\tau_z s}\partial_{\alpha}\right) + C_{44}^{k}\left(J_{\alpha}^{k\tau_z s}\partial_{\beta}\right),$$

$$\left(K_{uu}^{k\tau s}\right)_{31} = C_{11}^{k}\frac{1}{R_{\alpha}^{k}} J_{1/\alpha}^{k\tau s}\partial_{\alpha} + C_{13}^{k} J^{k\tau_z s}\partial_{\alpha} + C_{16}^{k}\frac{1}{R_{\alpha}^{k}} J^{k\tau s}\partial_{\beta} + C_{36}^{k} J_{\alpha}^{k\tau_z s}\partial_{\beta} - C_{45}^{k}\left(J_{\alpha}^{k\tau s_z}\partial_{\beta} - \frac{1}{R_{\alpha}^{k}} J^{k\tau s}\partial_{\beta}\right) - C_{55}^{k}\left(J^{k\tau s_z}\partial_{\alpha} - \frac{1}{R_{\alpha}^{k}} J_{1/\alpha}^{k\tau s}\partial_{\alpha}\right),$$

$$\left(K_{uu}^{k\tau s}\right)_{32} = C_{12}^{k}\frac{1}{R_{\alpha}^{k}} J^{k\tau s}\partial_{\beta} + C_{23}^{k} J_{\alpha}^{k\tau_z s}\partial_{\beta} + C_{16}^{k}\frac{1}{R_{\alpha}^{k}} J_{1/\alpha}^{k\tau s}\partial_{\alpha} + C_{36}^{k} J^{k\tau_z s}\partial_{\alpha} - C_{45}^{k}\left(J^{k\tau s_z}\partial_{\alpha}\right) - C_{44}^{k}\left(J_{\alpha}^{k\tau s_z}\partial_{\beta}\right),$$

$$\left(K_{uu}^{k\tau s}\right)_{33} = C_{11}^{k}\frac{1}{R_{\alpha}^{k}}\frac{1}{R_{\alpha}^{k}} J_{1/\alpha}^{k\tau s} + C_{33}^{k} J_{\alpha}^{k\tau_z s_z} + C_{13}^{k}\frac{1}{R_{\alpha}^{k}}\left(J^{k\tau_z s} + J^{k\tau s_z}\right) - C_{44}^{k} J_{\alpha}^{k\tau s}\partial_{\beta\beta} - C_{55}^{k} J_{1/\alpha}^{k\tau s}\partial_{\alpha\alpha} - 2C_{45}^{k} J^{k\tau s}\partial_{\alpha\beta}.$$

When both R_{α}^{k} and R_{β}^{k} are infinite, fundamental nuclei for plates are obtained (see Appendix A).

Appendix B:.2 Closed algebraic form

Nuclei presented in Appendix B:.1 can be written in closed form if Eqs.(207) and (209) are employed. In this case, $\bar{\alpha} = \frac{m\pi}{a}$ and $\bar{\beta} = \frac{n\pi}{b}$ where a and b are the shell dimensions.
Implemented algebraic form of nuclei for doubly curved shells are:

$$\left(K_{uu}^{k\tau s}\right)_{11} = \bar{\alpha}^2 C_{11}^{k} J_{\beta/\alpha}^{k\tau s} + \bar{\beta}^2 C_{66}^{k} J_{\alpha/\beta}^{k\tau s} + C_{55}^{k}\left(J_{\alpha\beta}^{k\tau_z s_z} - \frac{1}{R_{\alpha}^{k}} J_{\beta}^{k\tau_z s} - \frac{1}{R_{\alpha}^{k}} J_{\beta}^{k\tau s_z} + \frac{1}{R_{\alpha}^{k}}\frac{1}{R_{\alpha}^{k}} J_{\beta/\alpha}^{k\tau s}\right),$$

$$\left(K_{uu}^{k\tau s}\right)_{12} = \bar{\alpha}\bar{\beta} C_{12}^{k} J^{k\tau s} + \bar{\alpha}\bar{\beta} C_{66}^{k} J^{k\tau s},$$

$$\left(K_{uu}^{k\tau s}\right)_{13} = -\bar{\alpha}C_{11}^{k}\frac{1}{R_{\alpha}^{k}}J_{\beta/\alpha}^{k\tau s} - \bar{\alpha}C_{12}^{k}\frac{1}{R_{\beta}^{k}}J^{k\tau s} - \bar{\alpha}C_{13}^{k}J_{\beta}^{k\tau s_z} + C_{55}^{k}\left(J_{\beta}^{k\tau_z s}\bar{\alpha} - \frac{1}{R_{\alpha}^{k}}J_{\beta/\alpha}^{k\tau s}\bar{\alpha}\right),$$

$$\left(K_{uu}^{k\tau s}\right)_{21} = \bar{\alpha}\bar{\beta}C_{12}^{k}J^{k\tau s} + \bar{\alpha}\bar{\beta}C_{66}^{k}J^{k\tau s}, \tag{219}$$

$$\left(K_{uu}^{k\tau s}\right)_{22} = \bar{\beta}^{2}C_{22}^{k}J_{\alpha/\beta}^{k\tau s} + \bar{\alpha}^{2}C_{66}^{k}J_{\beta/\alpha}^{k\tau s} + C_{44}^{k}\left(J_{\alpha\beta}^{k\tau_z s_z} - \frac{1}{R_{\beta}^{k}}J_{\alpha}^{k\tau_z s} - \frac{1}{R_{\beta}^{k}}J_{\alpha}^{k\tau s_z} + \frac{1}{R_{\beta}^{k}}\frac{1}{R_{\beta}^{k}}J_{\alpha/\beta}^{k\tau s}\right),$$

$$\left(K_{uu}^{k\tau s}\right)_{23} = -C_{12}^{k}\frac{1}{R_{\alpha}^{k}}J^{k\tau s}\bar{\beta} - C_{22}^{k}\frac{1}{R_{\beta}^{k}}J_{\alpha/\beta}^{k\tau s}\bar{\beta} - C_{23}^{k}J_{\alpha}^{k\tau s_z}\bar{\beta} + C_{44}^{k}\left(J_{\alpha}^{k\tau_z s}\bar{\beta} - \frac{1}{R_{\beta}^{k}}J_{\alpha/\beta}^{k\tau s}\bar{\beta}\right),$$

$$\left(K_{uu}^{k\tau s}\right)_{31} = -\bar{\alpha}C_{11}^{k}\frac{1}{R_{\alpha}^{k}}J_{\beta/\alpha}^{k\tau s} - \bar{\alpha}C_{12}^{k}\frac{1}{R_{\beta}^{k}}J^{k\tau s} - \bar{\alpha}C_{13}^{k}J_{\beta}^{k\tau_z s} - C_{55}^{k}\left(-\bar{\alpha}J_{\beta}^{k\tau s_z} + \bar{\alpha}\frac{1}{R_{\alpha}^{k}}J_{\beta/\alpha}^{k\tau s}\right),$$

$$\left(K_{uu}^{k\tau s}\right)_{32} = -\bar{\beta}C_{12}^{k}\frac{1}{R_{\alpha}^{k}}J^{k\tau s} - \bar{\beta}C_{22}^{k}\frac{1}{R_{\beta}^{k}}J_{\alpha/\beta}^{k\tau s} - \bar{\beta}C_{23}^{k}J_{\alpha}^{k\tau_z s} - C_{44}^{k}\left(-\bar{\beta}J_{\alpha}^{k\tau s_z} + \bar{\beta}\frac{1}{R_{\beta}^{k}}J_{\alpha/\beta}^{k\tau s}\right),$$

$$\left(K_{uu}^{k\tau s}\right)_{33} = C_{11}^{k}\frac{1}{R_{\alpha}^{k}}\frac{1}{R_{\alpha}^{k}}J_{\beta/\alpha}^{k\tau s} + C_{22}^{k}\frac{1}{R_{\beta}^{k}}\frac{1}{R_{\beta}^{k}}J_{\alpha/\beta}^{k\tau s} + C_{33}^{k}J_{\alpha\beta}^{k\tau_z s_z} + 2C_{12}^{k}\frac{1}{R_{\alpha}^{k}}\frac{1}{R_{\beta}^{k}}J^{k\tau s} + C_{13}^{k}\frac{1}{R_{\alpha}^{k}}\left(J_{\beta}^{k\tau_z s} + J_{\beta}^{k\tau s_z}\right), + C_{23}^{k}\frac{1}{R_{\beta}^{k}}\left(J_{\alpha}^{k\tau_z s} + J_{\alpha}^{k\tau s_z}\right) + \bar{\beta}^{2}C_{44}^{k}J_{\alpha/\beta}^{k\tau s} + \bar{\alpha}^{2}C_{55}^{k}J_{\beta/\alpha}^{k\tau s}.$$

Implemented nuclei in case of cylindrical shells are :

$$\left(K_{uu}^{k\tau s}\right)_{11} = \bar{\alpha}^{2}C_{11}^{k}J_{1/\alpha}^{k\tau s} + \bar{\beta}^{2}C_{66}^{k}J_{\alpha}^{k\tau s}$$

$$+C_{55}^{k}\left(J_{\alpha}^{k\tau_z s_z}-\frac{1}{R_{\alpha}^{k}}J^{k\tau_z s}-\frac{1}{R_{\alpha}^{k}}J^{k\tau s_z}+\frac{1}{R_{\alpha}^{k}}\frac{1}{R_{\alpha}^{k}}J_{1/\alpha}^{k\tau s}\right),$$

$$\left(K_{uu}^{k\tau s}\right)_{12}=\bar{\alpha}\bar{\beta}C_{12}^{k}J^{k\tau s}+\bar{\alpha}\bar{\beta}C_{66}^{k}J^{k\tau s}, \tag{220}$$

$$\left(K_{uu}^{k\tau s}\right)_{13}=-\bar{\alpha}C_{11}^{k}\frac{1}{R_{\alpha}^{k}}J_{1/\alpha}^{k\tau s}-\bar{\alpha}C_{13}^{k}J^{k\tau s_z}+C_{55}^{k}\left(J^{k\tau_z s}\bar{\alpha}-\frac{1}{R_{\alpha}^{k}}J_{1/\alpha}^{k\tau s}\bar{\alpha}\right),$$

$$\left(K_{uu}^{k\tau s}\right)_{21}=\bar{\alpha}\bar{\beta}C_{12}^{k}J^{k\tau s}+\bar{\alpha}\bar{\beta}C_{66}^{k}J^{k\tau s},$$

$$\left(K_{uu}^{k\tau s}\right)_{22}=\bar{\beta}^{2}C_{22}^{k}J_{\alpha}^{k\tau s}+\bar{\alpha}^{2}C_{66}^{k}J_{1/\alpha}^{k\tau s}+C_{44}^{k}\left(J_{\alpha}^{k\tau_z s_z}\right),$$

$$\left(K_{uu}^{k\tau s}\right)_{23}=-C_{12}^{k}\frac{1}{R_{\alpha}^{k}}J^{k\tau s}\bar{\beta}-C_{23}^{k}J_{\alpha}^{k\tau s_z}\bar{\beta}+C_{44}^{k}\left(J_{\alpha}^{k\tau_z s}\bar{\beta}\right),$$

$$\left(K_{uu}^{k\tau s}\right)_{31}=-\bar{\alpha}C_{11}^{k}\frac{1}{R_{\alpha}^{k}}J_{1/\alpha}^{k\tau s}-\bar{\alpha}C_{13}^{k}J^{k\tau_z s}-C_{55}^{k}\left(-\bar{\alpha}J^{k\tau s_z}+\bar{\alpha}\frac{1}{R_{\alpha}^{k}}J_{1/\alpha}^{k\tau s}\right),$$

$$\left(K_{uu}^{k\tau s}\right)_{32}=-\bar{\beta}C_{12}^{k}\frac{1}{R_{\alpha}^{k}}J^{k\tau s}-\bar{\beta}C_{23}^{k}J_{\alpha}^{k\tau_z s}-C_{44}^{k}\left(-\bar{\beta}J_{\alpha}^{k\tau s_z}\right),$$

$$\left(K_{uu}^{k\tau s}\right)_{33}=C_{11}^{k}\frac{1}{R_{\alpha}^{k}}\frac{1}{R_{\alpha}^{k}}J_{1/\alpha}^{k\tau s}+C_{33}^{k}J_{\alpha}^{k\tau_z s_z}+C_{13}^{k}\frac{1}{R_{\alpha}^{k}}\left(J^{k\tau_z s}+J^{k\tau s_z}\right)$$
$$+\bar{\beta}^{2}C_{44}^{k}J_{\alpha}^{k\tau s}+\bar{\alpha}^{2}C_{55}^{k}J_{1/\alpha}^{k\tau s}.$$

When both R_{α}^{k} and R_{β}^{k} are infinite, fundamental nuclei for plates are obtained (see Appendix A).